

# EXPERIMENTAL AND COMPUTATIONAL STUDY OF TENSION LEG BUOY CONCEPTS FOR FLOATING WIND TURBINES

JOAKIM MIDTSEM BERG

NORWEGIAN UNIVERSITY OF LIFE SCIENCES  
DEPARTMENT OF MATHEMATICAL SCIENCES AND TECHNOLOGY  
MASTER THESIS 30 CREDITS 2013



## Preface and Acknowledgements

This thesis has been carried out to fulfill the requirement for Master of Science degree in Industrial Economics at the Department of Mathematical Sciences and Technology at the Norwegian University of Life Science (UMB), Norway. The thesis has been written by Joakim Midtsem Berg at the Norwegian University of Life Sciences from January to May in 2013. It was motivated by personal wish to contribute to development of renewable energy and an interest in the Finite Element Method as a simulation tool.

First of all, I would like to thank my supervisor Prof. Tor Anders Nygaard for giving me the opportunity to write this thesis under his supervision. I would also like to thank him for his advice, time for discussion and support.

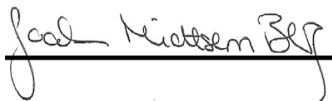
I am grateful to PhD. student Anders Myhr, for letting me participate in his work on the floating offshore wind turbines. He has provided me with a basis for my master thesis given me a part in a larger experiment. I wish to thank him for support, knowledge and time for discussion.

I wish to thank Anders Spæren for the construction of the test rig. The test rig would not have been so well suited for this experiment without his accurate work and eye for detail

I must also thank Marc le Boulluec and his team in the wave tank at IFREMER in Brest. They were very welcoming and deserves to be thanked for having us during the experiment. They were helpful in every way and made a substantial contribution to make it a successful experiment.

Great thanks to my wife Kristine Midtsem Berg for her patience and advice during the period of work on the master thesis.

Ås, 13th May 2013

A handwritten signature in black ink that reads "Joakim Midtsem Berg". The signature is written in a cursive style and is positioned above a solid horizontal line.

Joakim Midtsem Berg

## **Abstract:**

The need for more and cleaner energy has led many research groups to improve the technology of renewable energy harvesting. This project group seeks to verify the mooring line stabilized Tension Legged Buoy concept as a viable option for floating offshore wind turbines. It also seeks to verify 3DFloat, a simulation tool developed by Prof. Tor Anders Nygaard. This will in the next step lower the cost of offshore wind energy and make it more competitive with fossil energy.

This thesis is based upon a series of experiments that was carried out in January 2013 with intentions to study the behavior of a Tension legged structure in an ocean environment with different wave conditions.

The goal of this thesis is to document the experiment and afterwards attempt to replicate it in a series of simulations. The simulation gives the opportunity to understand the experiments better and discover what effects wave load have on the Tension Legged Buoy (TLB). We have measured the forces in the six mooring lines, six degrees of freedom movement of the top of each prototype. The wave height was measured both upstream and at the side of the prototype in water. The measured parameters were recorded synchronous. Video material from every experimental load case was recorded, both over and under sea level.

The simulations have been performed in ANSYS mechanical APDL v14.5 with nonlinear transient analysis. The software is a FEM software for structural analysis. The FEM simulation has also been used to calculate the eigen periods.

The results from the experiments and the simulations have been analyzed separately and then been compared. This makes it possible to sort out effects that are specific for each prototype, what effects that are load case specific and effects that are specific for the whole series of experiments.

It proves especially challenging to replicate the heave movements by simulating the prototypes in ANSYS. This is likely related to ANSYS lack of proper lid modelling opportunities in ocean environment. (EDR-Medeso, 2013) The deviating eigen periods and damping parameters are also likely sources for this.

There is no signs of significant errors in the experimental data. The results obtained from the experiments are proving to be good, and the experiment can be considered successful. The simulations delivered almost as good results as we could hope given the limitations in the software. This thesis shows that it is possible to simulate the behavior of the TLB with a certain level of accuracy, but more sophisticated tools than ANSYS mechanical APDL is recommended.

## Table of contents

Terminology and symbols.....	VI	
<u>1</u>	<u>Introduction.....</u>	<u>1</u>
1.1	The world is in need of more energy.....	1
1.1.1	Wind energy is one of the best options to generate renewable energy.....	1
1.1.2	Concepts of floating offshore wind turbines.....	6
1.2	Background and purpose.....	8
1.3	The project and project goals.....	9
1.4	Goals and Problem statement.....	9
1.5	Limitations.....	10
1.6	Method:.....	10
<u>2</u>	<u>Theoretical basis.....</u>	<u>11</u>
2.1	Wave theory:.....	11
2.2	Forces on structures in waves.....	13
2.3	Drag coefficients and inertia coefficients.....	15
<u>3</u>	<u>Experiment and prototype description.....</u>	<u>19</u>
3.1	The experiment set up.....	19
3.2	The towers.....	19
3.3	Test facility: IFREMER wave tank:.....	22
3.4	The components of the experiment.....	23
3.5	The three experimental prototypes.....	24
3.6	Measurements and properties of the prototypes:.....	25
3.6.1	TLB S.....	25
3.6.2	TLB B.....	26
3.6.3	TLB X3.....	28
3.7	Mooring line:.....	30
3.8	Adjustable springs:.....	31
3.9	The pulley plates:.....	32
3.10	Measurement equipment.....	33
3.10.1	Load cells.....	33
3.10.2	Wave gauges.....	33
3.10.3	Tracking system.....	34
3.10.4	LINAK Actuators.....	34
<u>4</u>	<u>Experimental results.....</u>	<u>35</u>
4.1	Choice of time domain to present and analyze:.....	35
4.2	Eigen values.....	35

4.3	Plots of movement and forces over wave height.....	36
4.4	Comparison of UX deflection on each prototype for different wave periods.....	37
4.5	Forces:.....	39
4.6	UZ movement from all the test cases: .....	39
4.6.1	TLB Simple: .....	40
4.6.2	TLB B .....	41
4.6.3	TLB X3: .....	42
4.7	The TLB B and TLB X3 dives into the wave.....	43
4.7.1	Center of rotation and wave force resultant .....	44
4.8	Wave frequency response plot.....	45
4.9	Uncertainties and error propagation .....	49
4.9.1	Variance in wave gauge results.....	51
4.10	Summarizing discussion of experimental results .....	52
<u>5</u>	<u>ANSYS APDL modelling.....</u>	<u>53</u>
5.1	Wave and ocean theory in ANSYS .....	53
5.2	Choice of elements .....	55
5.2.1	PIPE288.....	55
5.2.2	LINK180.....	56
5.2.3	COMBIN14 .....	57
5.2.4	MASS21.....	57
5.3	Assumptions and Simplifications.....	57
5.3.1	Constraining the model and choices .....	58
5.4	Modelling the three simulation models:.....	58
5.4.1	TLB Simple:.....	58
5.4.2	TLB B .....	59
5.4.3	TLB X3 .....	59
<u>6</u>	<u>Calibration and control of the simulation models:.....</u>	<u>61</u>
6.1	Controlling the geometry:.....	61
6.2	The figures for pretension in the lines were measured during the experiment: .....	61
6.3	Convergence analysis: .....	61
6.3.1	Time convergence analysis: .....	62
6.3.2	Element size analysis .....	63
6.4	Drag and Inertia coefficients.....	65
6.5	Eigen periods:.....	68
6.5.1	Yaw eigen period .....	68
6.6	Calibrating simulated damping parameters.....	70
6.6.1	TLB S.....	71
6.6.2	TLB B .....	72
6.6.3	TLB X3 .....	73

6.7	Control of wave loads in ANSYS .....	74
<u>7</u>	<u>ANSYS APDL Results.....</u>	<u>76</u>
7.1	Simulation 37: TLB S, 2.5 sec, 0.5 m .....	76
7.2	Simulation 45: TLB B, 1.58 sec, 0.3 meter.....	79
7.3	Simulation 61: TLB X3, 0.95 sec, 0.13 m.....	80
7.4	Simulation 67: TLB X3, 1.58 sec, 0.3 m.....	81
7.5	Summarizing discussion of simulation results .....	82
7.5.1	Separating surge movement from pitch movement.....	83
<u>8</u>	<u>Comparisons and discussion of experimental and simulated results.....</u>	<u>84</u>
8.1	Load case 37: TLB S, 2.5 sec, 0.5 m.....	84
8.2	Load case 45: TLB B, 1.58 sec, 0.3 m .....	86
8.3	Load case 67: TLB X3, 1.58 sec, 0.3 m .....	89
8.4	Summarizing discussion of results from comparison.....	91
<u>9</u>	<u>Conclusion: .....</u>	<u>92</u>
<u>10</u>	<u>Further work: .....</u>	<u>93</u>
<u>11</u>	<u>Bibliography.....</u>	<u>94</u>
<u>12</u>	<u>Appendix.....</u>	<u>97</u>

## Terminology and symbols

Term	Description of term
3DFloat	A FEA code written by Prof. Tor Anders Nygaard. The code is designed to simulate floating offshore wind turbines with higher accuracy than standard FEA codes.
Mooring line system	The system of mooring lines, adjustable springs, actuators and load cells in the experiment.
Anchor points	May refer to both anchor points on the model and the anchor points on the seabed.
Bracket	The actual mooring point on the prototype. Connects mooring lines to prototype
Catenary mooring lines	Loose mooring lines used to keep a floating in position, but not to stabilize it.
Code	Script for programming of computers
Deep water	Water depths above a certain level. What is considered deep water depends on the size of the waves.
DOF	Degrees of freedom.
Element	The structure that is subject to analyze is divided into elements. Because they are finite it is called the finite element method. The elements can have different properties, shapes and sizes depending on the structure and what we want to analyze. Nodes connect elements to the neighboring elements.
The experiment	The experiment conducted in Brest in January 2013. Sometimes it refers to the whole series of experiments, and sometimes it is used in the meaning of a special load case
FEM/FEA	Finite Element Method/ Finite Element Analysis: a numerical technique for finding approximate solutions to boundary value problems. It is used for many applications, but is the most widely used technique to solve complex structural problems in mechanical engineering.
Floating wind turbine	Wind turbine mounted on a floating structure. In this thesis it refers to the whole floating structure, including the floater.
Hydrodynamics	The study of liquids in motion
IFE	Norwegian institute for energy Technology.
Inertia forces	In wave theory, these forces are the result of acceleration and deceleration of a wave particle. The forces are related to the mass of the water
Keulegan Carpenter number	A dimensionless quantity describing the relative importance of the drag forces over inertia forces for bluff objects in an oscillatory fluid flow
Key point	Point in space defined by three coordinates, usually, x, y and z coordinate. Used to model a structure in FEM
Line	Line is used to create a connection between two key points. FEM is based upon laying properties on a line, area or volume. We put material properties and section properties on the lines to create the simulation model.
Lines or Mooring lines	Lines connecting the prototype to the "bottom" or anchors. There are six lines, three bottom lines and three top lines. In the experiment, they are connected to the prototype in one end and to the adjustable spring in the other end after going through a pulley on the fictional seabed. In the simulation the lines go from prototype to sea bed anchors.

Term	Description of term
Mesh	The set of connected nodes and elements in a Finite Element model
Motion tracking	System to determine how an object moves in space over time.
Nacelle	A housing on top of the wind turbine tower that includes the gearbox, generator and more. Nacelle is used to describe the dummy nacelle on top of the prototype B and X3. The weight of the dummy nacelle is also including the scaled weight of the rotor blades
Node	Point in space that connects elements. In structural analysis, it has three or six degrees of freedom depending on the elements they connect
Period	Time it takes before a sequence starts to repeat itself
The project	The project that do research on the TLB concept at Norwegian University of life sciences and Norwegian institute for energy Technology.
Reynolds number	Dimensionless number that gives a measure of the ratio of inertial forces to drag forces.
Shallow water	Water depths below a certain level. What we consider shallow water depends on the size of the waves.
The simulation	Meaning the simulation done to replicate the results from the Brest experiment. Sometimes it refers to the whole series of, simulations and sometimes it is used in the meaning of the simulation of a special load case
Test site	IFEMER wave tank in Brest, France.
Tension Leg Buoy	Vertically mounted buoy stabilized by its mooring lines. Mounted with taut mooring lines and floating with excess buoyancy
TLB S, TLB Simple	Refers to the plastic pipe prototype which serves as a reference model
TLB B, Prototype B	The second prototype, realistic with imitated nacelle. Floater with tapered section to minimize wave loads
TLB X3, Prototype X3	The third prototype, realistic prototype with imitated nacelle. Floater with the three-column section to minimize wave loads. Smaller diameter on floater than TLB B
Tower	Part of the offshore wind turbine that stands on the floater and bears the nacelle
Tracking ball	Piece of measurement equipment needed to track movement in space. In reality its four carefully positioned relative to each other. They are reflective balls visible for 3D cameras.
TWh	Terra Watt Hour: Energy produced or consumed. $1 \text{ TWh} = 3.6 \cdot 10^{15} \text{ Nm}$
TWh/a	Energy produced or consumed per year.
UMB	Universitetet for Miljø og Biovitenskap/Norwegian University of Life sciences.
Wave period	Time it takes before the wave is in the same phase again. For example between wave tops
Eigen frequency,	The natural frequency is the rate at which an object vibrates when it is not disturbed by an outside force.
Eigen period	$1/\text{eigen frequency [s]}$
Wave	Oscillating motion that travels. Often seen in transfer of energy. In this thesis wave refers to wave in the ocean that has its source in the wind transferring its energy into waves on the ocean.



Term	Description of term
Wave steepness	How high the wave is, compared to how long the wave is. The higher the wave given the same wavelength, the steeper the sides of the waves.
WEO	World Energy Outlook, a semiannual publication from The International Energy Association on the Energy situation in the world in the coming 20 years.
Wind turbine	Unit that is set up to harvest energy from wind. Usually to produce electricity. Sometimes wind turbine is used to describe the experimental model in this thesis
X3-columns	The three columns connecting the floater to the tower on the X3 prototype
$F_x$	Force in X-direction
$F_y$	Force in Y-direction
$F_z$	Force in Z-direction
$M_x$	Moment around the x-axis
$M_y$	Moment around the y-axis
$M_z$	Moment around the z-axis

Table 1: Labels on the simulated and experimental results

	In simulation	In experiment
Force line 1	Force1	LoadCell1
Force line 2	Force2	LoadCell2
Force line 3	Force3	LoadCell3
Force line 4	Force4	LoadCell4
Force line 5	Force5	LoadCell5
Force line 6	Force6	LoadCell6
X translation	UX	TLBBody1 X
Y translation	UY	TLBBody1 Y
Z translation	UZ	TLBBody1 Z
X rotation	Roll	TLBBody1 Roll
Y rotation	Pitch	TLBBody1 Pitch
Z rotation	Yaw	TLBBody1 Yaw

### Movement of a structure in the sea:

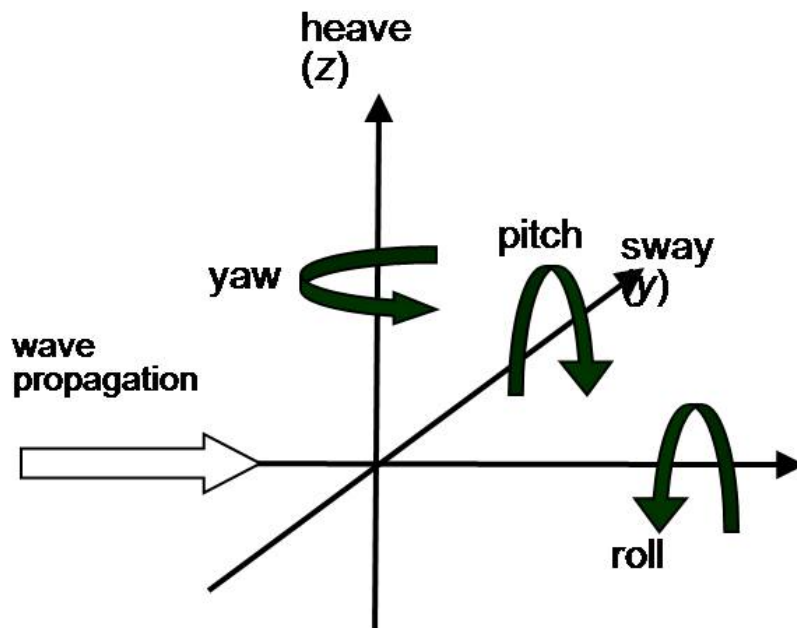


Figure 1: Modes of motion in water. Credit: Lancaster University Renewable Energy Group

# 1 Introduction

## 1.1 The world is in need of more energy

The world needs more power now, and especially in the future. The 2010 World Energy Outlook from the International Energy Agency estimates that the world will consume between 31 981 and 38423 *TWh* of electricity in 2035. That is 90 – 129 % more electricity than in 2008 where 16 800 *TWh* were consumed. (International Energy Agency, 2010)

Which source of energy that will have the largest growth is uncertain, but wind energy is expected to contribute with a substantial part. The average scenario in the WEO2010 estimates that the world will produce 2 851 *TWh* of wind energy in 2035 (with 1035 *GW* of installed capacity). (International Energy Agency, 2010). That is 13 times more than in 2008 and 3.8 times more than the expected production in 2015.

Table 2: World electricity production and capacity

	2008	2015	2035	Growth (%)
Electricity production [ <i>TWh</i> ]	20183	24513	35336	175 %
-Wind [ <i>TWh</i> ]	219	756	2851	1302 %
Electrical Capacity [ <i>GW</i> ]	4719	5942	8613	183 %
-Wind [ <i>GW</i> ]	120	358	1035	863 %

Between 180 and 340 *GW* is assumed to come from offshore wind power in 2035. The average size of an offshore wind turbine is assumed increase to between 8 and 10 *MW* in 2020. (Det Norske Veritas AS, 2012). This means that the world will build between 20 000 and 30 000 offshore wind turbines in the next 20 years. Higher focus on global warming in the years after the report gives reason to believe that the estimate is conservative. Less interest in nuclear power after the Fukushima accident does also mean a shift towards other energy sources such as wind energy. On the other hand, the United States has found an enormous amount of shale gas. This may take the estimate in another direction. The opinions of people and the political trends are shifting faster than technology development can adapt. The only sure thing here is that those who can supply energy at a reasonable price with a minimum of pollution will have a chance.

### 1.1.1 Wind energy is one of the best options to generate renewable energy

Wind is a renewable energy source coming from current solar radiation. The sun heats the air and sets it in motion together with the rotation of the earth (*Knapp, 2012*). Table 3 states that the theoretical potential of wind energy on the planet is 100 times the assumed electricity consumption in 2035. The

theoretical potential of wind energy is much larger than hydro energy, but more costly to harvest. The challenge of the wind industry is to generate electricity at a profit allowing cost.

Table 3: Table of the theoretical potential energy from renewable energy sources (Knapp, 2012)

	Theoretical potential [TWh/a]
Solar radiation	694 000 000
Biomass energy	833 000
hydro energy	44 000
wind energy	3 055 000
ocean energy	1 389 000
geothermal energy	278 000

$$\text{Energy } E = \frac{1}{2} \times m \times c_{\infty}^2, \text{ where } \frac{m = \text{mass of the wind}}{c_{\infty} = \text{average wind speed}} \quad \text{Equation 1}$$

$$\text{Power } P = \frac{E}{t} = \frac{1}{2} \times \dot{m} \times c_{\infty}^2 = \frac{1}{2} \times \rho \times A \times c_{\infty} \times c_{\infty}^2 = \frac{1}{2} \times \rho \times A \times c_{\infty}^3 \quad \text{Equation 2}$$

$$\text{where } \frac{\dot{m} = \text{mass flow} = \frac{m}{t}}{t = \text{time}}$$

$$\text{Wind Power Density } WPD = \frac{P}{A} = \frac{1}{2} \times \rho \times c_{\infty}^3 \quad \text{Equation 3}$$

Equation 3 states that the amount of energy that we can harvest from wind increases with the cube of the wind speed. It is crucial to the profitability of wind energy that wind parks are located at the location with highest and most stable wind speeds. The wind speed is the one factor that determines how much power we can extract from the wind. The sea has a smoother surface than there is over land. Hills, forests buildings are obstacles that slows down the wind over land, but there is no such obstacles at the sea. This means lower friction between the wind and ground or sea and higher wind speeds at lower altitudes over sea.

2.4. Types of wind turbines  
2.4.5. Offshore plants

wind velocity distribution above ground at different ground roughness values:

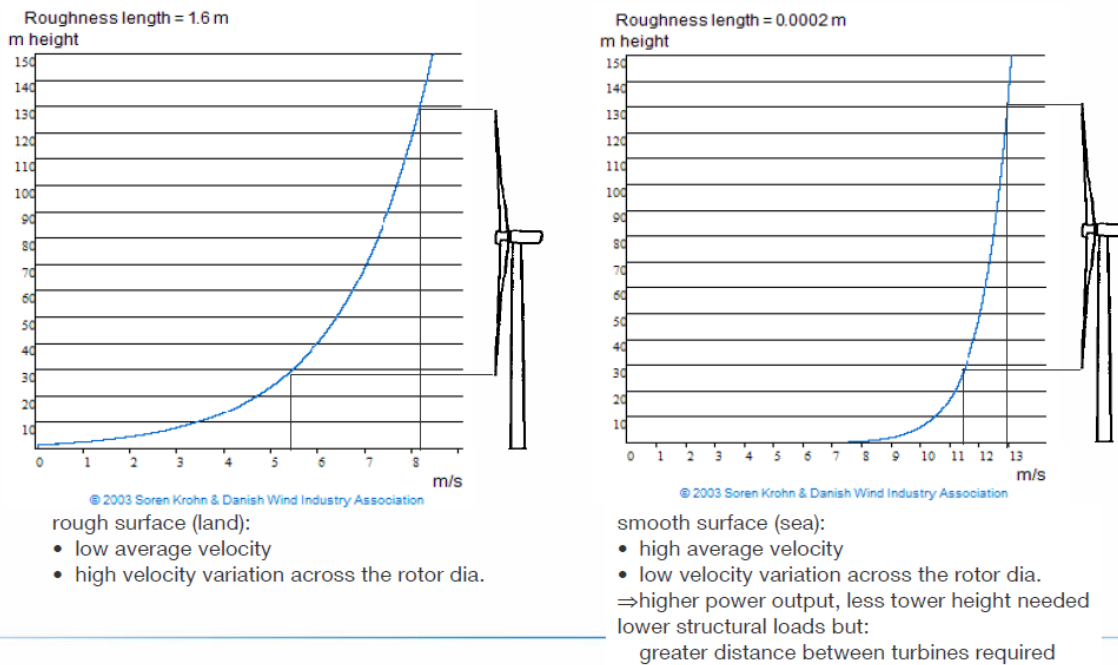


Figure 2: Illustration of wind speed and roughness (Knapp, 2012)

The friction between surface and wind is called ground roughness (Knapp, 2012). The ground roughness value states how much of the wind speed decays as we come closer to the surface.

One of the advantages of lower roughness is lower variation in velocity over the rotor diameter that results in lower bending forces on the turbine axel and thus the expected lifetime of the axel.

The velocity of the wind at a chosen height H is given by the function:

$$v_h = v_{ref} \times \frac{\ln\left(\frac{H}{z_0}\right)}{\ln\left(\frac{H_{ref}}{z_0}\right)} \quad \text{Equation 4}$$

Where:

$$\frac{v_h = \text{velocity at height } H}{v_{ref} = \text{velocity at reference height } H_{ref}}$$

$$z_0 = \text{Roughness length}$$

$$\rho = \text{mass density of air}$$

Table 4: Roughness of the ground (Knapp, 2012)

surface	roughness	roughness	energy
sea	0	0.0002	100
flat	0.5	0.0024	73
fields,	1	0.03	52
fields	2	0.1	39
villages,	3	0.4	24
large	4	1.6	13

The  $v_h = v_{ref} \times \frac{\ln(\frac{H}{z_0})}{\ln(\frac{H_{ref}}{z_0})}$  Equation 4 and Table 4 states that the wind speed close to ground or sea level is higher at sea given the same wind speed in the reference height.

Figure 3 from Wind Conditions and Resource Assessment by Petersen and Troen (2012) illustrates the wind speeds at sea and at shore. In some onshore locations such as north on the British Isles, we find locations with high average wind speeds. It is also easy to see that the longer away from shore the higher average wind speed. The downside is that the distance to shore increases the cost of bringing the electricity to the users.

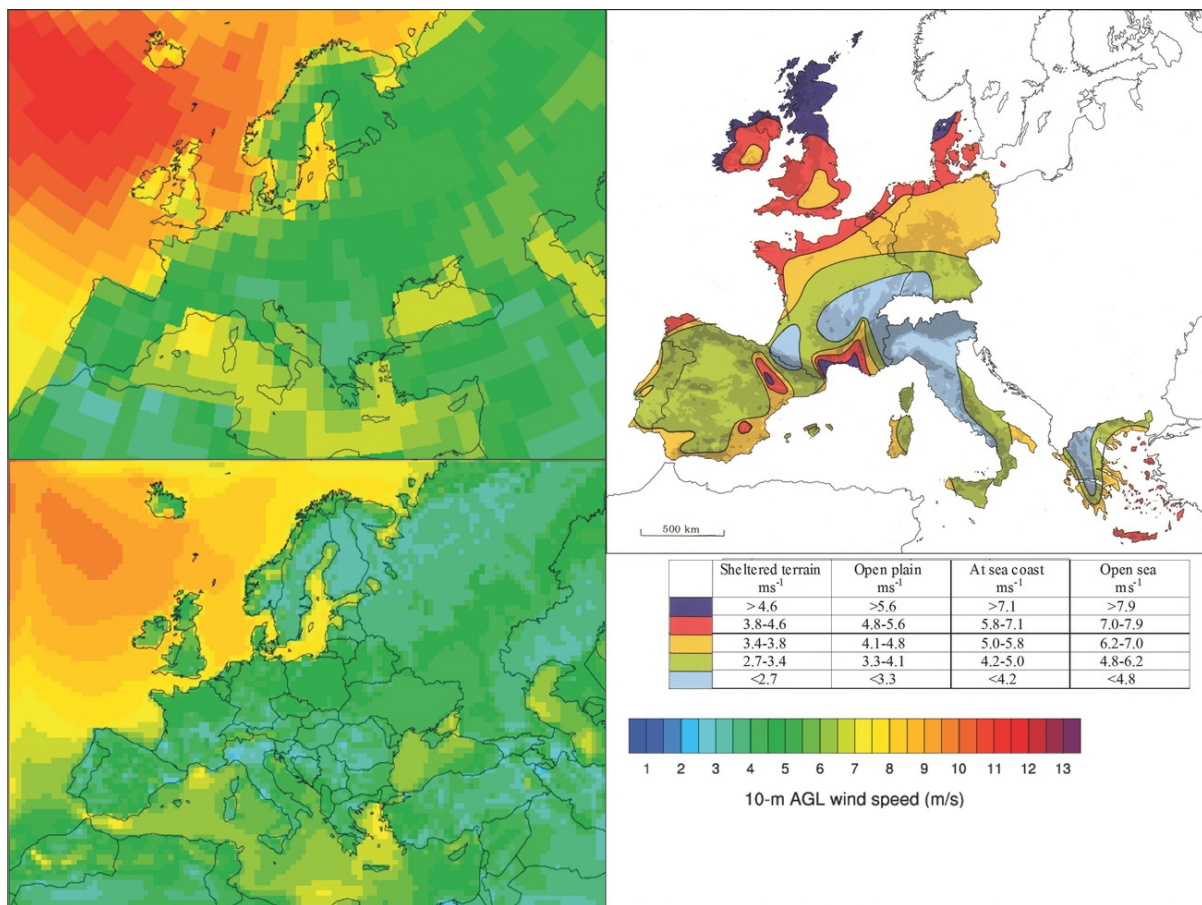


Figure 3: Wind speeds at sea and at shore in Europe (Petersen & Troen, 2012)

Offshore wind energy is divided into floating wind turbines and bottom mounted wind turbines. The bottom fixed turbines are most commonly used today and they are used in relatively shallow water. Compared to bottom fixed offshore wind turbines, floating wind turbines has several advantages and disadvantages:

Advantages:

- Can be placed further from shore to find better and more stable wind and wave conditions
- Possible to build lightweight constructions with less material usage.

Disadvantages:

- Higher grid cost because installation is further from shore.
- Higher cost of maintenance if the installation is further from shore.

With more research on floating offshore wind turbines there are reasons to believe that it is possible to produce electricity from floating offshore wind turbines profitably in the future. (Volden & Sanden, 2010) In their 2010 World energy Outlook IEA projects increasing prices on oil and decreasing prices on electricity generated by renewable energy sources. (International Energy Agency, 2010)

Table 5: Cost of generating renewable energy toward 2035. (International Energy Agency, 2010)

	Generating costs						Learning rates
	2010-2020 (\$2009 per MWh)			2021-2035 (\$2009 per MWh)			
	Min	Max	Avg	Min	Max	Avg	
Hydro - large	51	137	94	52	136	95	1%
Hydro - small	71	247	143	70	245	143	1%
Biomass	119	148	131	112	142	126	5%
Wind - onshore	63	126	85	57	88	65	7%
Wind - offshore	78	141	101	59	94	74	9%
Geothermal	31	83	52	31	85	46	5%
Solar PV - large scale	195	527	280	99	271	157	17%
Solar PV - buildings	273	681	406	132	356	217	17%
CSP	153	320	207	107	225	156	10%
Marine	235	325	281	139	254	187	14%

Note: MWh = megawatt-hour.

### 1.1.2 Concepts of floating offshore wind turbines

For floating offshore wind turbines there are three different main concepts for the floater:

1. Buoyancy stabilized floater
2. Ballast stabilized floater
3. Mooring line stabilized floater

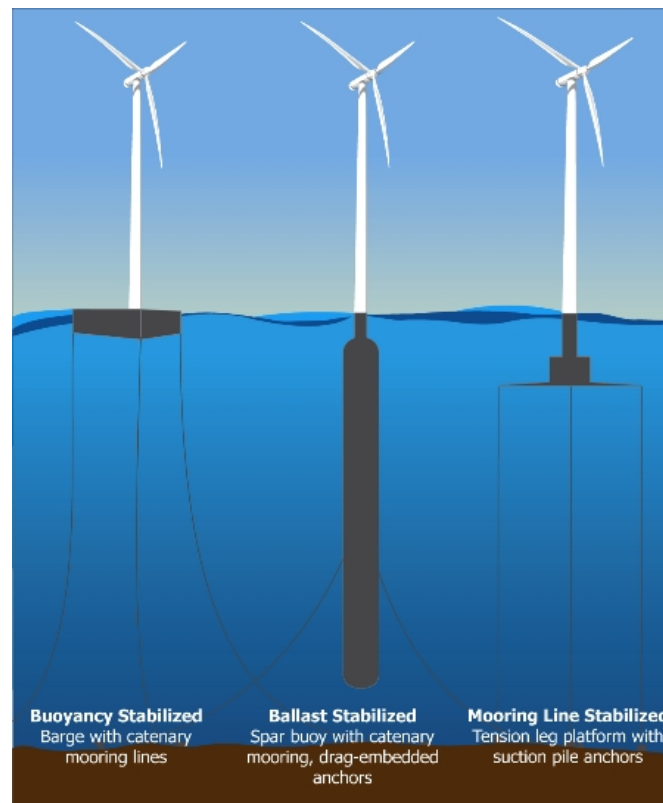


Figure 4: Example of mooring types. Illustration by renewableenergyworld.com

Volden and Sanden (Volden & Sanden, 2010) states that the mooring line stabilized concept is more economical than ballast stabilized concept they have compared it with. The mooring line stabilized concept has a more efficient material usage. The construction of the mooring line stabilized wind turbine gives it more flexibility concerning location because of its lower draft. Ballast stabilized floater need a lot of ballast to be stabilized and a larger floater to float the extra ballast. The Tension Leg Buoy (TLB) is stabilized by the mooring lines and excess buoyancy. This means that there is no need for ballast inside the floater and no extra floating capacity. The findings of Volden and Sanden (Volden & Sanden, 2010) shows that the TLB concept has cost advantages over the other types mooring.

TLB are floating, but the mooring lines determine the vertical position and not the water line. The buoy is pulled below the water line and has excess buoyancy. It is fully stabilized by its mooring lines and do to some extent behave as if it is bottom fixed. A version of the same concept, the Tension legged platform (TLP) is known from the oil and gas industries. The TLB controls all Degrees-Of-Freedom (DOF) by the axial stiffness of taut mooring lines attached to the platform at two or more heights. Professor Sclavounos of



Massachusetts Institute of Technology (MIT) (Butterfield, 2005) was the first to introduce the TLB in a wind energy context under the name MIT double taut leg.

The behavior of tension legged wind turbines are not very well documented and the calculation method used today is yet to be properly proven as most offshore simulation tools rely on rigid structures which is necessary to simulate the stiffness dominated TLB-systems. One of the goals of this project is to examine if the TLB is an option when it comes to floating wind turbines and if it is good option in terms of both stability, cost and material efficiency.

No code has been verified to do a complete computer simulation of the TLB and it is therefore not possible at this point without big uncertainties around calculation. Prof. Tor Anders Nygaard has written a code for the software 3DFloat that take the hydrodynamic, aerial and servo forces exerted on a complete floating wind turbine into consideration in an elastic model at the same time. The code still to be fully verified, and a side goal of the experiment is to verify this code by comparing experiments and simulations.. With a code that is proved to be working, it is possible to calculate the behavior of TLB wind turbines.

The project strategy is to go stepwise from small scale wind turbines to full scale. This reduces the cost and the risk of making unsuccessful prototypes. The optimal design for a TLB wind turbine can be pursued in smaller scale and wind parks built at reduced cost.

An experiment in the IFREMER wave tank late January 2013 has been conducted to obtain better knowledge of the Tension legged buoy behavior in ocean waves. The experiment is a 1:40 scaled prototype of a full-size wind turbine concept. The project group made a test rig the autumn and early winter of 2012-2013. The test rig was planned and built at the Norwegian University of Life Sciences (UMB). PhD. Student Anders Myhr had the main responsibility for concept development for this experiment, but several persons has been involved at earlier stages. Anders Myhr and Amund Føyn developed and built the electronic equipment. Anders Spæren had the construction of the test rig as his master thesis and worked on the project from the autumn of 2012. Joakim Midtsem Berg was assisting them in the period before we went to Brest in France to carry out the experiment.

Several floating offshore wind turbine projects have been started in recent years. (Volden & Sanden, 2010) The Ballast stabilized wind turbine concept from Statoil, The Hywind is one of the prototypes that is already functional at sea (Statoil ASA, 2013). The blue H concept is a tension leg platform concept of a floating offshore wind turbine by the Blue H group. This prototype was tested at in 2008 (Blue H group, 2013). A third concept is the WindFloat, a semi-submersible platform for floating offshore wind turbines (Principle power inc., 2013).



*Figure 5: The TLB Concept (Myhr & Nygaard, Load Reductions and optimizations on a tension legged buoy offshore wind turbine platforms., 2012)*

## **1.2 Background and purpose**

The background of this thesis is the ongoing project on offshore floating wind turbines at the Norwegian University of Life sciences and the Norwegian institute for Energy technology.

This thesis is written as a part of the project to help verifying that the Tension legged buoy is a viable solution to build floating offshore wind turbines. It is written under the supervision of prof. Tor Anders Nygaard. Nygaard is also responsible for the project.

The purpose of the thesis is to document the results from the experiment in Brest and write a code for ANSYS APDL to simulate the load cases from the experiment. If the simulations are successful, they will be used in further studies to verify that the 3DFloat code produces reliable results.

The first month (January 2. – February 3. 2013) of the work with this master thesis was dedicated to build the test rig. The test period lasted from 21 – 31 of January with three days of transportation before and after. The first week dedicated to set up the experiment and the second week to conduct the test sequences. Tor Anders Nygaard, Catho Bjerkseter, Amund Føyn, Anders Myhr and Joakim Midtsem Berg was on the site during the set up period, while Anders Myhr and Joakim Midtsem Berg was on site during the test period.

This master thesis seeks to verify the TLB as a stable construction with a minimum of movement at the nacelle. The thesis also seeks to verify the work done by Anders Myhr in this project. He does the same simulation but with the more specialized and sophisticated program 3DFloat.

### 1.3 The project and project goals

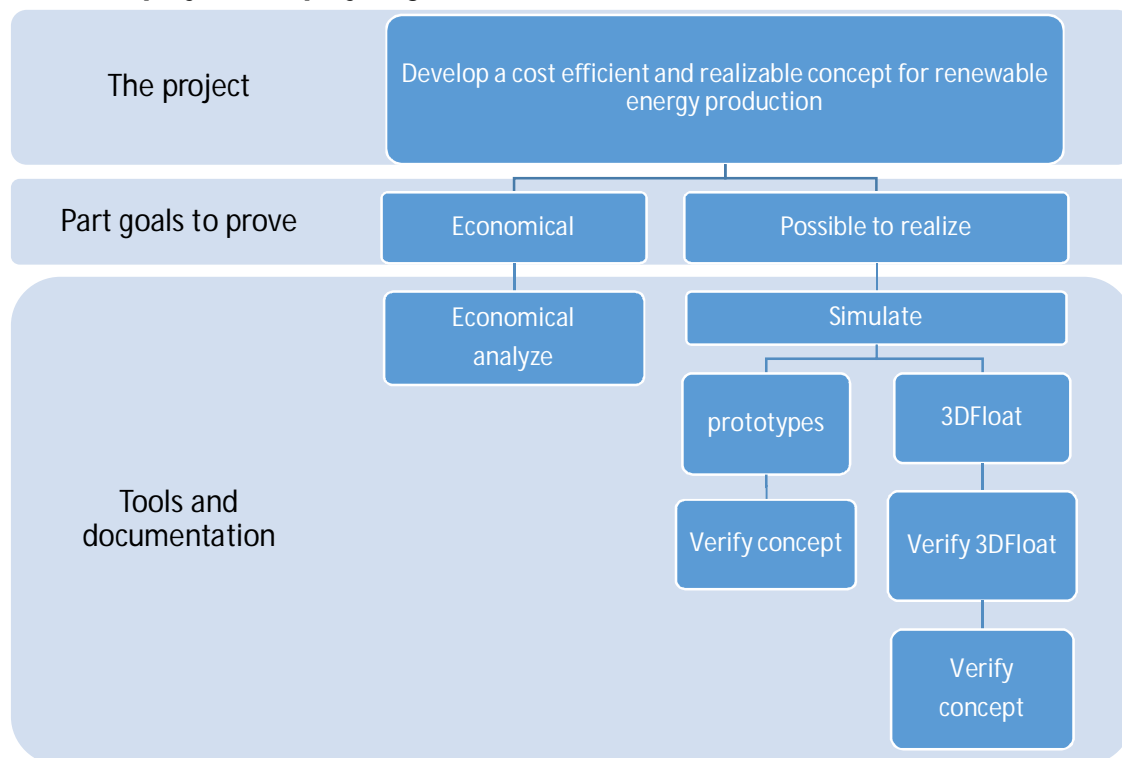


Figure 6: Illustration of the TLB research project

The goal of the project is to develop the best concept for renewable energy production. That goal is realized by finding an economically reasonable concept and a concept that is possible to realize in terms of construction.

### 1.4 Goals and Problem statement

The problem statement is to do an experimental and computational evaluation of tension leg buoy concept for floating wind turbines in ocean waves.

The thesis has three main goals that that is fulfilled to the achievement of part goals:

1. Present experiment and result
  - a. Construct and assemble test rig for experiment
  - b. Document experimental results
  - c. Analyze the experimental results
2. Present simulation models and simulation results from simulation of the experiment
  - a. Build three simulation models to simulate the prototypes in FEM software
  - b. Calibrate the models after experiment
  - c. Present and analyze the results from simulation
3. Compare experiment and simulation

## **1.5 Limitations**

This thesis will only concentrate on the downsized floater. It seeks only to document and analyze the results of the experiment.

Only wave loads will be studied in this thesis, because the experiment is limited to such loads.

ANSYS APDL is not able to run irregular waves without significant extra work. This thesis will focus on the regular waves only except for four plots in the experiment result section where it is appropriate to involve them. This is because they put light to the results from the regular wave cases. Splashing and other loads from the ocean will not be considered in this master thesis, since the theoretical level is too high and ANSYS is not able to include such loads.

## **1.6 Method:**

The main source of data in this thesis is quantitative material gathered in the experiment. There are side data in qualitative form such as video material made to control and verify findings in the main data source.

The data material has been structured and plots has been made through use of Excel data sheets. It has been studied and analyzed by comparing data series in plots and statistical methods. Excel was chosen as tool for analyzing the data because of its ability to manage relatively large amounts of data and its ability create plots of different data rapidly. Done

This simulation was prepared in excel data sheets and completed in ANSYS mechanical APDL simulation software. ANSYS provides the necessary solution to solve this kind of simulation by combining simulation of hydrodynamic environment and an elastic FEM modelling. ANSYS mechanical APDL is widely acknowledged world wide as one of the best providers of multi physics software. It supports ocean and wave commands to simulate the right environment. ANSYS mechanical APDL does only provide simplified hydrodynamics, but it is sufficient for the simulation of this experiment. ANSYS Mechanical APDL is also chosen for its simple and safe modeling. Other options are ANSYS Workbench, ANSYS ASAS or ANSYS Aqua, but these lack the ability to simulate hydrodynamic loads or they can only model with rigid objects. When a structure is subject to a dynamic load, not only the external forces must be considered, but also the forces created by the inertia of the structure and the internal friction or external damping. (Huebner, Dewhirst, Smith, & Byrom, 2001) Computational fluid dynamics tools are not an option because they lack the possibility to use an elastic object in a fluid flow. ANSYS Workbench, ANSYS ASAS or ANSYS Aqua have the possibility to use CAD drawings from SolidWorks or similar, but it will give a high number of equations. Computationally expensive simulations is not desirable because of limited time.

The simulation model has been calibrated upon the measurements from the experiment.

The reader is assumed to be familiar to the Finite Element method.

The simulated results were compared through excel data sheets and graphical plots. The comparison of the data sets were done through analyzing the difference between the data sets for the three prototypes and over several different load cases.

## 2 Theoretical basis

The theoretical base for this thesis is hydrodynamics. The following chapter includes how forces is exerted on a body semi submerged in water. The forces from waves are applied with Morrison's equation.

### 2.1 Wave theory:

A basic way to understand the hydrodynamic forces on a structure is to divide them into inertia forces and drag forces. The inertia forces being the weight of the water pushing on the structure and the drag forces being the frictional force from the water moving past the structure.

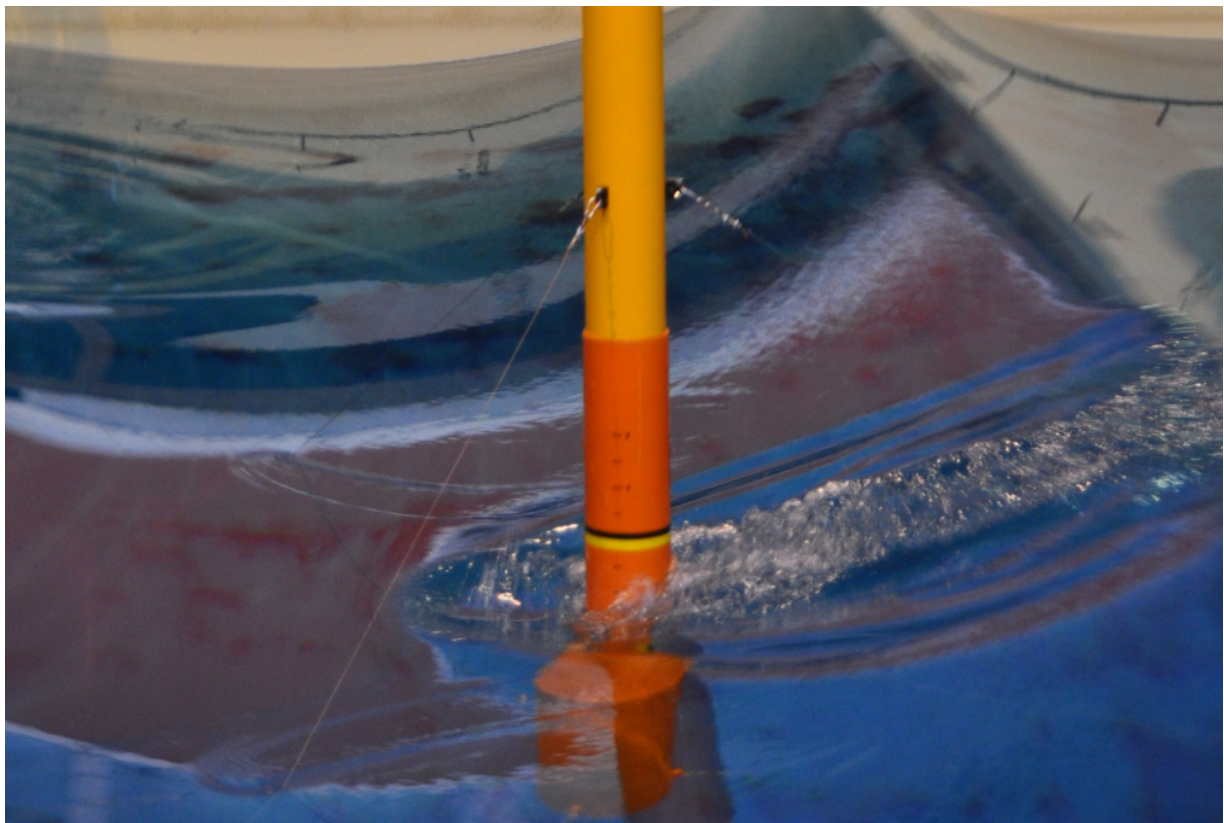


*Figure 7: Wave moving past model B in the IFREMER water tank.*

Waves have both vertical and horizontal movement, with associated velocity and acceleration. Airy's linear wave theory and Stokes wave theories are two of several different theories to describe the wave motion. The Airy linear wave theory and Stokes non-linear wave theory is two of the most commonly used theories.

Waves act different in deep water and shallow water. Both the Airy theory and Stokes wave theory are designed mainly for deep water problems.

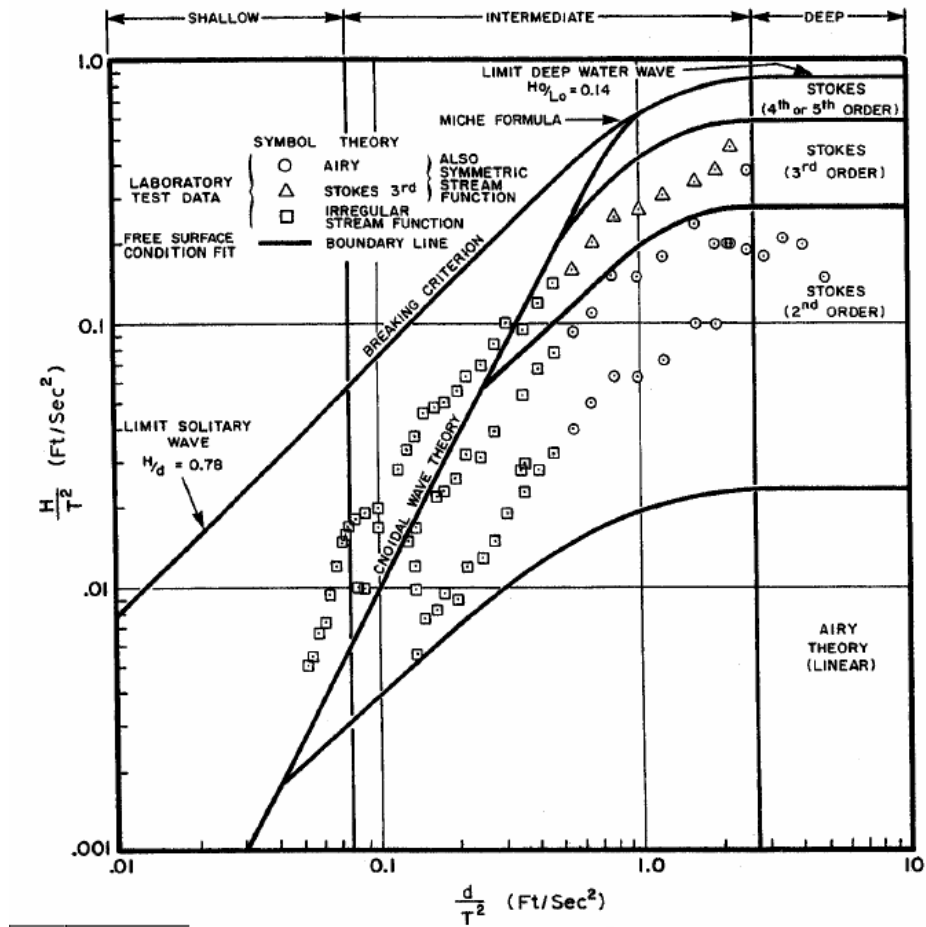


Figure 8: Ranges of wave theory validity. Be aware of the length unit (Det Norske Veritas, 2013)

There are no universal wave theory for every sea condition, but several wave theories that are applicable in different sea conditions. Figure 8: Ranges of wave theory validity. Be aware of the length unit (Det Norske Veritas, 2013) shows that different wave theory that are valid at different wave conditions and different depth of the sea. Which theory to apply to a problem depends on these formulas (Det Norske Veritas, 2010)

- Wave steepness parameter (Det Norske Veritas RP-C205, 2010):

$$S = 2\pi \frac{H}{gT^2} = \frac{H}{\lambda_0} \quad \text{Equation 5}$$

- Shallow water parameter (Det Norske Veritas RP-C205, 2010):

$$\mu = \frac{2\pi d}{gT^2} = \frac{d}{\lambda_0} \quad \text{Equation 6}$$

- Wavelength of deep-water ocean wave: (Twidell & Weir, 2006)

$$\lambda = \frac{2\pi g}{\omega^2} \quad \text{Equation 7}$$

Table 6: Extreme wave cases in experiment: highest and lowest wave period and wave height

Extreme wave cases	Wave period [s]	Wave height [m]
Short wave period, low wave height	0.95	0.13
Short wave period, high wave height	1.8	0.5
Long wave period, low wave height	2.8	0.13
Long wave period, high wave height	2.5	0.5

The depth in the test basin is 10 meters and the longest period for the waves is 2.8 seconds.

$$\frac{d}{T^2} = \frac{10m}{2.8^2 s^2} = \frac{10}{7.84} \frac{m}{s^2} > 0.8 \frac{m}{s^2}.$$

Because this is the smallest ratio between depth and period, all of load cases in the experiment are in what DNV considers as deep water.

The choice is therefore between Airy theory and Stokes 2<sup>nd</sup>, 3<sup>rd</sup>, 4<sup>th</sup> or 5<sup>th</sup> order waves.

The wave height to period ratio is between:

$$0,011 \frac{m}{T^2} \leq \frac{H}{T^2} \leq 0,780 \frac{m}{s^2} \quad \text{Equation 8}$$

This means that Stokes 2<sup>nd</sup> order and 3<sup>rd</sup> order wave theory should be used, but since ANSYS only simulate Airy waves or Stokes 5<sup>th</sup> order waves. this is not possible in the simulation. Stokes 5<sup>th</sup> order wave theory is applicable for wave case of lower order (Nygaard, 2013) and chosen for all cases in the simulation.

## 2.2 Forces on structures in waves

Newton's second law states that  $\vec{F} = m\vec{a}$  and drag force:  $\vec{F}_D = -b\vec{v}$  (Tipler & Mosca, 2007). These are the two forces in hydrodynamics. A fluid is accelerating and decelerating, and that causes forces on an object in water. This is what is called inertia forces in the hydrodynamics. When a fluid moves with a relatively higher or lower velocity compared to an object in the fluid, this creates frictional forces. This friction is between the fluid and the object, but the object can also cause turbulence in the fluid which in turn creates internal friction in the fluid.

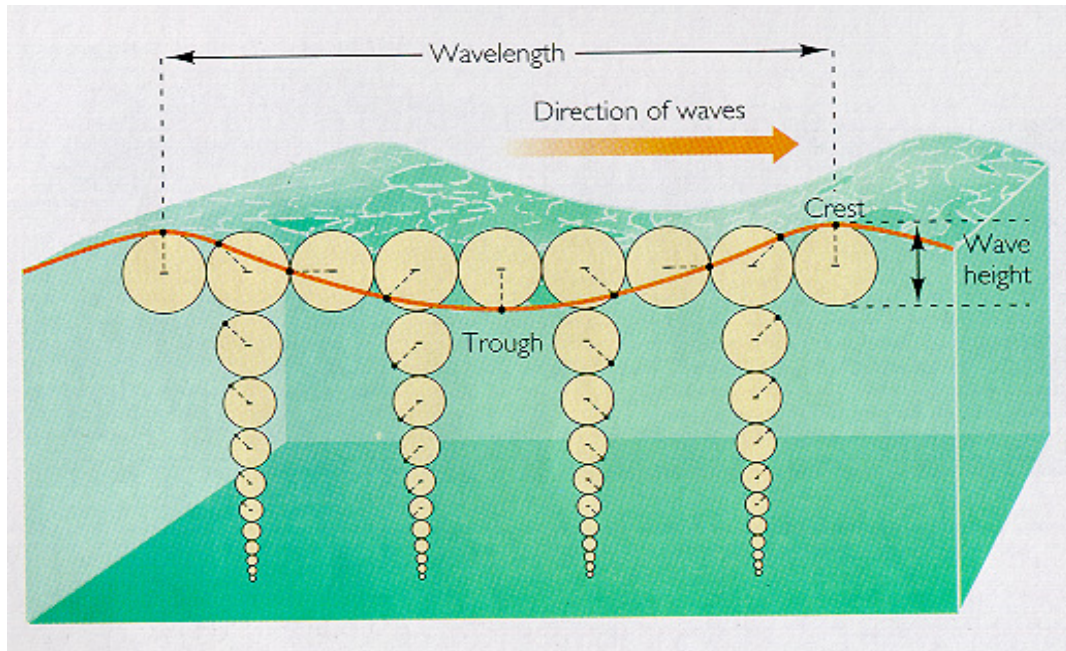


Figure 9: Illustration of wave motion (Lohmann, 2013)

Forces on partly or fully submerged slender structures such as cylinder can be described with Morison's equation (Det Norske Veritas, 2013):

$$dF = dF_M + dF_D = C_M \rho \frac{D}{2} \ddot{x} dz + C_D \rho \frac{D}{2} |\dot{x}| \dot{x} dz \quad \text{Equation 9}$$

Where

- $dF$  is the horizontal force on an element with height of  $dz$
- $dF_M$  is the force from inertia or mass of water
- $dF_D$  is the force from drag or friction
- $C_M$  and  $C_D$  is the inertia and drag coefficients
- $\rho$  is the density of seawater in 15°C
- $D$  is the diameter of the cylinder
- $\dot{x}$  is the horizontal wave induced velocity of water
- $\ddot{x}$  is the horizontal wave induced acceleration of water

The first part of Morison's equation is the force from the inertia the second part of the equation is the drag force. Morison's equation is applicable when the wavelength is larger than five times the diameter of the cylinder. This holds for all the wavelengths in the experiment and Morison's equation can be applied in all load cases.

The Morison equation requires that the flow acceleration is uniform or close to uniform around the body. Morison's equation is only valid when the dimension of the structure is small relative to the wavelength, i.e. when  $D < 0.2\lambda$ . The integrated version of Morison's equation given



here is only valid for non-breaking waves. (Det Norske Veritas, 2013).

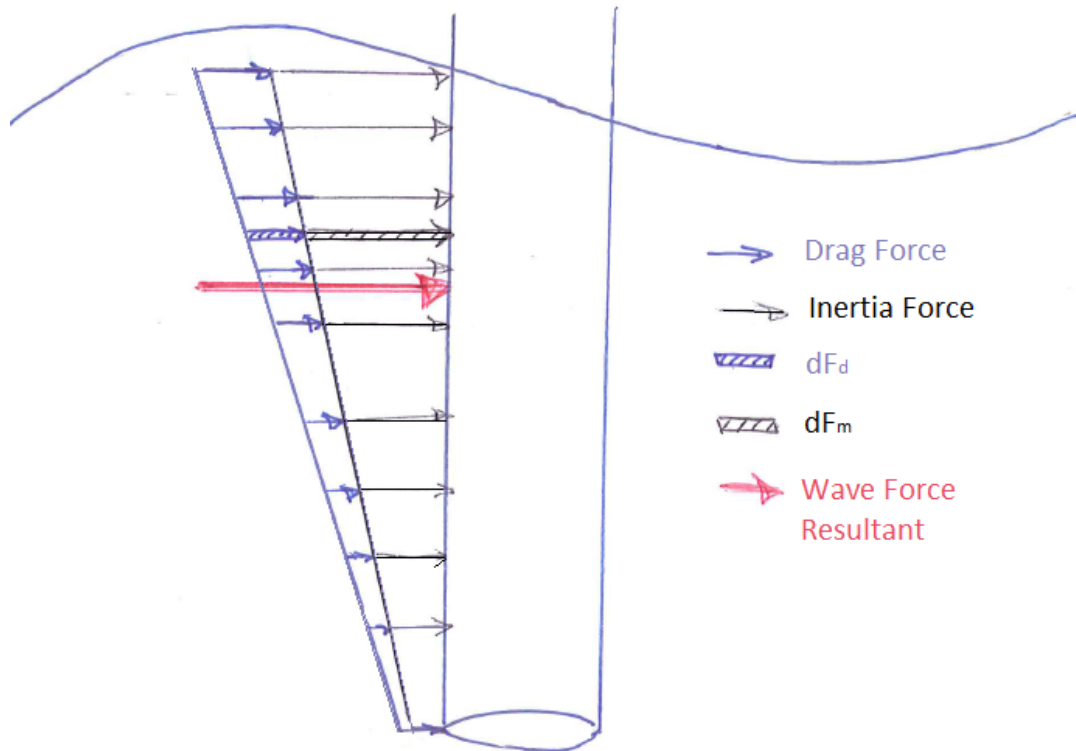


Figure 10: Illustration of horizontal drag and inertia wave forces

### 2.3 Drag coefficients and inertia coefficients

The Reynolds number and Keulegan Carpenter number is required to find the correct drag coefficient for the simulation. The Reynolds number offers a measure of the ratio between inertial forces to viscous forces and quantifies the relative importance between these two types of forces. (Reynolds, 1883)

Reynolds number  $Re$ :

$$Re = \frac{U_{Max}D}{\nu} \quad \text{Equation 10}$$

Where

- $U_{Max}$  is the maximal horizontal velocity at of a wave particle
- $D$  is the diameter of the cylinder submerged in the fluid.
- $\nu$  is the kinematic viscosity

The Keulegan Carpenter number (KC) describes the relative importance of drag forces on an object over inertia forces. It is a measure of the ratio between the distance moved by a water particle between its extreme positions in oscillating flow and the diameter of the tower. The inertia dominates for small KC while for large numbers, the drag forces are more important. (Keulegan & Patterson, 1940)

The Keulegan-carpenter number

$$KC = \frac{U_{Max}T_i}{D} \quad \text{Equation 11}$$

Where

- $T_i$  is the intrinsic period of the waves

Table 7: Wave and sea parameters

		from	to	
Period	T	2.8	0.95	sec
Kinematic Viscosity (Det Norske Veritas RP-C205, 2010)		1.19E-06	1.19E-06	m <sup>2</sup> /s
H/T <sup>2</sup>		0.0166	0.315	m/s <sup>2</sup>
wavelength	$\lambda$	12.24	1.41	m
Wave number	k	1.24	4.46	
water density	$\rho$	1025	1025	kg/m <sup>3</sup>
Diameter of TLB S cylinder	D	0.25	0.25	m
Height of waves	H	0.50	0.13	m
length of TLB S cylinder under water	z	-1.09	-1.09	m

Table 8: Reynolds number and Keulegan Carpenter number

	max	Min	
U max	0.87	0.43	m/s
Reynolds number Re	118000	90000	
Keulegan Carpenter number KC	6,28	1.63	

The Keulegan carpenter number is relatively small. Because the diameter of the tower is relatively small compared to the wavelength, the inertia forces are more important than the drag forces. For  $KC < 4$ , the values of  $C_m$  is larger than 2.0 (Sarpkaya & Isaacson, 1981). Sarpkaya does not say how much larger  $C_m$  values is than 2.0. Since DNV recommends to use  $C_m = 2.0$  this thesis will comply to that recommendation (Det Norske Veritas RP-C205, 2010).

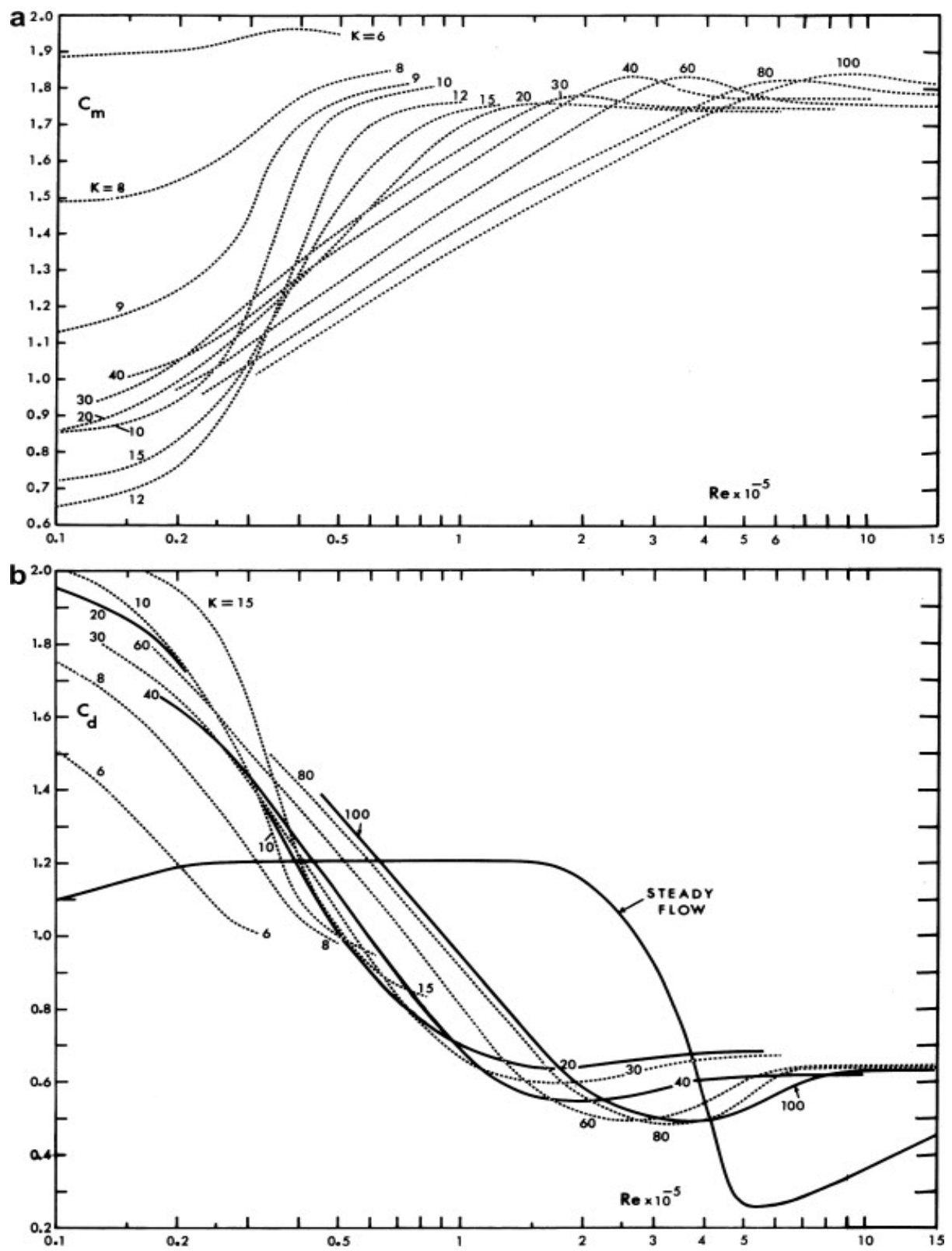


Figure 11: The combined influence of KC and Reynolds numbers on inertia coefficient and drag coefficient (Sarpkaya & Isaacson, 1981)

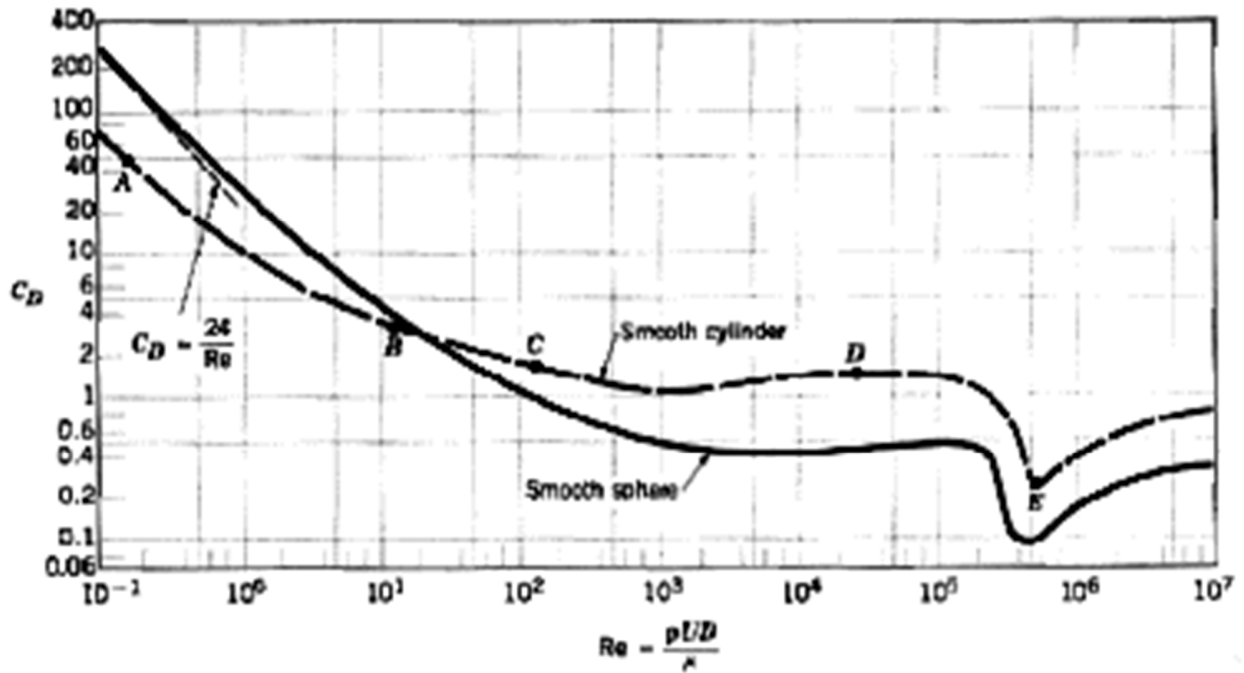


Figure 12: Drag coefficients for cylinder and sphere (Smits, 2013)

Figure 12 says that the drag coefficient is approx. 1.5 for Reynolds numbers between 20 000 and 300 000. It is only possible to input a scalar value for the drag coefficient. It is therefore convenient that drag coefficient is 1.5 for almost the whole range of Reynolds number in the experiment.

Different values for  $C_d$  within the ranges that the theory allows (Sarpkaya & Isaacson, 1981) has been tried in the simulations to seek out the one that gives better results.

Figure 11 shows that the drag coefficient should perhaps have been set lower. The figure does not show values for the range of Keulegan Carpenter number in the experiment. For Reynolds number around 100 000 and  $KC < 6$  it is assumed that the drag coefficient should be less than 1.0. The inertia coefficient is also uncertain since the  $C_m$  chart stops at 2.0.

Taking the recommendations of DNV, Sarpkaya and Isaacson and Smits (Det Norske Veritas, 2010) (Sarpkaya & Isaacson, 1981) (Smits, 2013) in consideration it is decided to use  $C_d = 1.3$  and  $C_m = 2.0$  for all prototypes as initial values. These numbers are an approximate mean value of the recommended drag coefficients and inertia coefficients. A parameter study will be conducted for each simulation model in the calibration chapter in attempt to find the exact coefficients.

### 3 Experiment and prototype description

The following chapter describes how the experiment was set up, conducted and how the results were obtained.

#### 3.1 The experiment set up

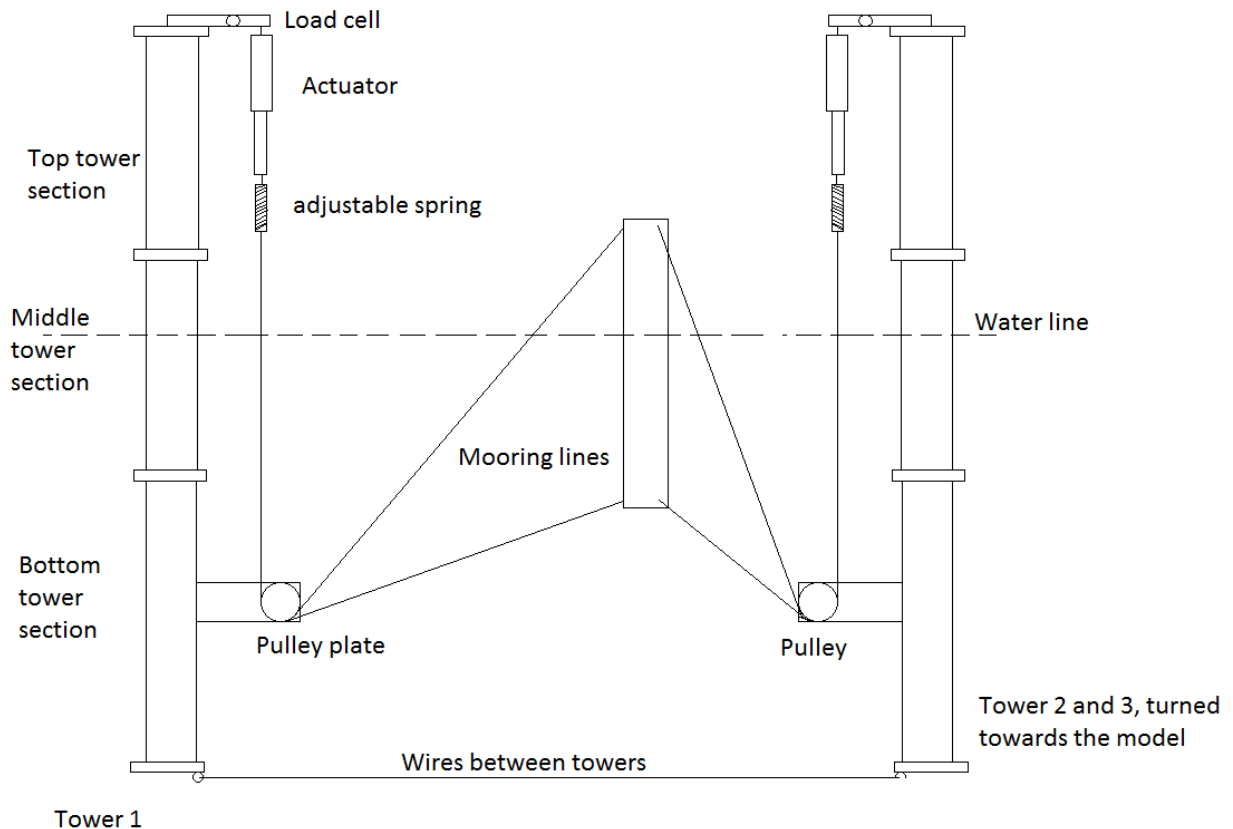


Figure 13: Illustration of experiment set up

The experiment is set up with the prototypes in the center moored down by six line, three upper lines and three lower lines. One of the lower lines and one of the upper lines is connected to each tower as Figure 13 illustrates.

#### 3.2 The towers

The towers were assembled from three sections as shown in Figure 23.. The middle section was in the waterline. The load cells, actuators, springs and mooring lines was connected in pairs at the top of each upper section. The three towers was placed with equal distance between them, as an equilateral triangle. The prototypes were placed in the middle, with equal distance to each tower. The three towers were placed in a triangle and connected in the bottom sections with three wires of a known length. The wires were fastened at the same point to have control over the distance between the towers. The pulley plate

was mounted to the lower part of the tower. The Load cells were attached at the top of three identical towers. Two load cells was placed at each tower, one for the bottom line, and one for the top line.

Illustration of experiment

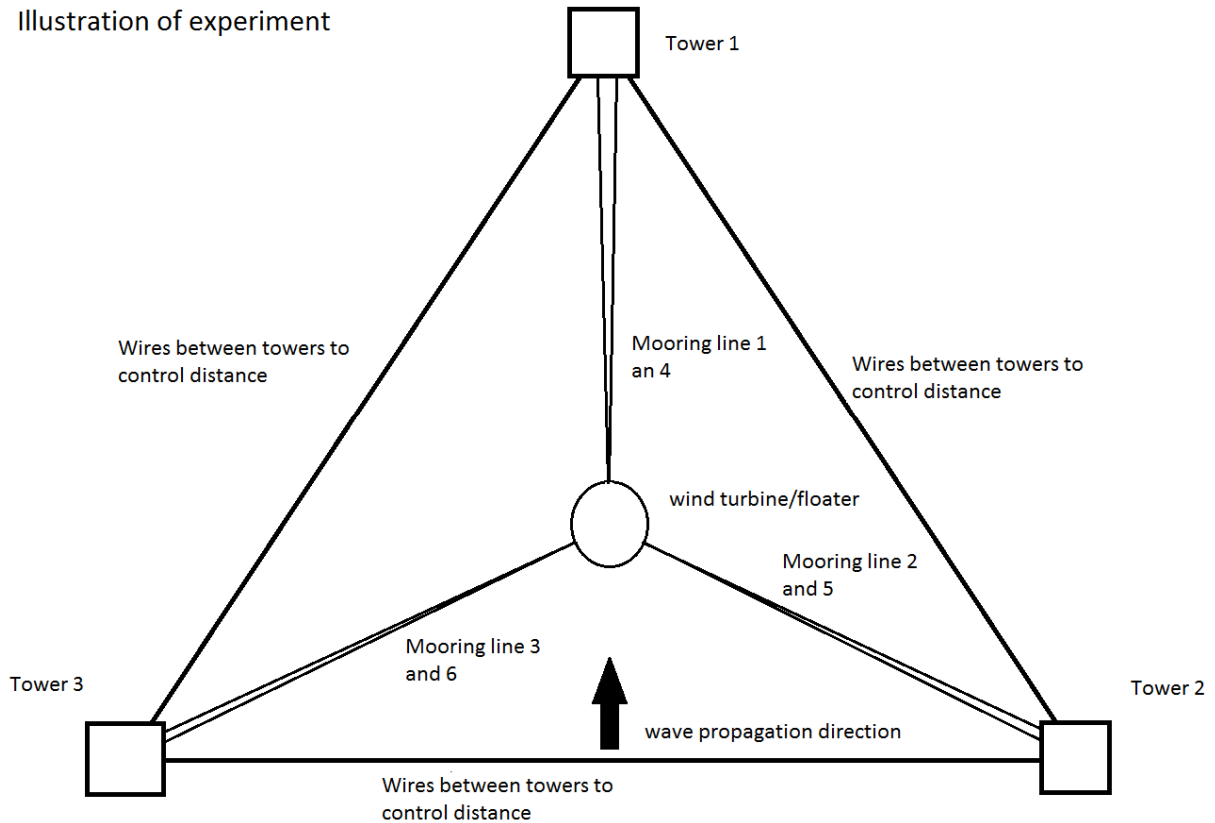


Figure 14: Bird view of the experiment setup

Table 9: Placing of towers

Measurement	Value	Unit
Distance between towers	6.642	m
Horizontal distance from tower to center of prototypes	3.835	m
depth of anchor point (pulley)	-1.868	m

The waterline in the center of the prototype is the origin of the coordinate system and the towers are placed around with equal radius to the pulley plate of 3.835 meters. The position of the prototype was calibrated with the knowledge of the wanted geometry for the experiment. If the prototype was placed correctly in the middle, the force in all the upper lines should be equal and at the same time the force should be equal in the bottom lines. This requires that the upper lines have the same stiffness and same for the lower lines. If the prototype is placed wrongly, it is not possible that the forces in the lines are equal. The mooring depth of the prototype was regulated by placing the mark of the water line on the prototype the actual water line

The anchor radius is the distance measured from the point the mooring lines were free of the pulleys to the center of the coordinate system. The pulleys on each pulley plate have a distance of 60 mm between them.

The stiffness of the springs were measured and adjusted separately before each prototype was launched. This was to tune the stiffness to suit the buoyancy of each prototype. To find the total stiffness of the mooring line, the stiffness of the mooring line between the spring and the prototype and the adjustable spring must be taken into account. The total stiffness of each spring + mooring wire will be used as stiffness for the simulated mooring lines.

Table 10: Anchor point coordinates

	X	Y	Z
Anchor point 1, lower line, tower 1	3.835	-0.030	-1.868
Anchor point 2, lower line, tower 2	-1.891	3.336	-1.868
Anchor point 3, lower line, tower 3	-1.943	-3.306	-1.868
Anchor point 4, lower line, tower 1	3.835	0.030	-1.868
Anchor point 5, lower line, tower 2	-1.943	3.306	-1.868
Anchor point 6, lower line, tower 3	-1.891	-3.336	-1.868

Table 11: Stiffness of anchor lines

Line nr:	TLB S	TLB B	TLB X3	Unit
Stiffness mooring line 1 (k1)	2899	2899	2494	N/m
Stiffness mooring line 2 (k2)	2842	2842	2479	N/m
Stiffness mooring line 3 (k3)	2870	2870	2425	N/m
Stiffness mooring line 4 (k4)	2341	2341	2312	N/m
Stiffness mooring line 5 (k5)	2320	2320	2325	N/m
Stiffness mooring line 6 (k6)	2299	2299	2234	N/m

### 3.3 Test facility: IFREMER wave tank:

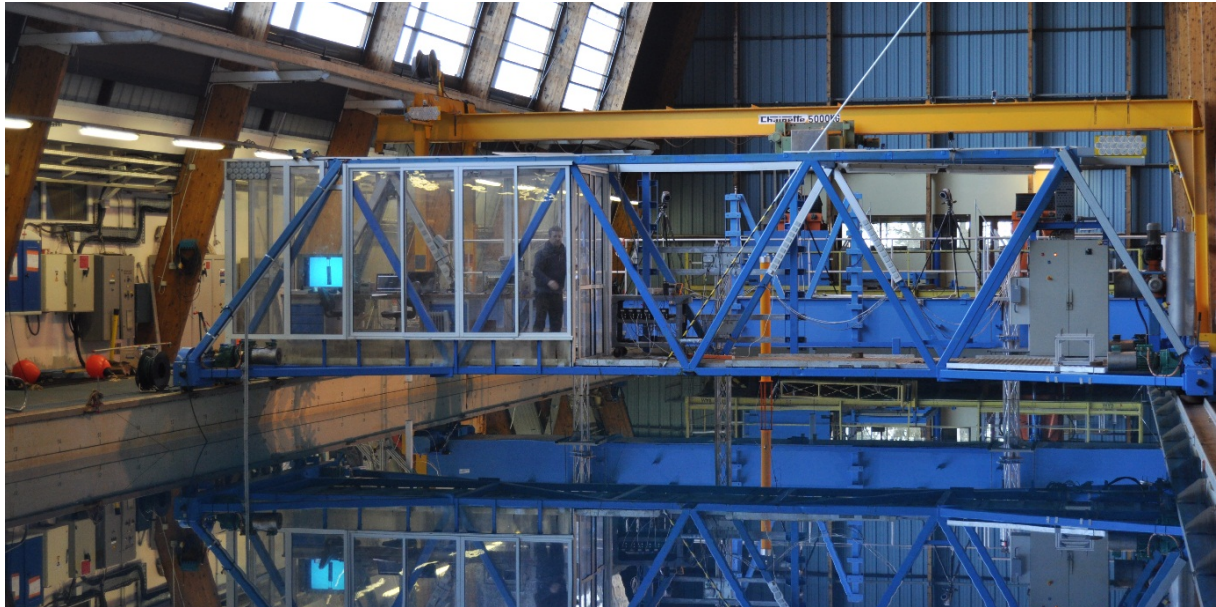


Figure 15: Picture of the test site, the wave tank at IFREMER

The experiment was carried out in the IFREMER Deep Sea Water Wave Tank in Brest, France. IFREMER is a French research organization for oceanographic studies founded by the French government in 1984. The IFREMER wave tank is a 50 m long basin with seawater for marine testing. 37.5 m of the basin is 10 m deep, and 12 m of the basin is 20 m deep. It is possible to generate unidirectional regular or irregular waves in the tank. Maximum wave height is 0.5 m with periods from 0.8 to 3.0 sec. The tank is equipped with 3-D aerial and submarine optical tracking, with six DOF motion tracking. (IFREMER, 2013) They have sea surface elevation measurement equipment and aerial and submarine video recording possibilities.

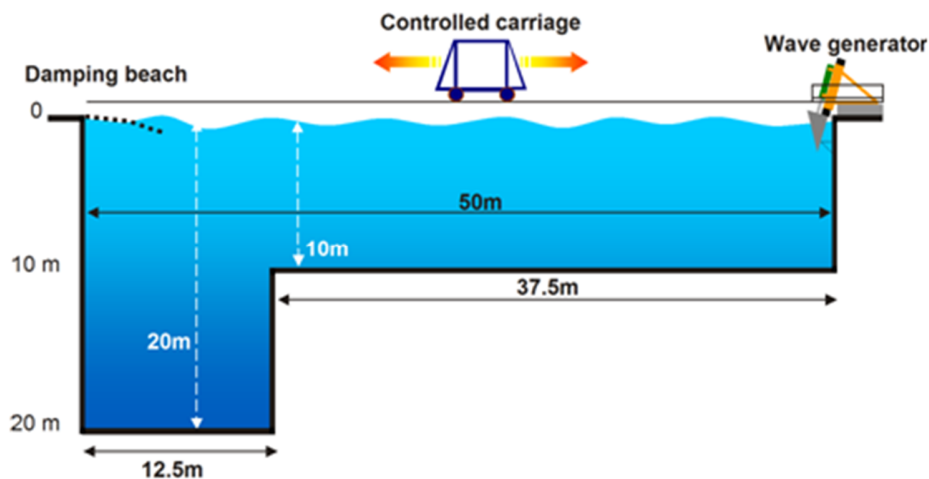


Figure 16: IFREMER Deep seawater tank. (IFREMER, 2013)



### 3.4 The components of the experiment

The components in the experiments are:

- Three scaled prototypes.
- Three towers standing in a circle with 120 degrees between them
- Actuators to move the prototypes into the exact position and raise and lower the prototype in the water
- Adjustable springs to obtain the right stiffness in the mooring line system
- 6 wires mooring the prototypes to the springs
- Measuring equipment (sensors and computers for recording of results)

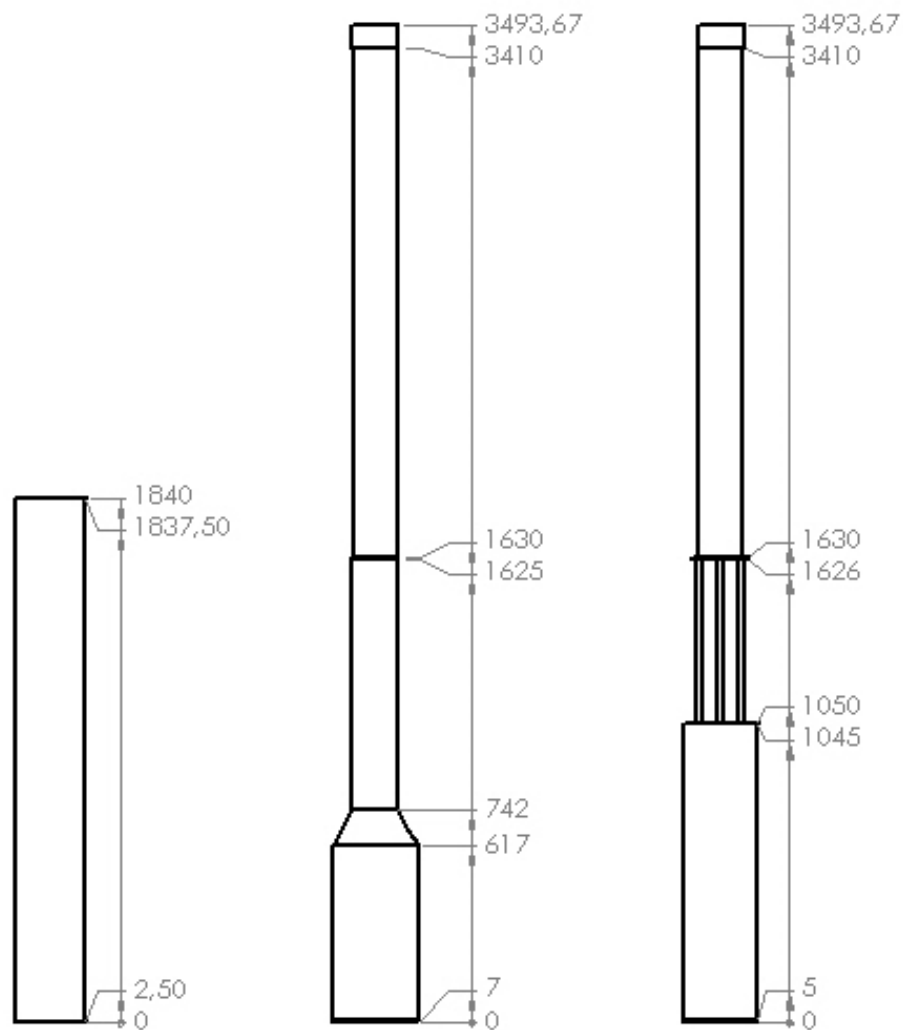


Figure 17: Illustration of prototypes with height in mm

### 3.5 The three experimental prototypes

Three prototypes has been made to do the experiment; the TLB S, The TLB B and TLB X3. The TLB S is a very simplified prototype that a plastic pipe with lids and anchoring points on it. The TLB S is used for reference. This prototype should be easy to model on a computer without losing any details. The TLB S will also make it possible to single out errors that are prototype specific and not systematical for the whole experiment.



Figure 18: Photography of the prototypes (from left: Tower, TLB S, TLB B and TLB X3)

The TLB B and X3 are two different variations of the floater section of the TLB. The floater is the lower section of the wind turbine that provides the buoyancy. The floaters of TLB B and TLB X3 are designed to have a smaller area going through the water line. These two prototypes are imitations of a real wind turbine. These are designed to let waves pass easier and put less stress on the turbine.

The yellow tower to the left in Figure 18 is the tower placed on top of TLB B and TLB X3 with an aluminum weight to imitate a full-scale wind turbine with a nacelle. The same tower is used on both TLB B and TLB X3.

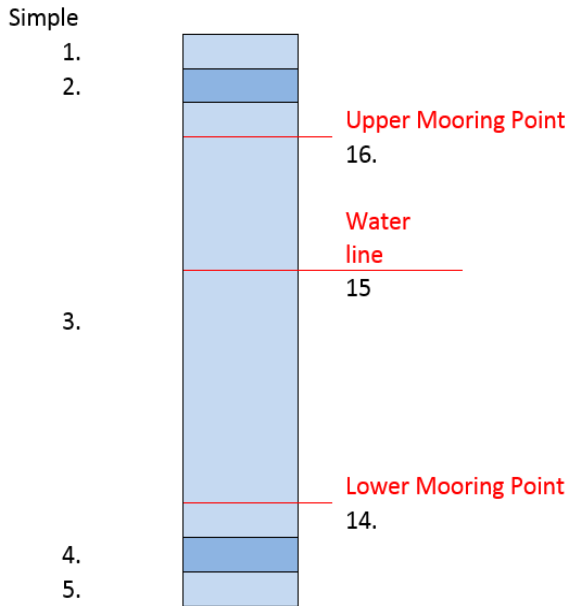
The red-black line on the simple and the yellow-black line on TLB B and TLB X3 is the water line.

The ears on the prototypes are the mooring points. There are three low mooring points on each prototype and three upper mooring points (for TLB B and TLB X3 the upper mooring points are on the tower). The mooring points are placed with 120-degree distance around the pipe.

### 3.6 Measurements and properties of the prototypes:

The measurements of the prototypes under are given as used in the simulation. The geometry were measured several times, both when the prototypes were in parts and as fully assembled. The total weight was measured fully assembled, while the part weights were weighed in parts. The full section properties as used in the simulation is found in the appendix

#### 3.6.1 TLB S



The parts of the TLB S

1. The top lid (Polycarbonate)
2. The top lid inside the top of the pipe. (Polycarbonate)
3. The main pipe (Polycarbonate)
4. The bottom lid inside the bottom of lower pipe/floater pipe. (Polycarbonate)
5. The bottom lid. (Polycarbonate)

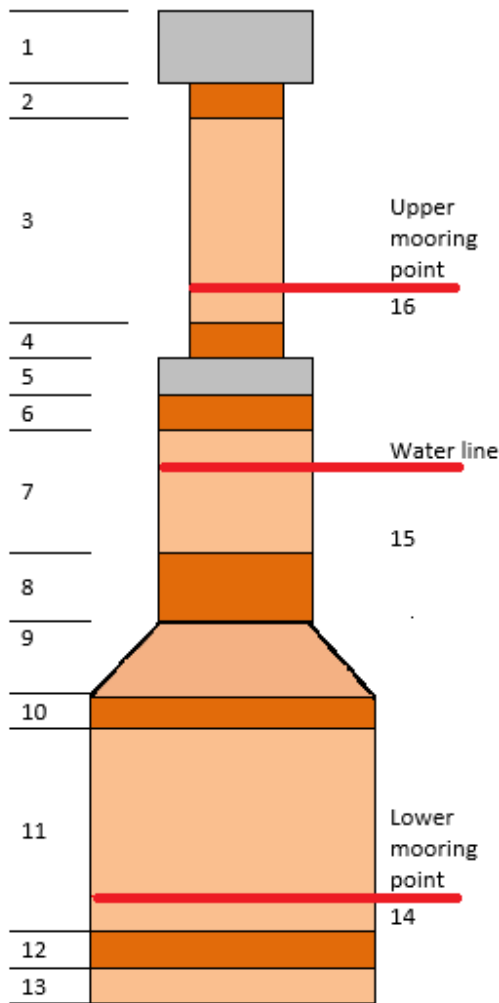
Figure 19: Sections of the simple prototype

Table 12: The TLB S with geometry.

Section	H [m]	z [m]	D outer [m]	Thickness [m]	d (inner) [m]	Vol. [m <sup>3</sup> ]	Mass [kg]	E [N/m <sup>2</sup> ]
1	0.0025	0.7170	0.25	0.1200	0.001	1.47E-04	0.216	1.20E+09
2	0.0025	0.7145	0.25	0.1200	0.001	2.45E-04	0.226	1.20E+09
3	1.8300	0.7120	0.2500	0.0050	0.240	7.02E-03	7.978	1.20E+09
4	0.0025	-1.1180	0.25	0.1200	0.001	2.45E-04	0.229	1.20E+09
5	0.0025	-1.1205	0.25	0.1200	0.001	1.47E-04	0.218	1.20E+09
14	0.04		0.31				0.090	
15	1.094							
16	1.811		0.31				0.090	
Total weight in parts							9.047	
Total measured weight at IFREMER							9.074	

*H = height of pipe section, z = distance from waterline, D outer = Outer diameter of pipe section, Thickness = wall thickness of pipe section, d (inner) = Inner diameter of pipe section, volume = volume of material in section, mass = mass of section, E = young's modulus of section*

### 3.6.2 TLB B



#### The parts of the TLB B

1. The top of the Nacelle. (aluminum)
2. The bottom of the nacelle and the top of the upper pipe. (aluminum)
3. The upper pipe (Polycarbonate)
4. The bottom of the upper pipe and top of upper transition piece. (aluminum)
5. The upper transition piece. (Aluminum)
6. The upper transition piece inside the mid pipe. (Aluminum)
7. The mid pipe (Polyvinylchloride PVC)
8. The tapered transition piece inside the mid pipe (aluminum)
9. The Tapered transition piece (aluminum)
10. The tapered transition piece inside the lower pipe (aluminum)
11. The lower pipe. (aluminum)
12. The bottom lid inside the bottom of lower pipe/floater pipe. (aluminum)
13. The bottom lid. (aluminum)

Figure 20::Illustration of section in the TLB B

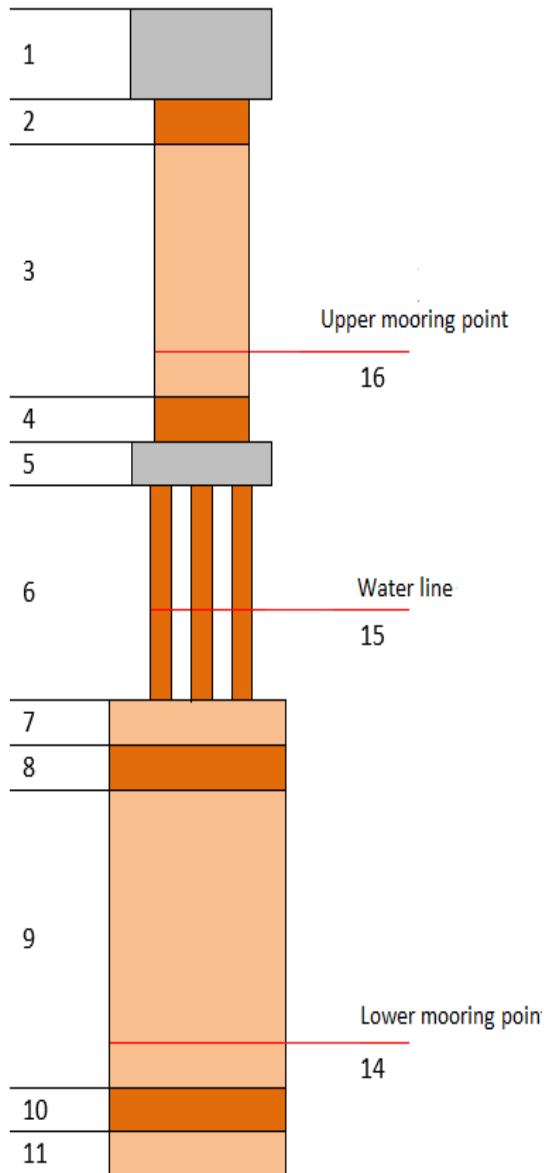
The TLB B is the first of two realistic prototypes in the experiment. It is recognizable by its tapered section and the large volume in the lower section of the floater. The lower transition piece is a tapered section that allows a large diameter bottom part of the floater and a smaller diameter pipe in the waterline. This is to lower the horizontal force from waves on the prototype, but have enough buoyancy from the lower part of the floater. The next transition piece is above water to connect the tower to the floater.

Table 13: Geometry of TLB B

section	H [m]	z [m]	D outer [m]	Thickness [m]	d [m]	Volume [m3]	Mass [kg]	E [N/m2]
1	0.084	2.284	0.163	0.051	0.060	1.50E-03	4.680	7.00E+10
2	0.020	2.200	0.150	0.045	0.060	2.97E-04	0.830	7.00E+10
3	1.780	2.180	0.150	0.004	0.142	3.27E-03	3.920	1.20E+09
4	0.020	0.400	0.150	0.009	0.132	7.97E-05	0.170	7.00E+10
5	0.005	0.380	0.160	0.017	0.126	3.82E-05	0.120	7.00E+10
6	0.020	0.375	0.160	0.010	0.140	9.42E-05	0.160	7.00E+10
7	0.843	0.355	0.160	0.005	0.150	2.05E-03	3.170	3.00E+09
8	0.020	-0.488	0.160	0.008	0.144	7.64E-05	0.150	7.00E+10
9	0.125	-0.508	NA	0.004	NA	4.14E-05	1.200	7.00E+10
10	0.018	-0.633	0.298	0.006	0.287	9.11E-05	0.270	7.00E+10
11	0.582	-0.651	0.298	0.003	0.293	1.35E-03	3.880	7.00E+10
12	0.010	-1.233	0.298	0.006	0.287	5.06E-05	0.100	7.00E+10
13	0.007	-1.243	0.297	0.119	0.060	4.65E-04	0.750	7.00E+10
	3.534	-1.250						
14	0.033		0.360				0.126	
15	1.25							
16	1.896		0.210				0.066	
Total masses:				Nacelle			5.513	
				Tower			4.162	
				Floater			9.931	
				Total			19.606	19.606

### 3.6.3 TLB X3

The consists of four main section: The lower part of the floater, the three column section, the tower and the nacelle (equal to the tower and nacelle of TLB B). The signature feature of TLB X3 is the three columns in the section breaking through water. That results in a smaller area perpendicular to the waves. The lower section of the X3 has a smaller diameter than the lower section of the TLB B, but the lower section of X3 is taller. They have approximately the same area perpendicular to the wave propagation when they stand at their initial position.



The parts of the TLB X3

1. The top of the Nacelle (Aluminum)
2. The bottom of the nacelle and the top of the upper pipe (Aluminum)
3. The upper pipe (Polycarbonate)
4. The bottom of the upper pipe and top of upper transition piece (Aluminum)
5. The upper transition piece. Weight includes the bolts to fasten the X3 rods (Aluminum)
6. The three X3 columns (Aluminum)
7. The lower transition piece/lid with bolts to X3 columns (Aluminum)
8. The lower transition piece inside the top of lower pipe/floater pipe (Aluminum)
9. The pipe of the floater (Aluminum)
10. The bottom lid inside the bottom of lower pipe/floater pipe (Aluminum)
11. The bottom lid (Aluminum)

Figure 21: Sections of the TLB X3

Table 14: Geometry of TLB X3

Section	H [m]	z [m]	D outer [m]	Thickness [m]	d inner [m]	Volume [m <sup>3</sup> ]	Mass [kg]	E [N/m <sup>2</sup> ]
1	0.084	2.298	0.163	0.076	0.010	1.75E-03	4.681	7.00E+10
2	0.020	2.214	0.150	0.070	0.010	3.52E-04	0.832	7.00E+10
3	1.780	2.194	0.150	0.004	0.142	3.27E-03	3.922	1.20E+09
4	0.020	0.414	0.150	0.013	0.124	1.12E-04	0.259	7.00E+10
5	0.004	0.394	0.200	0.038	0.124	7.74E-05	0.594	7.00E+10
6	0.576	0.390	0.022	0.003	0.016	3.09E-04	0.837	7.00E+10
7	0.005	-0.186	0.261	0.125	0.010	2.67E-04	1.021	7.00E+10
8	0.008	-0.191	0.261	0.005	0.252	2.90E-05	0.095	7.00E+10
9	1.040	-0.199	0.261	0.003	0.256	2.11E-03	5.960	7.00E+10
10	0.008	-1.239	0.261	0.005	0.252	2.90E-05	0.087	7.00E+10
11	0.005	-1.247	0.261	0.125	0.010	2.67E-04	0.577	7.00E+10
	3.550	-1.252						
14	0.035						0.066	
15	1.252							
16	1.897		0.210				0.066	
					Mass of Prototype:	Nacelle	5.510	
						Tower	4.250	
						Floater	9.240	
						Total	18.997	18.997

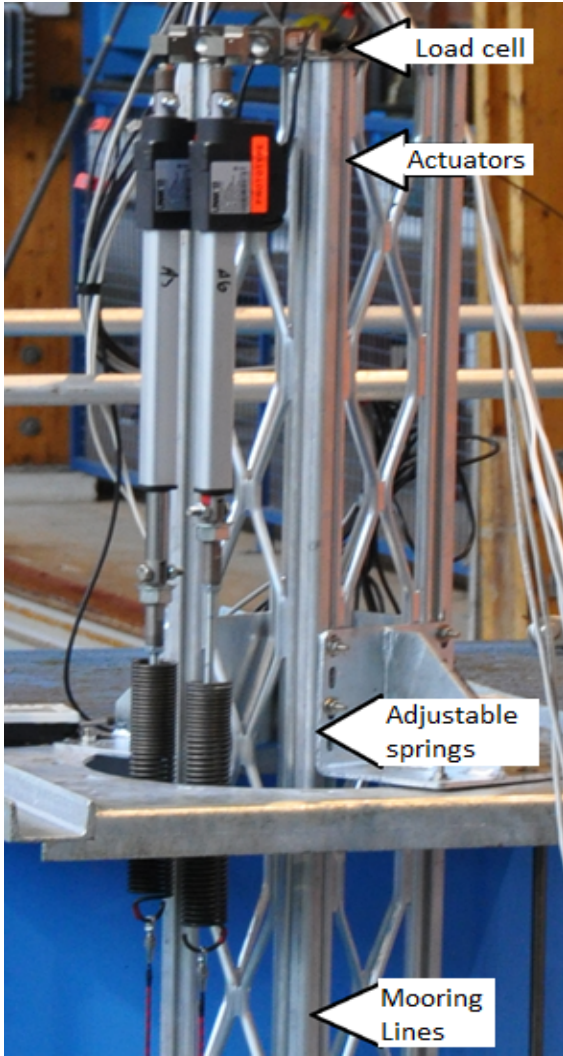


Figure 22: Setup of Tower, Load cell, Actuator, spring and mooring line

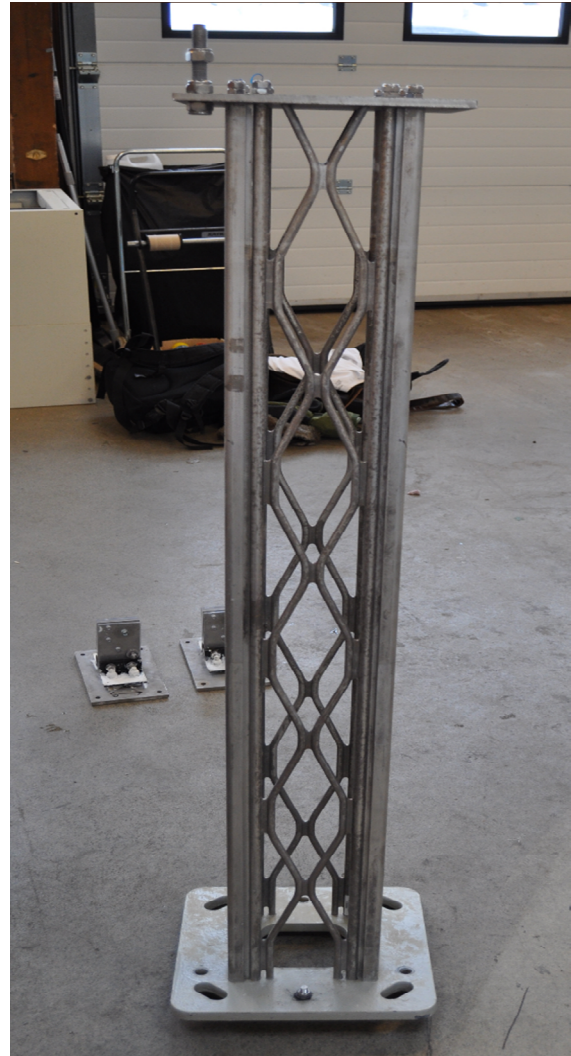


Figure 23: Tower section

### 3.7 Mooring line:

The mooring line was a 1 mm diameter steel wire. With Young's modulus of  $2.0 \times 10^5 \text{ N/mm}^2$

$$\varepsilon = \frac{\Delta l}{l} = \frac{F}{A \times E} = \frac{200 \text{ N}}{0.785 \times 2 \times 10^5} = 0.00159 \frac{\text{mm}}{\text{mm}} \quad \text{Equation 12}$$

The strain in the mooring line for the experiment is not of great importance since the adjustable springs make sure that the total stiffness of the mooring line system is according to the specifications.



### 3.8 Adjustable springs:



Figure 24: Adjustable spring

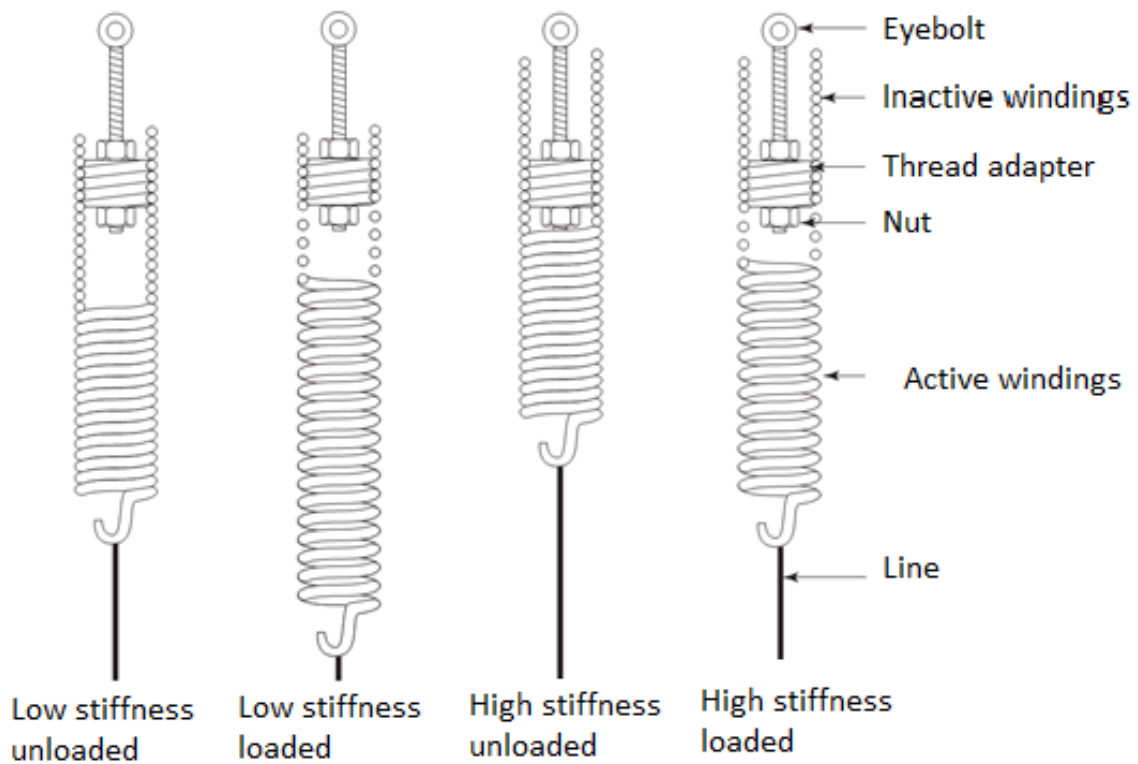


Figure 25: Illustration of adjustable springs (Spæren, 2013)

The adjustable springs were developed especially for this experiment. They can be adjusted by changing the number of active windings. The more windings, the lower spring constant. The springs have a designed capacity of 504 N with a safety factor of 2.

### 3.9 The pulley plates:

The pulley plates were modified in Brest, after friction problems. The pulley plate in Figure 26 is the modified version. The mooring point used in the simulations is where the mooring line leaves the pulley. This is the last place where the line is straight between the mooring point on the prototype, and the pulleys.

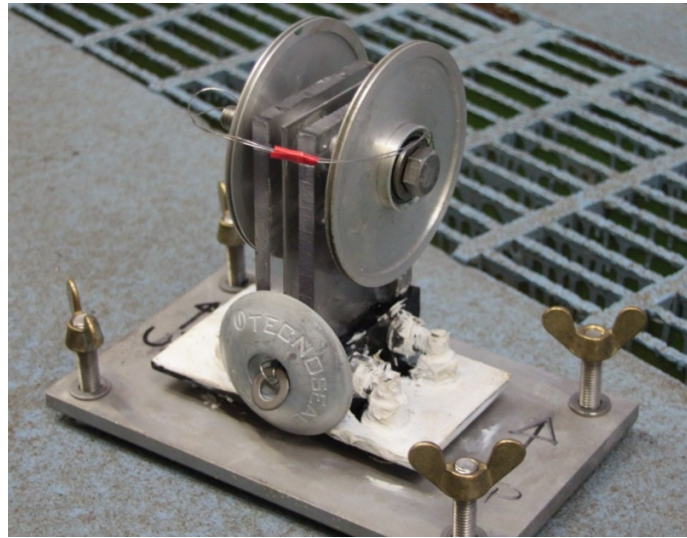


Figure 26: Pulley plates with the modified pulleys

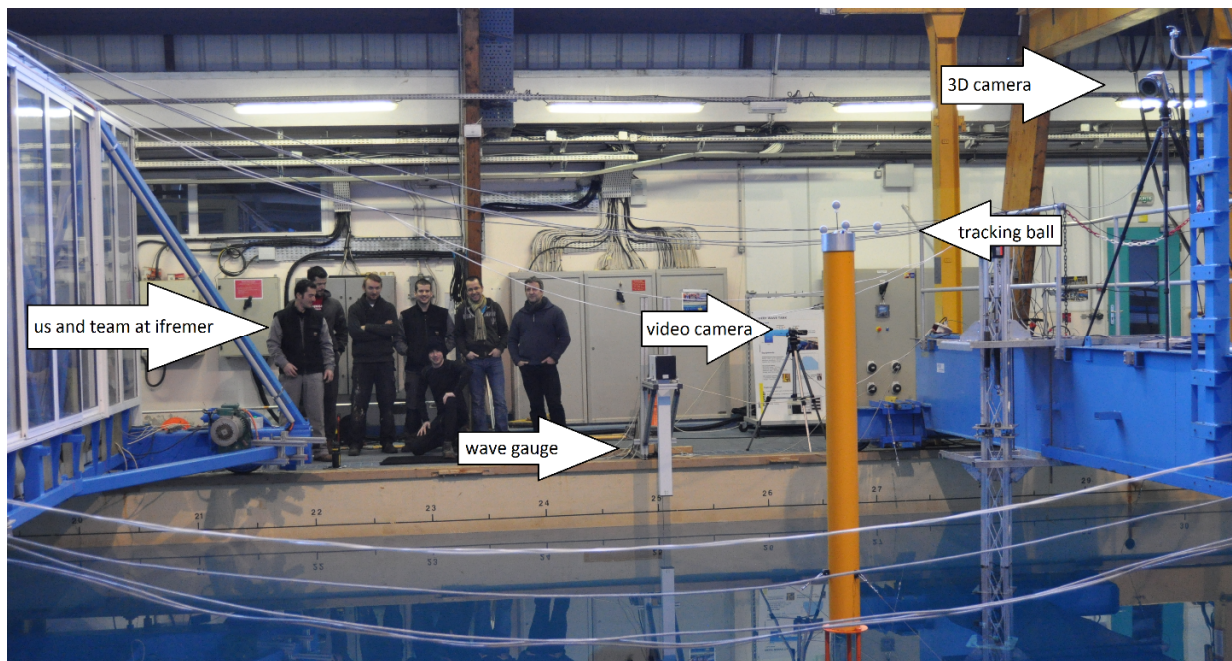


Figure 27: Illustration of 3D camera, tracking ball, video camera and wave gauge.

### 3.10 Measurement equipment

The measurement equipment consists of a load cell, a 3D tracking system and two wave gauges.

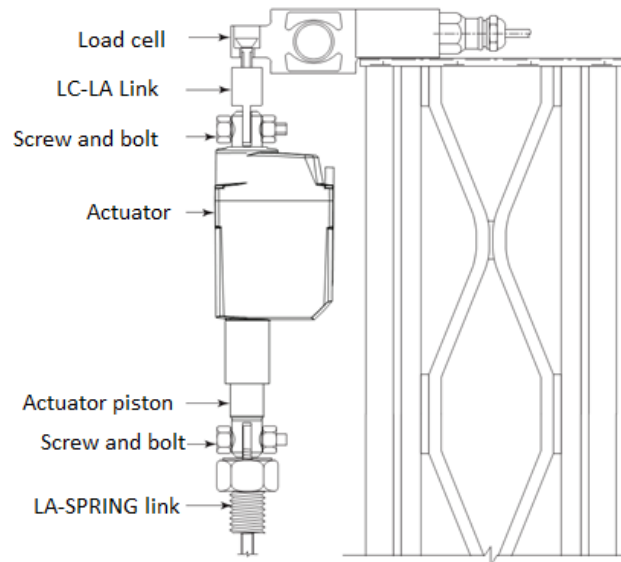


Figure 28: Illustration of load cell, actuator and spring setup (Spæren, 2013)

#### 3.10.1 Load cells

Six beam type load cells from Flintec sensor solution of the type SB6 were used to measure the loads in the lines at all times. The load cells have a designed capacity of 1 kN to reduce the risk of over load. (Spæren, 2013)

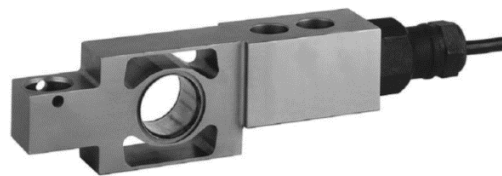


Figure 29: Beam type load cell (Flintec sensor solutions, 2013)

#### 3.10.2 Wave gauges

There were two wave sensor in the tank under the experiment. One were upstream, five meters right in front of the prototypes, and one were on the side of the prototype to measure the wave height.

IFREMÉR used mechanical wave gauges were with a sensor following the moves of the water line. The wave gauges was manufactured at IFREMÉR under the name ORCA. The data from the wave gauges was logged simultaneously with the load cell data and 3D tracking data.

### 3.10.3 Tracking system

The tracking system was chosen because it was available on the test site and familiar to the operators. They had a 3D tracking system to track motion in six degrees of freedom. The system consisted of a computer system, three cameras and a tracking ball on the prototype in addition to a reference tracking ball.

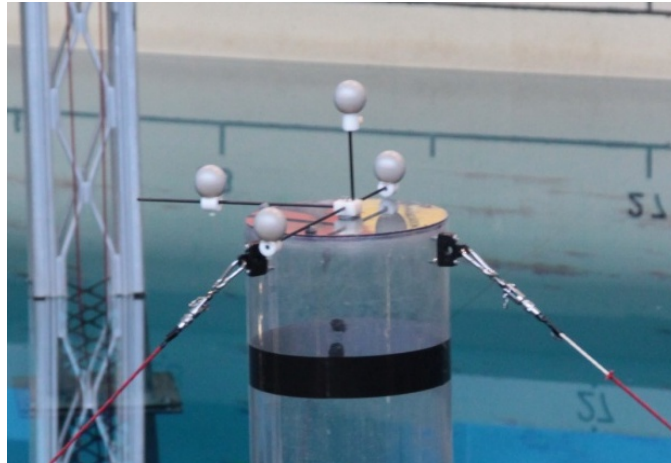


Figure 30: Tracking balls on top of prototype

### 3.10.4 LINAK Actuators

The position of the prototype was controlled through the mooring lines by six custom-made 12V linear actuators from LINAK. The actuators were also used to apply the right pretension in the lines. For this job, the LINAK LA23 linear actuators were chosen. It is an electrically controlled piston with internal positioning system with a returning position signal. (LINAK (a), 2013) The actuator had a stroke length of 300 mm (Spæren, 2013). Control unit TR-EM-288-S (LINAK (b), 2013) from LINAK was used to control the actuators and receive the position signal.



Figure 31: Linear actuator LA23 from LINAK

For further details on the experiment the reader is referred to the Master thesis Development and Construction of floating wind turbine prototypes and test rig for wave tank test by Anders Spæren. He has been responsible for the build and documentation of the build.

## 4 Experimental results

The following chapter presents an excerpt of the experimental results. It includes:

1. Eigen period results from the decay tests
2. Plots where the three prototypes are compared over similar load cases.
3. Plots where one prototypes is subject to load cases with similar wave height but different wave periods to see the response difference.
4. Frequency response plots

Video documentation, both above and under sea level has been recorded for each load case. This make it possible to go back and look for answers if something seems unclear in the data sets. Photos of the test rig, prototypes and experiment has been taken to further strengthen the documentation. A table with the load cases in the experiment can be found in the appendix.

### 4.1 Choice of time domain to present and analyze:

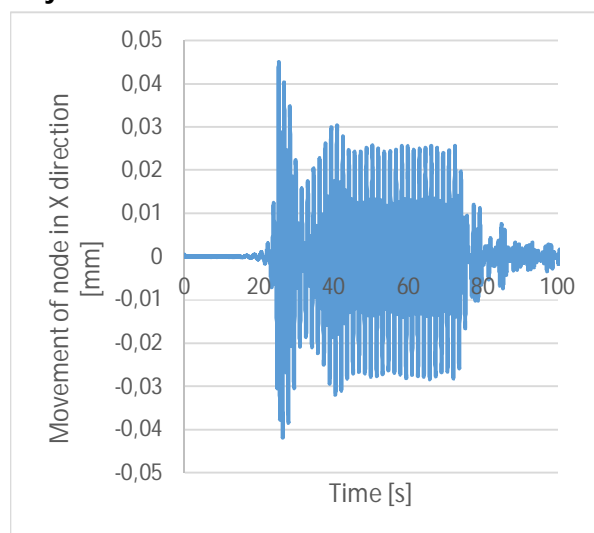
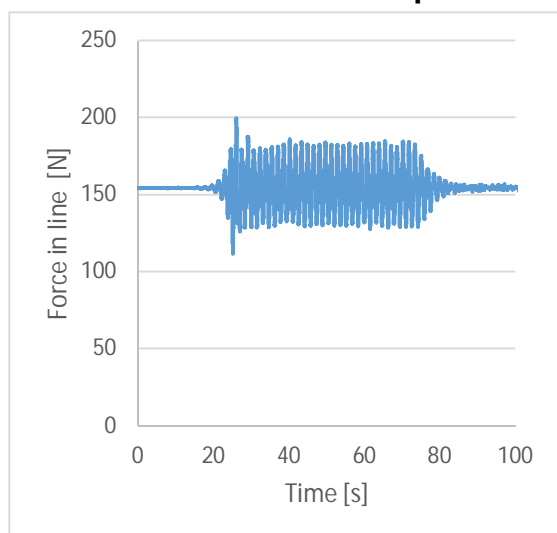


Figure 32: TLB B: Experiment 45, Force line 1: 0.3 m, 1.58 sec    Figure 33: TLB B: Experiment 45, UX movement: 0.3 m, 1.58 sec

Figure 32 and Figure 33 are from load case 45 with TLB B in the water. The wave period is 1.58 seconds and the wave height is 0.3 meters. The plots shows that it is not arbitrary what time domain that is chosen to analyze. The first time domain after the first wave hits the wind turbine is characterized by disturbance. When the effect of this first wave has decayed, the results stabilize, and it is possible to find reliable results in terms of periodical movements. From Figure 77 states that the pitch movement of TLB B decays fully after about 15 seconds. The analysis will not be meaningful before at least 15 seconds after the first wave meets the model. For all simulations and comparisons, it must be ensured that the disturbance from the first wave hitting the tower has decayed and the results are stable and reliable.

### 4.2 Eigen values

Three different types of decay tests were conducted in the wave tank for each prototype to find the eigen periods for the prototypes. These are the results:

Table 15: Eigen periods measured in the wave tank

	Unit	TLB S	TLB B	TLB X3
Pitch	Sec	0.25	0.74	0.74
Heave	Sec	0.35	0.58	0.56
Yaw	Sec	-	0.21	0.21

The Eigen periods are all over shorter for TLB S because it is a lighter prototype. The mass of the TLB S is closer to the mass center and rotational center. That gives it less mass moment than TLB S and TLB X3. There is no result from the yaw test of the TLB S because there was too much disturbance in the result of the decay test.

### 4.3 Plots of movement and forces over wave height

The experimental results can be plotted with time on the x-axis or with wave height on the x-axis. When the results are plotted with wave height on the x-axis it is possible to:

1. Compare load cases with the same wave height and period across prototypes
2. Compare wave periods with the same prototype and wave height

This provide an opportunity to analyze how the prototypes behave in different wave conditions with changing wave height and wave period. It also provides a good visualization of the variance in the results. The results displayed in this chapter are extruded from the best range in the dataset. That means the part with least variance in the parameters.

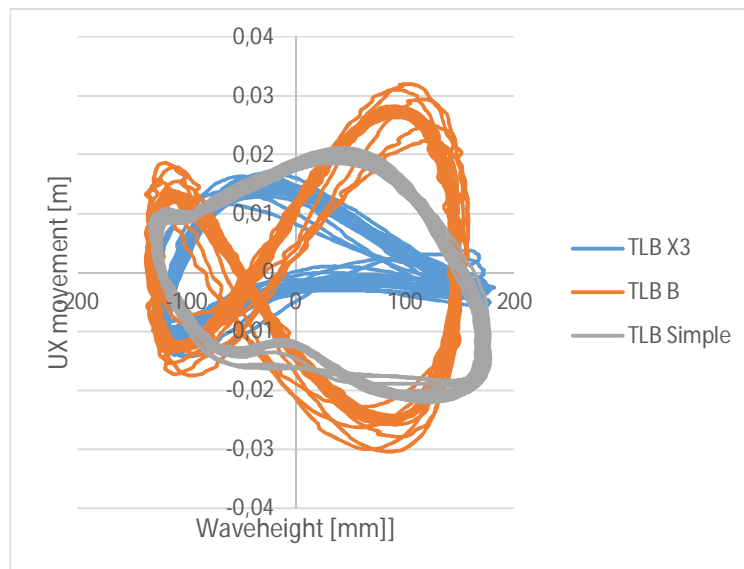


Figure 34: Comparing UX Movement: 0.3 meter and 1.58 sec period

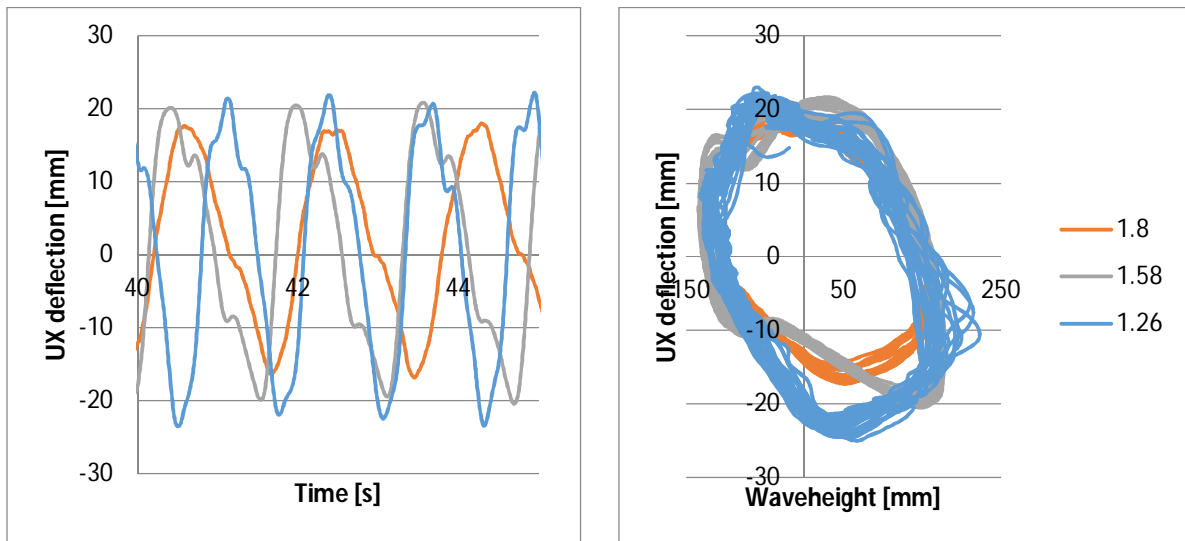
In the time domain from 50 to 60 seconds, the results are stable and periodical. It can be seen that there is something interfering with the sinusoidal curve, giving it two tops and two bottoms in each period. It is likely that this is the eigen periods. The time between the largest top and the smallest top is 0.72 seconds,

which corresponds to the Eigen period of Surge and Sway. It is unsure what this means since the rest of the period is 1.18, and it does not correspond to any of the eigen periods directly. The distance between the deep bottom and the shallow bottom is 0.76 seconds. The distance between the shallow bottom and the deep bottom is 0.81. Neither of this corresponds to any of the eigen periods directly.

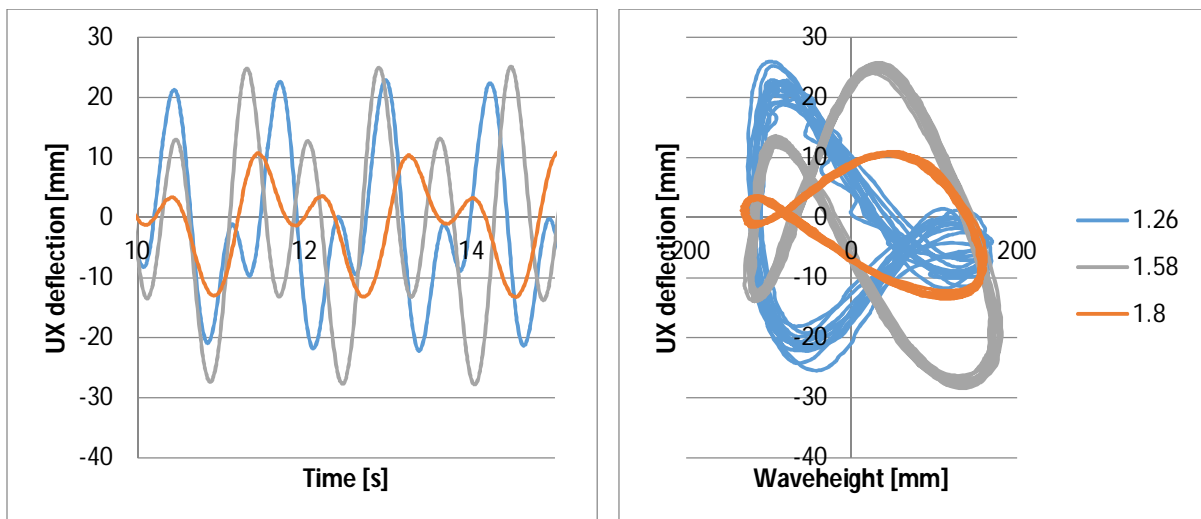
#### 4.4 Comparison of UX deflection on each prototype for different wave periods

Table 16 displays the UX deflection of TLB S on 0.3 m wave height for different wave periods. These plots shows how the different prototypes react to different wave periods.

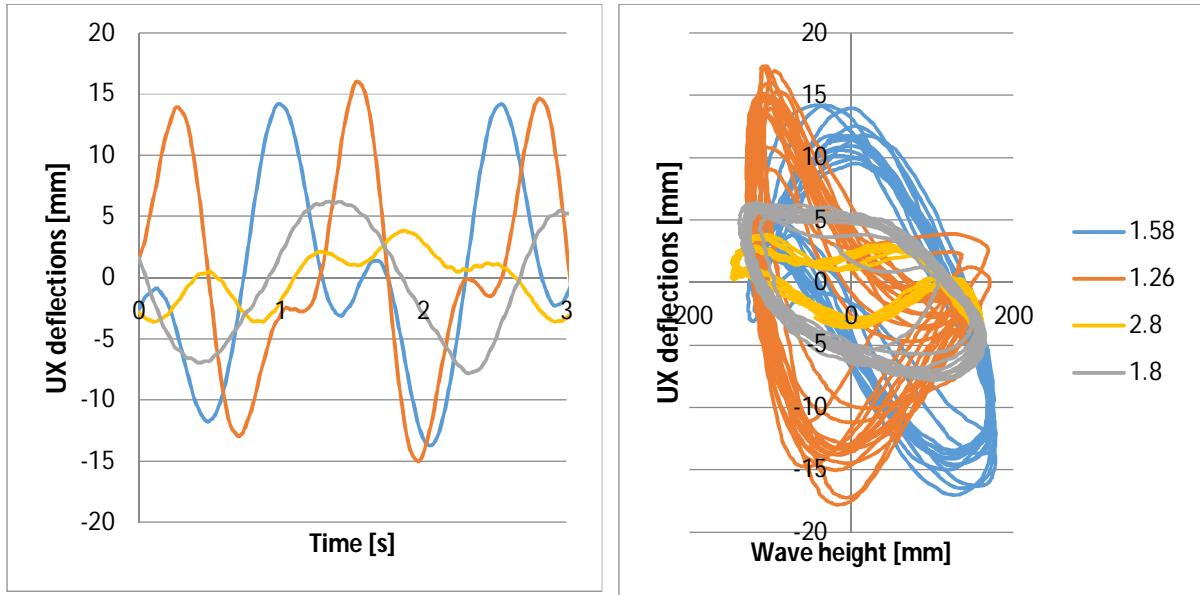
Table 16: UX deflections from all the simulations with 0.30 m waves



The TLB S shows a relatively similar behavior for the different wave periods. This is likely because it is very light and follows the wave movement easily even in short wave periods.



The TLB B is sensitive to the wave period. Shorter wave periods causes larger movement in the x direction. This is likely caused by the eigen period interfering since the eigen period in pitch for the TLB B is 0.74. The double of the eigen period is 1.48 seconds and that is very close to the spectrum of wave periods in these results. The results from 1.8 second period show very little variance, while the results from the 1.26 second period show more variance.



The TLB X3 shows a lot of variance in results for the 1.26 sec and 1.58 sec wave case. It seems like the TLB X3 is more sensitive to variations in the wave height for the 1.58 and 1.26 sec wave cases. These are cases close to the double of the pitch eigen period for TLB X3. The 1.8 and 2.8 second wave cases shows a movement with little variance, but there are some double tops in the 2.8 wave case. The little movement in the long period indicates that the X3 is relatively insensitive to horizontal forces as long as they are outside the range of eigen periods. The horizontal movement is smaller than for TLB B. This is likely because of the small area perpendicular towards the waves in the upper region of the floater (X3 columns)



## 4.5 Forces:

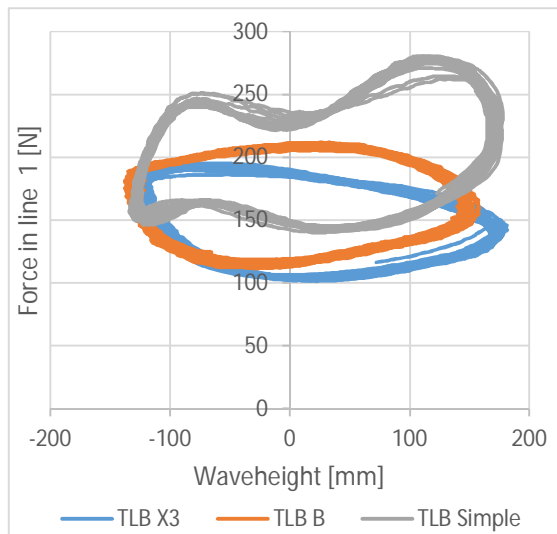


Figure 35: Forces in line 1: from all prototypes in 0.3 m waves and 1.58 sec period

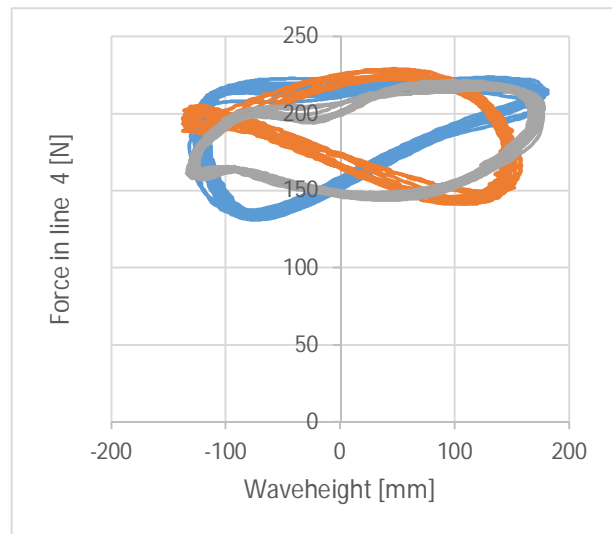


Figure 36: Forces in line 4 from all prototypes in 0.3 m waves and 1.58 sec period

Figure 35 and Figure 36 shows the forces in the lines for all of the prototypes. The amplitude of the force is between 50 and 100 N depending on which line that is studied. The forces in the lines are steadier and show less variation than the tracking results. The upper lines, line 4 -6, has a little more than half of the amplitude of the lower lines.

The forces in the bottom lines TLB S deviates from the bottom lines of the two other prototypes. This is likely to be caused by the large area it has perpendicular to the wave propagation direction around the water line. This causes the TLB S to be more affected by horizontal drag and inertia forces. The lower mooring lines on the TLB S is also 20 cm closer to the water line than on the TLB B and X3. This changes the angle of mooring line and they will take up more of the vertical forces that goes through the lower lines of TLB S. The same effect can also be seen in load cases with large waves and long wave period.

## 4.6 UZ movement from all the test cases:

Figure 37 to Figure 46 shows the plots of all the UZ movements in the load cases plotted against wave heights. The plots are sorted by prototypes, and separated by wave height in the load case. There are one series for each wave period.

#### 4.6.1 TLB Simple:

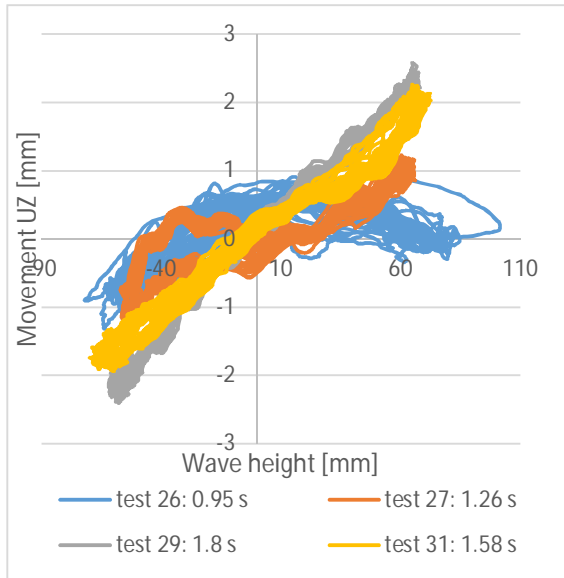


Figure 37: TLB Simple: 0.13 m waves

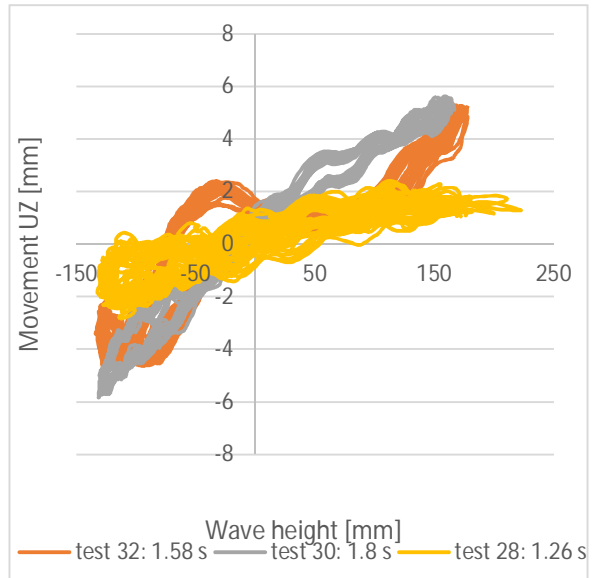


Figure 38: TLB Simple: 0.30 m waves

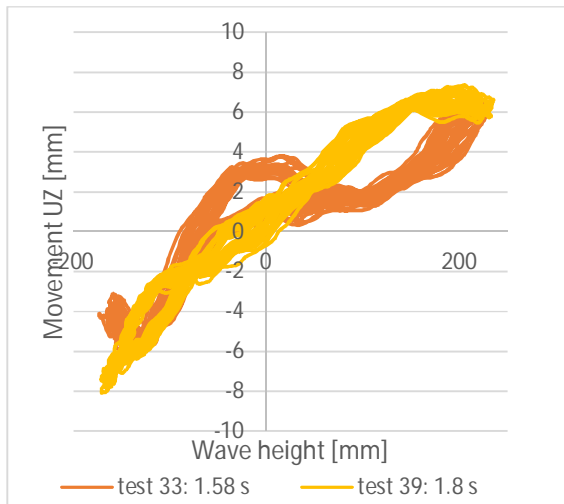


Figure 39: TLB simple: 0.40 m waves

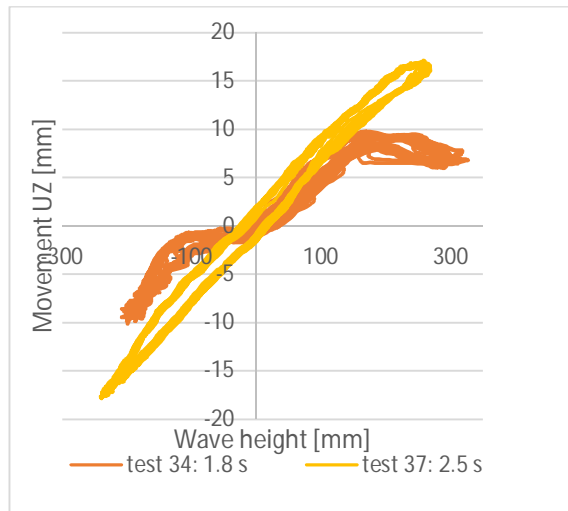


Figure 40: TLB Simple: 50 m waves

Some of the cases from the experiments with the TLB S show a lot of disturbance while others has minimal disturbance. Longer periods seem to give less disturbance, and more even movement. This can be seen in all wave heights and for all the prototypes. The disturbance can almost look like vibrations as the wave passes the prototype.

With a long wave period the prototype moves in a harmonic mode. When the wave period is to short the prototype is not able to return to its origin. The movement becomes uneven and this distributes to the lines. All of these movements and more must be expected at sea.

#### 4.6.2 TLB B

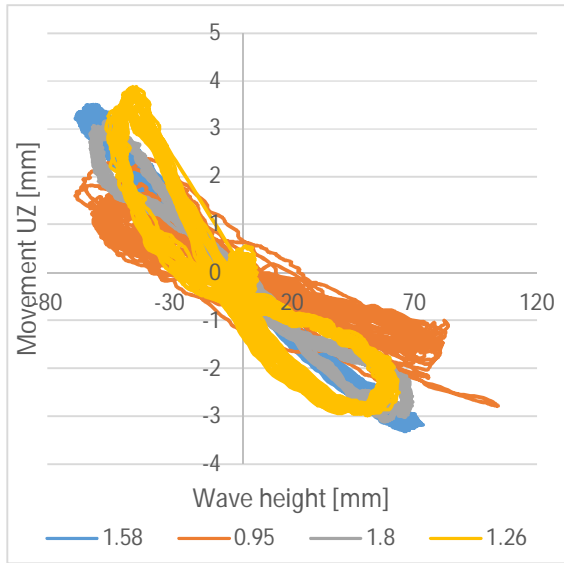


Figure 41: TLB B: 0.13 m wave

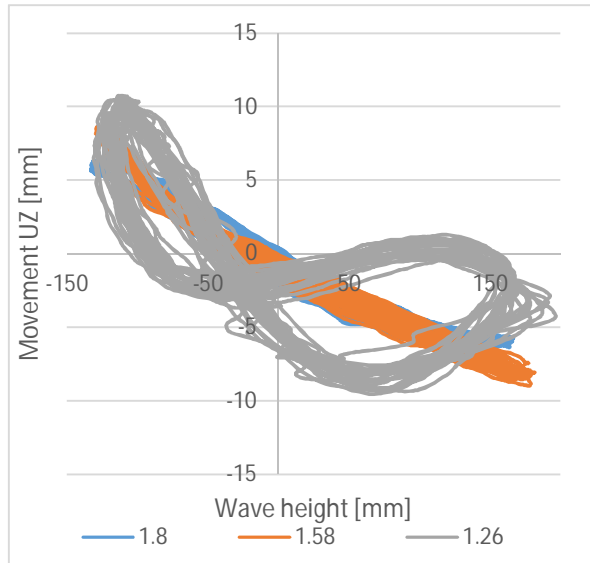


Figure 42: TLB B: 0.30 m wave

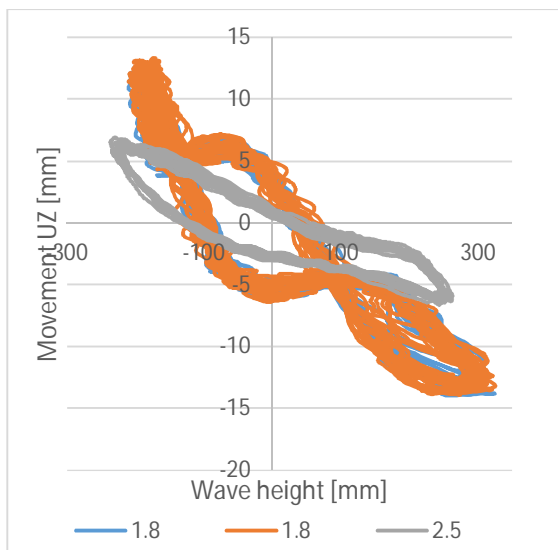


Figure 43: TLB B: 0.5 m wave height

The same disturbances are observed in the short period waves for the TLB B. Shorter periods give more variance in the results, and a rougher movement. It is also the 0.5 meter wave with the longest period that gives the smoothest result. This is similar to the TLB S.

Notice that the top of UZ movement is at the bottom of the wave trough and bottom UZ is at top of wave crest. This phenomenon is also seen in the results of TLB X3 and will be examined further in chapter 4.7.

The TLB B has larger amplitudes on UZ movement than the TLB S on small waves, while it has smaller amplitudes than TLB S on large waves. It is likely that this has something to do with the tapered section. The effect of the tapered section is very little in small waves. In wave cases with small waves, the TLB B behaves like a slimmer version of TLB S. A slimmer version that is subject to less forces from the waves. When the waves get larger, the effect of the tapered section gets stronger. The horizontal area of the tapered section damps the UZ movement of the turbine more in larger waves.

### 4.6.3 TLB X3:

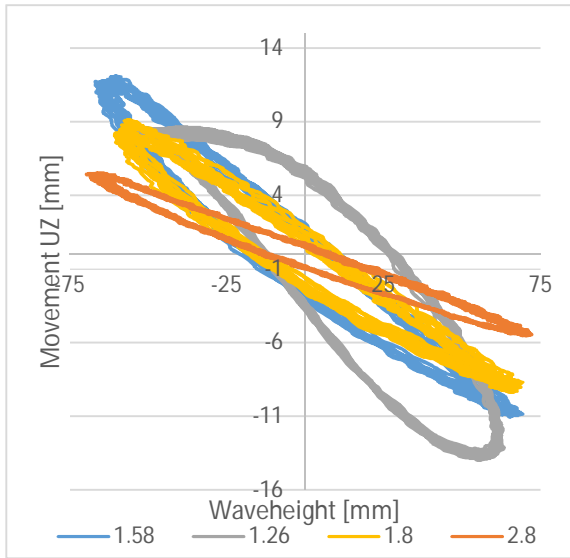


Figure 44: TLB X3: 0.13 meter wave



Figure 45: TLB X3: 0.3 meter wave

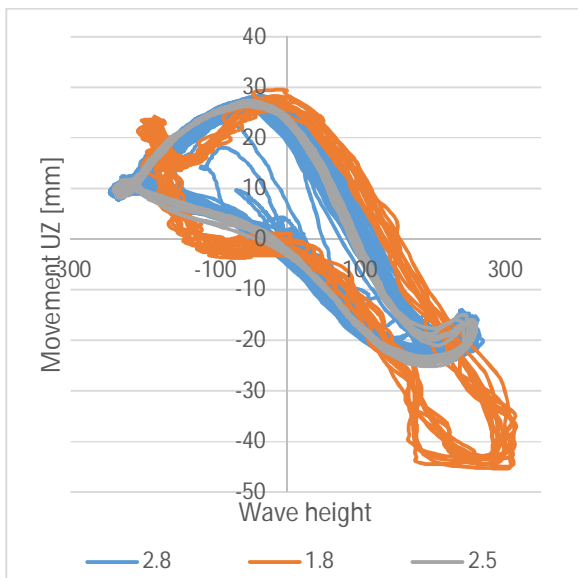


Figure 46: TLB X3: 0.5 m wave

There are rougher movements on the shorter period waves than the long wave periods.. This may indicate that these experiments are more influenced by interference from eigen periods.

The long period results have little variance and very smooth movements, especially for 0.13 m wave height. Larger waves and shorter wave periods makes the prototype unable to return to its initial position before the next wave comes, and the movement becomes uneven.

The TLB X3 moves easily through the waterline because of the small area crossing it. In the load cases with largest waves, it is possible to observe that the lid on the floater comes through the water. That damps the heave movement because the volume of displaced water suddenly decreases more rapidly. The TLB X3 moves easier in heave direction than the other two prototypes.

#### 4.7 The TLB B and TLB X3 dives into the wave

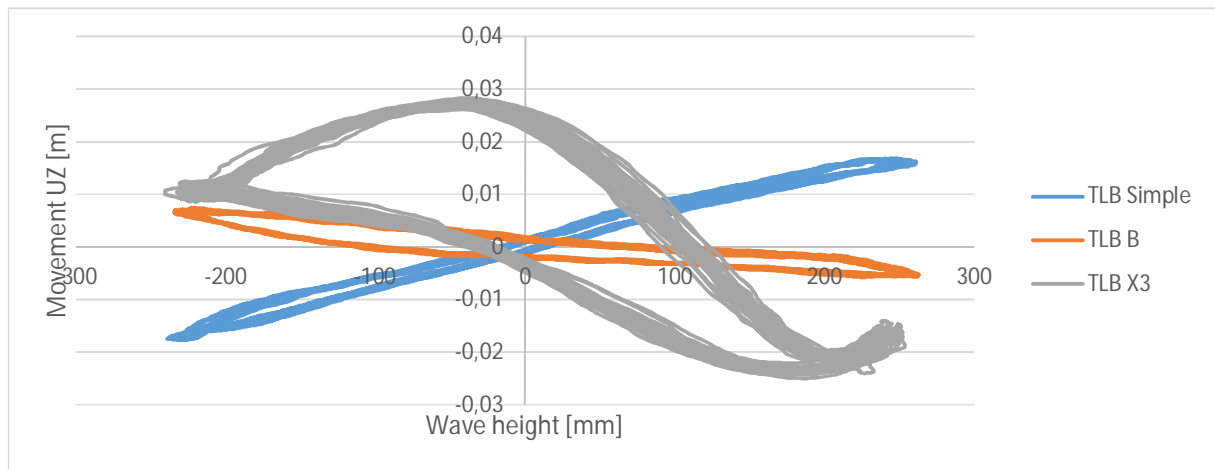


Figure 47: UZ movement in wave cases 0.5m wave and 2.5 sec period

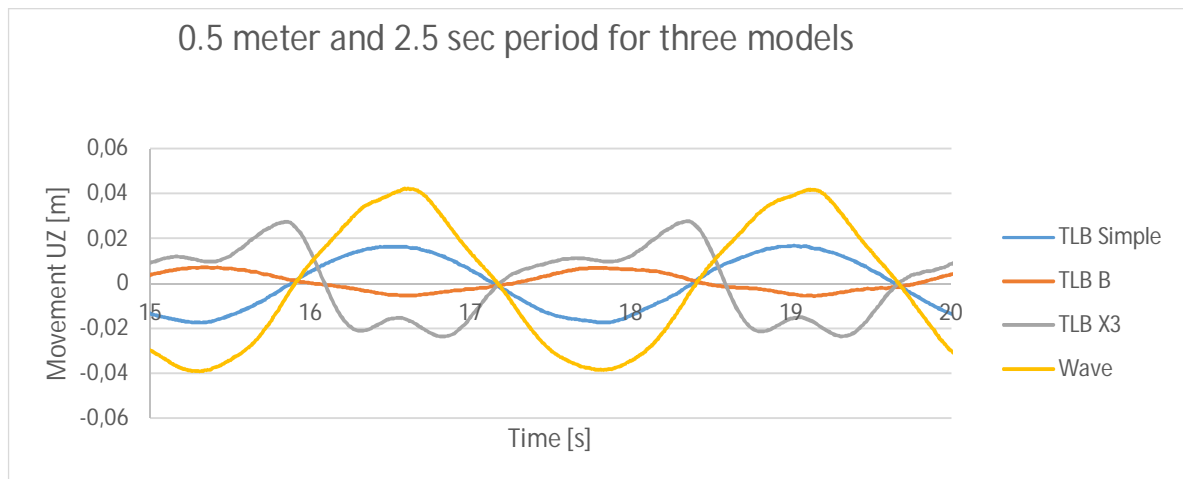


Figure 48: UX movement of prototypes in 0.5 meter and 2.5 sec period

When the experimental results for each prototype are compared with one another, it can be observed that TLB B and X3 moves against the waves. The UZ is at its highest when the wave is at its lowest, except for X3 in 0.3-meter waves. At first, it seems like the results from TLB B and X3 are wrong. The prototype is at its lowest point when the wave is at its highest. This is not very intuitive, at least not at first glance. However, if high forces in the x-direction is assumed, this will result in high reaction forces in the x direction. Because of the angle of the mooring lines, it induces reaction forces that pulls the prototype down instead of letting it float up with the wave top. This effect will vary depending on how much of this force that moves through the top lines and how much moving through the bottom lines. This again depends on how high above water line the top lines are mounted to the prototype and how deep below water line the bottom lines are mounted. This is probably why a different behavior by the TLB S is observed. It seems like it is a question of the magnitude of drag and inertia force at the wave top compared to the extra buoyancy at the wave top.

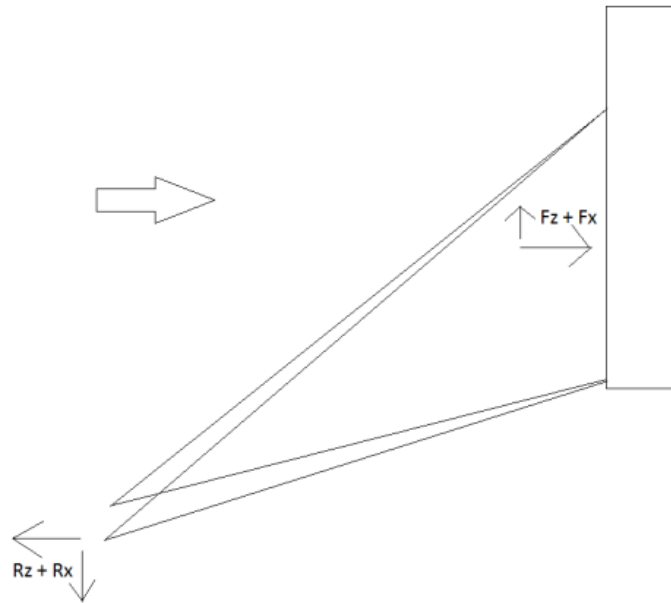


Figure 49: Illustration of forces pulling the TLB B and X3 under water at wave top

This effect is also amplified by the waves applying a torque in the pitch direction that moves the prototype forward and down. This effect is larger on TLB B and X3 because the radius from the center of pitch rotation to the tracking ball is several times higher.

#### 4.7.1 Center of rotation and wave force resultant

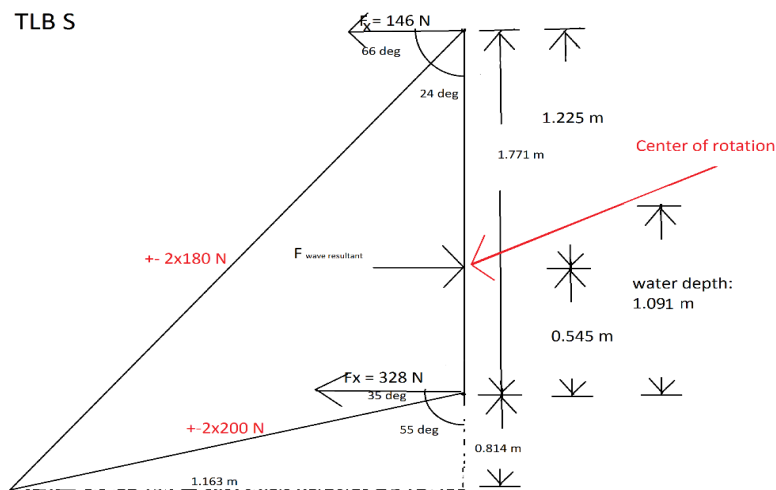


Figure 50: Illustration of balance point (drawing not to scale)

If the resultant force from the waves is different in experiment and simulation, large differences in force in lines may be seen because more pitch movement means more force in the upper lines. If a force with same magnitude attacks the structure at a lower point there will be more surge movement and also more forces in the lower lines. This is because the lower lines takes up more of the surge movement relatively to the upper lines. The upper lines takes up more of the heave and pitch movement. This is mainly dependant on the angle of the mooring lines, but of course also on the stiffness in the upper lines vs the lower lines and also the initial pretension set up.

The mean force in the lines in load case 37 is used for this example. The force in the two upstream lines are 180 in the upper lines and 200 in the lower lines. The down stream lines balances this on the other side. The added horizontal force in the upper lines are 146 N and 328 N in the lower lines. This puts the center of rotation 0.545 m from the lower anchor point, which is closer to the lower lines. The center of rotation can be found with a balance equation.

$$328 \text{ N} \times x = 146 \text{ N} \times (1.771 \text{ m} - x) \quad \text{Equation 13}$$

$$x = 0.546 \text{ m}$$

How much pitch that will appear in the results depends on how much the resultant move up and down. The question is: At a given point of time, where is the wave resultant and how large is it in the experiment? At the same point of time, where is the resultant of the wave force in the simulation, and how large is it? If the answers of these two questions are different, we will see different behavior of the TLB. The further away from the center of rotation we find the resultant, the more pitch we find compared to surge. Relative to the force magnitude ofcourse.

The center of rotation changes from prototype to prototype and the resultant force changes from wave case to wavecase and from prototype to prototype.

#### **4.8 Wave frequency response plot**

The plots in this chapter are wave frequency response plots. They display the response (mm movement / mm waveheight or force/mm waveheight) of the prototypes to the waves depending on the period/frequency of the waves. The plots show the results from both the regular and the irregular wave cases. The irregular cases are shown as lines in the plots while the regular plots are small squares, triangles or circles depending on the wave height. The purpose of the plots is to present how the prototypes change their behavior with increasing wavefrequency. The results of the regular loadcases are consistent with the irregular wave cases.

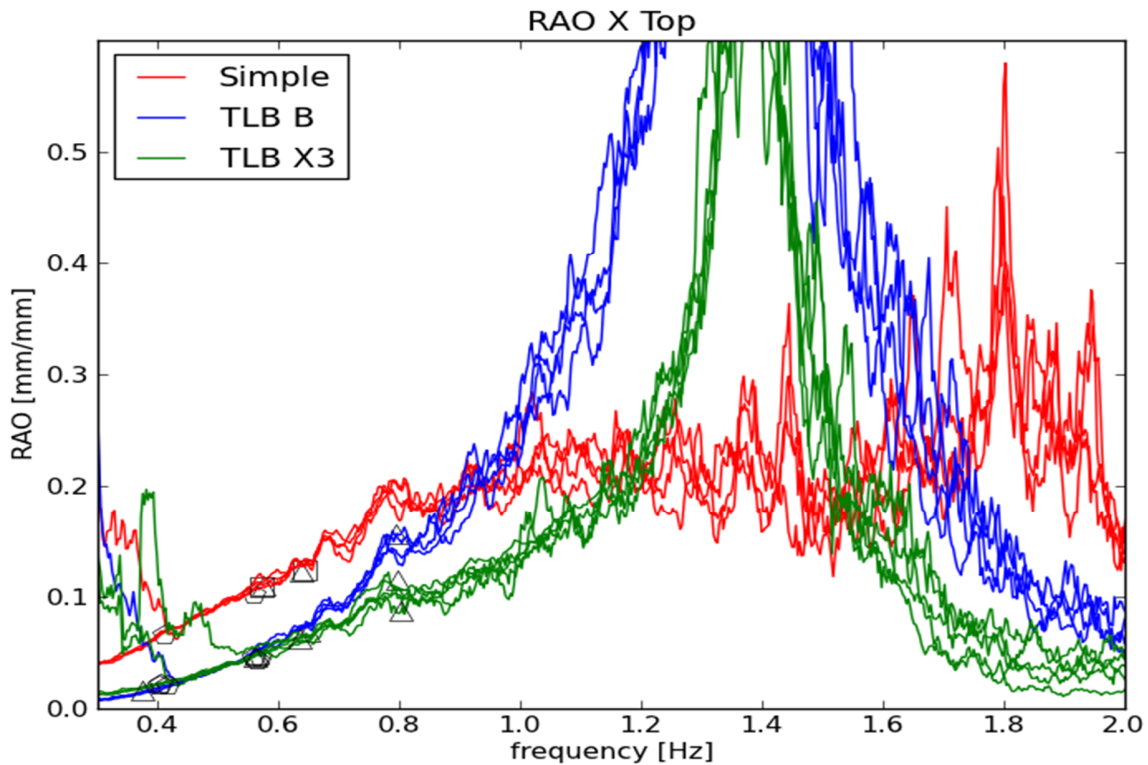


Figure 51: Plot of x direction movement against wave frequency (Myhr, 2013)

The response of x-direction movement (mm movement / mm waveheight) of TLB S increases with increasing wave frequency/falling wave period but shows no signs of eigen period interference. The response of TLB B and TLB X3 increases exponentially as the wave period encounters the zone of eigen values (eigen frequency pitch/surge TLB B: 1.5/1.4; pitch/surge TLB X3: 1.5/1.3) The response of TLB B is stronger than X3 because it has a larger area fronting the waves. The TLB S has a higher pitch response in low frequency waves, but it has its pitch eigen period at 0.26 and surge at 0.63. This means that it does not have the combined effect of the two eigen frequencies to create wave response. The responsiveness of TLB S may be a result of its low weight compared to the others. A heavier model seems to be preferable in terms of wave responsivity as it is less responsive and more stable.



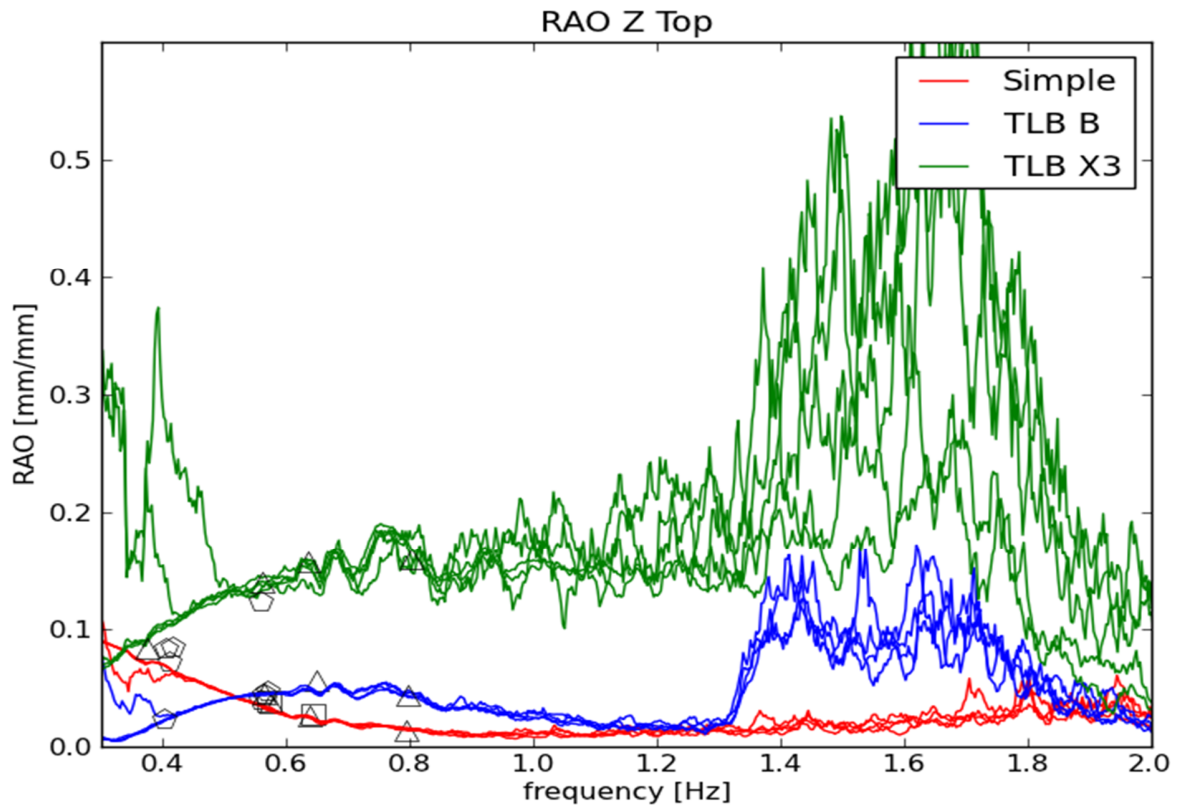


Figure 52: Plot of z direction movement against wave frequency (Myhr, 2013)

The effect of eigen values can be seen in Figure 52 as in Figure 51, but for the heave eigen values. It also seems like the pitch eigen values interfere in the responsivity plots.

The TLB S has shorter eigen periods than TLB B and TLB X3 and has an even curve within the range of frequencies in the plot. The TLB S reacts stronger to long wave periods than TLB B and TLB X3, but apart from that it does not seem to be sensitive in the heave direction to changes in wave periods.

The TLB X3 is more responsive in the Z-direction. This is because it has a smaller area coming through the water line. This lets it move more easily up and down. The volume of water that is displaced by the floater stays almost constant when the X3 moves in heave direction. The X3 shows more signs of disturbance earlier in frequency range. It might be caused by turbulence between the X3 columns.

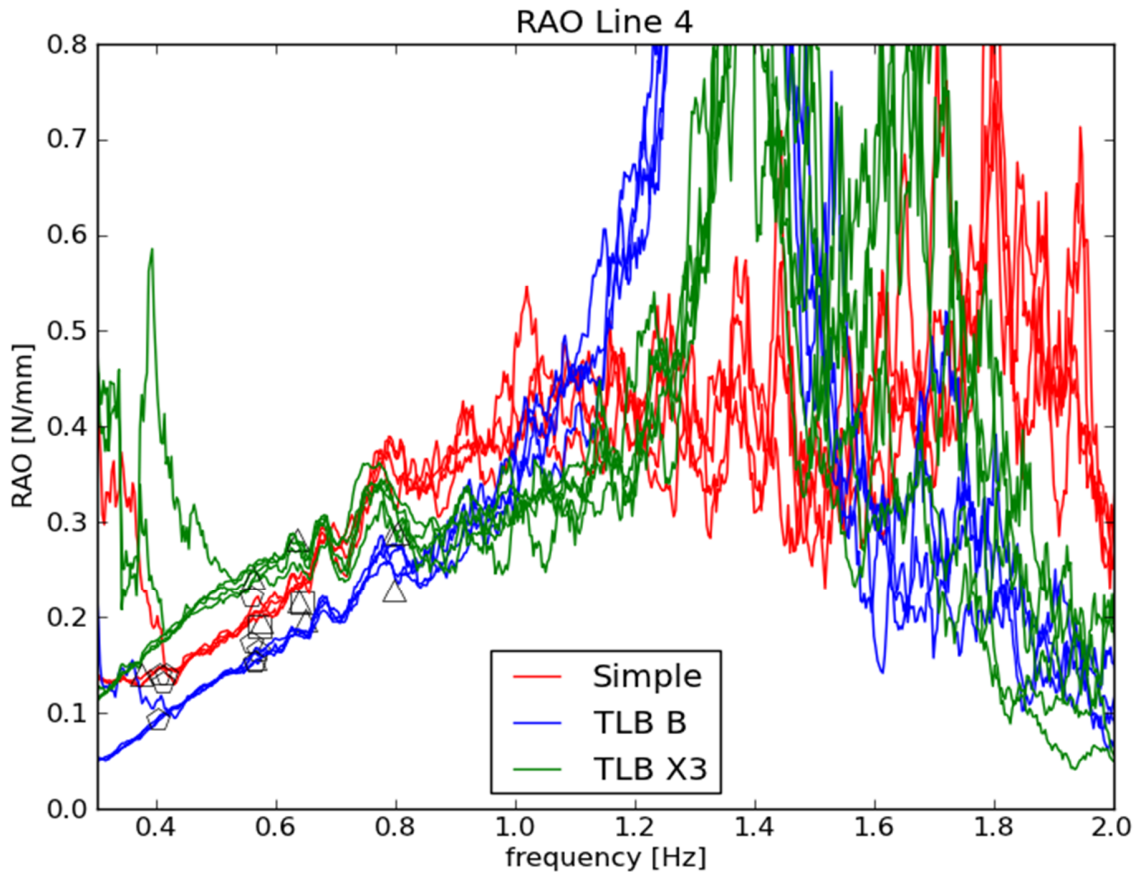


Figure 53: Plot of force in line 4 against wave frequency (Myhr, 2013)

The wave response of force in line 4 increases for all the prototypes with increasing wave frequency. Line 4 is affected both by horizontal movement and vertical movement because it's the upper line. The response of TLB B and X3 falls at higher frequencies. This is likely because the wave periods are too short for the TLBs to react to the waves before they have passed. This effect is more apparent on TLB B and X3 which is natural considering the weight of the prototypes.

A look at the TLB S line shows that the response increases until around 1 Hz. After that it continues more horizontally, but with large disturbance. It seems like there is a top in response around 1 Hz, but the response of TLB B and TLB X3 continues to increase because of interference of Eigen periods/frequencies. The TLB has increasing wave response until a certain point and then the response in the mooring line is constant, but with disturbance.

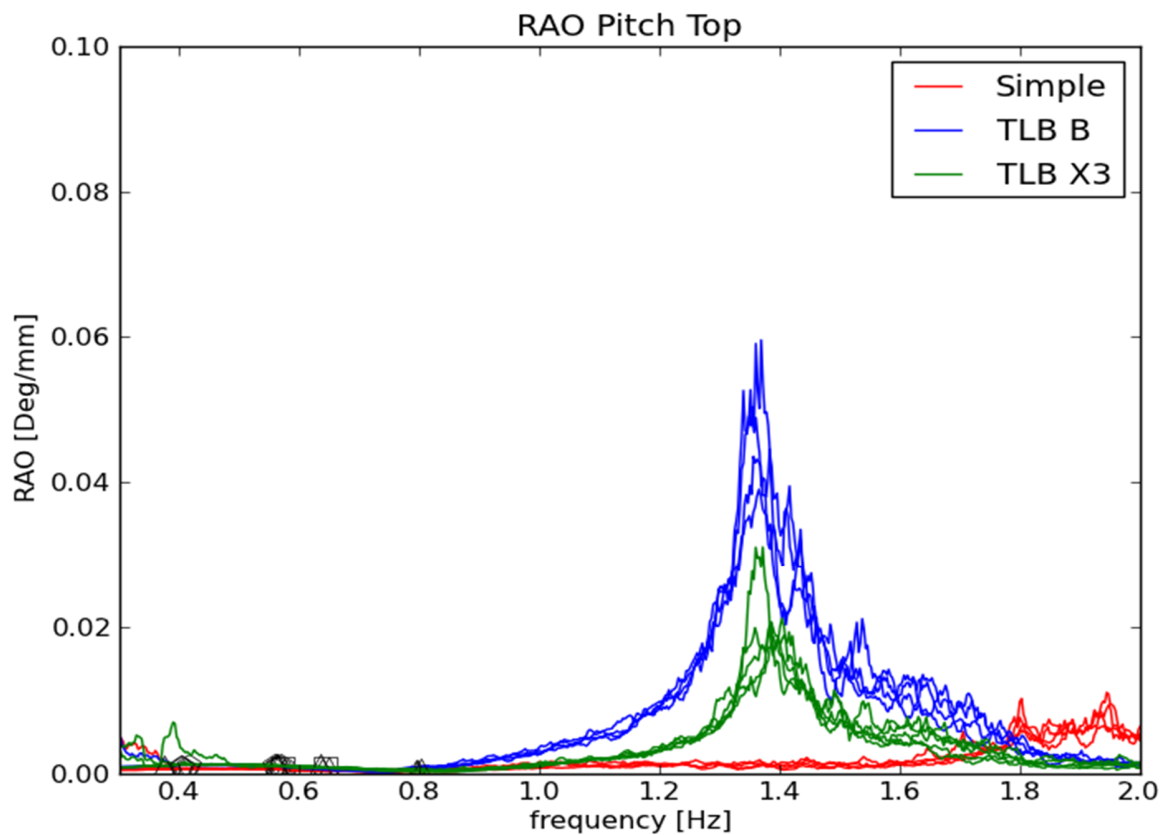


Figure 54: Plot of pitch movement against wave frequency (Myhr, 2013)

This plot shows much of the same behavior as the previous. The response of TLB B is twice as high as for TLB X3 at the highest. This is probably because TLB B has a larger area facing the waves. It simply catches up more forces in the horizontal direction.

All of the prototypes seem to have a fairly constant response on the pitch movement to the waves. When the wave frequency encounters the eigen periods there is a higher response to the waves.

#### 4.9 Uncertainties and error propagation

In general, if we have a result  $Q$ , and it is a function of  $a$  and  $b$

$$Q = a + b \tag{Equation 14}$$

then the uncertainty of  $Q$ ,  $\delta Q$  is a function of the uncertainty of  $a$  and  $b$ ,  $\delta a$  and  $\delta b$

$$\delta Q = \sqrt{\delta a^2 + \delta b^2} \tag{Equation 15}$$

In the case of this experiment there are numbers on some of the parameters, while others are missing. Since there are a many variables contributing to the final result in the measurement it might give a

wrong picture of the uncertainty if only some of them were used to calculate the total uncertainty of the experiment.

If quantitative numbers of the uncertainty on each parameter existed it would be possible to calculate the uncertainty in an experiment.

<p>The force are measured in the lines, F1 to F6. They are a function of the following variables</p>	<p>The movements are measured at the top of the prototypes. It is a function of the following variables</p>
<ul style="list-style-type: none"> <li>• The measurement equipment</li> <li>• Forces in the other lines</li> <li>• Friction in the pulleys</li> <li>• The buoyancy of the prototype</li> <li>• The load from the waves.</li> <li>• Wave height</li> <li>• Wave period</li> <li>• Wave shape</li> <li>• Energy conservation in the prototypes</li> <li>• Errors in the measuring the prototypes (weight and geometry)</li> <li>• Errors in the test rig (angles and distances)</li> </ul>	<ul style="list-style-type: none"> <li>• The measurement equipment</li> <li>• Friction in the pulleys</li> <li>• The buoyancy of the prototype</li> <li>• The load from the waves.</li> <li>• Wave height</li> <li>• Wave period</li> <li>• Wave shape</li> <li>• Energy conservation in the prototypes</li> <li>• Stiffness error in the mooring lines</li> <li>• Errors in the measuring the prototypes (weight and geometry)</li> <li>• Errors in the test rig (angles and distances)</li> </ul>

There is no way to isolate all the different sources of uncertainty, but an estimation of the error can be made by taking the variance of the results. Errors from friction will still be left out of such an analysis because it is systematical and not detectable from the force results in the lines. There are variance in the results but the magnitude of variance changes from load case to load case. Table 16: UX deflections from all the simulations with 0.30 m waves. Table 16 shows that there is a difference in the variance for the same load case on the different prototypes. There is often more variance in the results for the TLB X3 than for the two others, but it is not always the case.

It is difficult to put number on the variance in the experiment, but by studying the movement plotted against the waves it can be seen that there is a lot of variance in some load cases and much less in other cases. The smallest  $\pm 0.001$  around a UZ-value of 0.05. That is  $\pm 2\%$ . Other places there is variances of  $\pm 0.005$  around measured UZ-value of 0.03. That is  $\pm 17\%$ . The uncertainty in measurement equipment is smaller than the smallest number and probably  $< 1\%$ .

The effect of friction in the lines is unknown. It is likely that there is an unknown effect of friction around the pulleys, which takes up some of the forces in the lines. This means that the amplitude of the measured force in the lines are smaller than the force that is actually in the mooring line between the prototype and the pulleys. The friction in the pulleys were measured to be 0.05 kg at 20 kg loading (Spæren, 2013). If it

is assumed that the friction is linear between 100 and 300 N of load in the line, there will be a friction of 0.25 % or between 0.25 and 0.75 N.

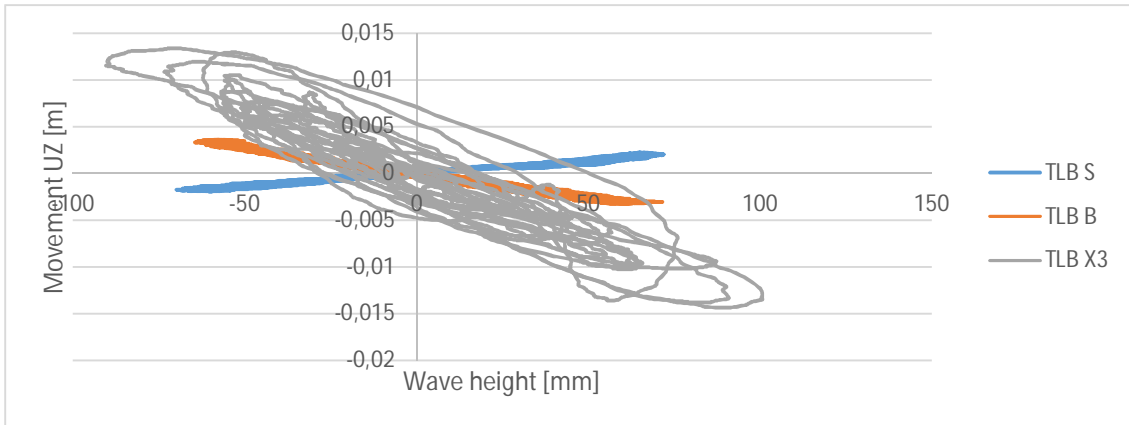


Figure 55: 0.13 meter and 1.58 sec period for three prototypes

Figure 55 illustrates how two prototypes have results with no signs of disturbance from a wave case, while the third has much disturbance. It also illustrates the challenge in giving a proper estimate on the variance in the results. The variance varies over each wave case, and between the measured parameters.

#### 4.9.1 Variance in wave gauge results

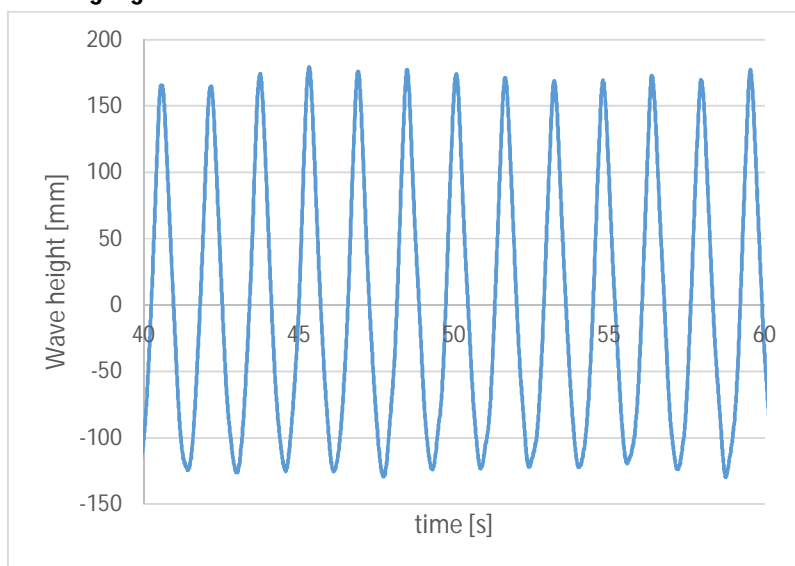


Figure 56: Wave measurement in load case 45

This means that some of the uncertainty has its roots in the uncertainty of wave height and wave shape. Figure 56 shows that there are variations in the heights of the wave crests and also on the wave troughs. In case 45 there is a standard deviation of 2.5 % around a mean wave top amplitude of 150.6 mm. This is a small sample, but it is taken from the range of the best results, in this case 20 seconds after the first wave has met the wind turbine. The average level of the wave through in the same range is -132.4 mm.

This means that there is an average wave height of 290.4 mm in a wave cases that is supposed to have an average of 300 mm. In further work on the simulation models, it should be considered to use the measured waves to create a custom wave case for each model. This would likely close the gap between the results in simulation and experiment.

The shape of the wave and small variations in wave periods from period to period may cause disturbance. This will disturb a harmonic movement in the prototype, The period of the wave varies Equation 5 states that the shape of the wave changes with both the wave height and the wave period. This will in turn cause variations in forces on the wind turbine.

#### **4.10 Summarizing discussion of experimental results**

There are no sign of significant error sources in the experiment. The results do not indicate significant friction. The loadcells are tested thoroughly and have not shown signs of error.

The two pairs of symmetrical upstream lines (line 2, 3, 5 and 6) has the same amplitude, shape and phase. This indicates that the model is stable in the water and distributes the forces correctly to the mooring lines.

The placing of the tracking ball has made it difficult to see the surge movement because the UX results are very influenced by the pitch movement. This effect is also stronger on TLB B and TLB X3 than it is on TLB S. It is not possible to compensate for the pitch movement with high accuracy because we cannot assume that the pitch at the top is equal to the pitch around its center of rotation. This is because of bending in the tower affect the pitch rotation on top.

There is most likely nothing wrong with any of the load cases, but some might be more challenging to simulate.

In some of the test cases the movement of the TLB has the shape of a figure 8. TLB B is the prototype where this effect is most obvious. most In the example of load case 45 the eigen period is close to half of the wave period. This lets it move back and forth almost twice before a new wave top hit it again. If this is right it should be possible to simulate the same behavior if the simulation has the same eigen periods.

## 5 ANSYS APDL modelling

The following chapter describes how the simulation model has been built and what input that has been used in ANSYS. The first part describes how ANSYS has been used for the three simulations in general and the second part of this chapter contains the setup of the YLB S, the TLB B and TLB X3. The following chapter contains the calibration and control of the simulation models. This thesis does not seek to replicate real ocean environment, but to come as close to the environment in the test basin as possible.

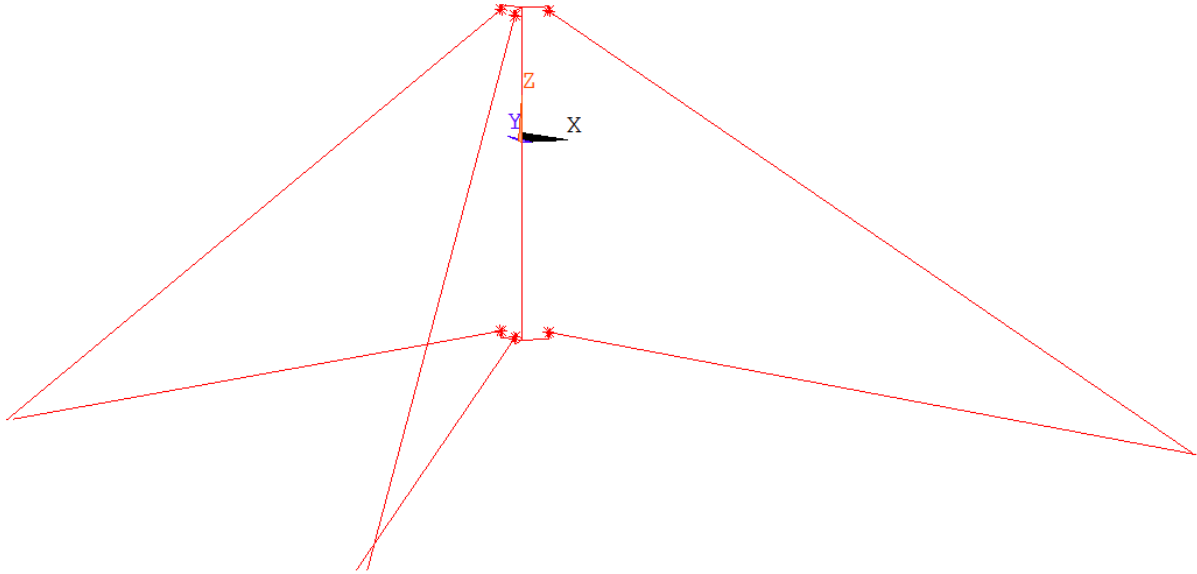


Figure 57: Line model of the TLB S. (6 dots on model are point masses of mooring points. Water line at origin in xy-plane)

### 5.1 Wave and ocean theory in ANSYS

A global analyze of the whole wind turbine with its anchor lines is needed to simulate the experiment.

To set up an analysis in ANSYS there are the following options:

1. Line model
2. Shell model
3. Solid model

ANSYS does only provide pipe elements that is compatible with ocean loads in ANSYS Mechanical APDL (EDR-Medeso, 2013). The line model with PIPE288 and PIPE289 elements is the only option. (ANSYS Inc. (d), 2013)

Three simulation models has been built, one for each wind turbine prototype. They are similar except for the geometry. The TLB S has the simpler geometry with fewest equations, while the TLB X3 is the more complex one. The models are built as input files so that they are easily modified when it is needed. The input files provide a good overview on the model. There is a low level of details on the models because it

rapidly becomes too heavy to run. It has not been necessary with a high detail level to analyze stresses in the model.

The simulation has simplified this system to just include the mooring lines from the pulleys and the floater. All degrees of freedom are locked at the end of the mooring line. The stiffness of the simulated mooring line is the same as the stiffness of the spring and total mooring line in the experiment.

The lines follow the z-axis and the six brackets are modeled as one line radial direction from the z- axis and then one line parallel with the z axis up to the right height of the bracket.

This is a hydrodynamic problem with waves changing the pressure and load from the ocean. hydrodynamic ocean commands must be used, instead of just pressure on the cylinder. Pressures and motions from waves at a given phase of the wave are found in hydrodynamic data file. The data are mapped onto line element pressures based on Morison's equation (ANSYS Inc. (d), 2013) ANSYS provide several wave theories, but for deep water wave theory we can only choose between AIRY waves without modifications and Stokes 5th order waves.

Ocean data input in ANSYS is:

- Depth of sea
- Density of sea
- Choice of wave theory
- Wave height
- Wave period
- Reynolds number
- Drag coefficients in normal directions of the waves (in the element y and z directions)
- Drag coefficient in tangential direction of the waves
- Coefficient of inertia in the element y and z directions
- Defining independent pressures on the inside and outside of the pipe,
- The ratio of added mass,
- The ratio of buoyancy.

Pressures and motions from waves, current and forward speed at a given phase of the wave are found in hydrodynamic data file. The data is mapped into either surface element pressures or line element pressures based on Morison's equation. The relevant wave types to select from is small amplitude AIRY waves without modifications and Stokes 5th order waves. Small amplitude wave with Wheeler empirical modification of depth decay function can also be chosen, but it does not suit the sea depth in the simulation.

*"It is not necessary for the hydrodynamic and structural meshes to be identical, and the loading is mapped automatically from one to the other; however, it is assumed that the hydrodynamic axis system is identical to that used for the structural analysis. Small displacements are assumed in the load-mapping process, and mapping may not be accurate if this condition is not met. "* (ANSYS, inc., 2012)



Ocean loads can only be applied to PIPE288 and PIPE289 elements with circular sections (EDR-Medeso, 2013). Since there only are circular sections in the models, this is enough.

## 5.2 Choice of elements

The FEM simulation is conducted with two element types only: The PIPE288 element and the LINK180 element. The PIPE288 element is used for all structural elements except for the mooring lines where the LINK180 element is used. Under is an explanation of the two elements:

### 5.2.1 PIPE288

The element is a two-node pipe element with six degrees of freedom in each node the way it is used in this thesis. These are translations in  $x$ ,  $y$ , and  $z$  directions and rotations around the  $x$ ,  $y$ , and  $z$  axis in the local coordinate system.

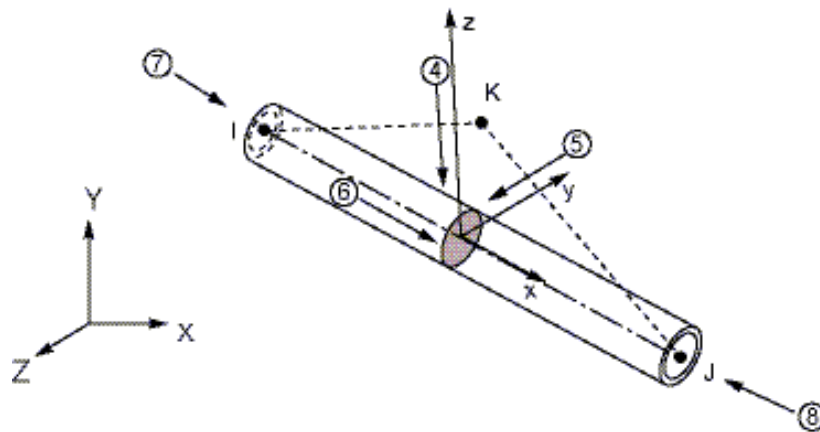


Figure 58: Figure of the PIPE288 element (ANSYS, inc., 2012)

The element is chosen because it is the only element besides PIPE289 that is compatible with the ocean commands. Forces are applied to the I and J node at each end of the element.

“The PIPE288 element is suitable for analyzing slender to moderately stubby/thick pipe structures. The element is based on Timoshenko beam theory. Shear-deformation effects are included. (ANSYS, inc., 2012) Beam elements can be subject to axial forces, shear forces and bending forces.

End cap loads can be applied by using the key option 6. This option is used to have the effects of vertical wave forces on the element. How the effect waves are at the intersection of two elements of different cross section is unknown. It is not fully known if the end caps incorporates the wave loads or if they only use the pressure differences.

The global origin is at mean sea level with the  $z$ -axis pointing in the vertical direction, away from the center of the earth.

Using the Key option for End lids on the PIPE288 elements did make a difference in the results. On average, the results from the simulation change by 0.0036 % for the measured variables. The default option is on for this key option, and the default option is used for all simulation.

Relevant assumptions and restrictions for PIPE288 element:

- The pipe cannot have zero length.
- Cross-section distortion or collapse is not considered.
- Rotational degrees of freedom are not included in the lumped mass matrix if offsets are present.
- The element works best with the full Newton-Raphson solution scheme (the default option in solution control).
- Only moderately "thick" pipes can be analyzed.
- Stress stiffening is always included in geometrically nonlinear analyses.

### 5.2.2 LINK180

LINK180 is two-node, three dimensional spar. The element to model trusses, springs and cables. A tension only option is available, but not necessary for this model since there are pretension in the mooring lines and the elements will always be under tension. The element has three degrees of freedom at each node, the UX, UY and UZ translations. Loads are transferred only along the axis of the element meaning it can take axial forces only.

The LINK180 is chosen because it is the only element that is suitable for this application. The link167 element is used for explicit dynamic analysis only.

The element includes large deflection effects when large deflection is activated (NLGEOM,ON)

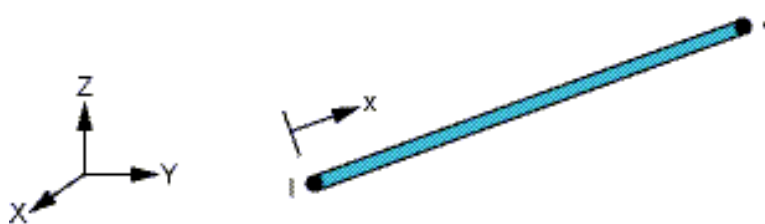


Figure 59: Illustration of the LINK180 element (ANSYS Inc. (b), 2013)

The section properties (area of mooring line) are input via the SECTYPE and SECADATA commands (ANSYS Inc. (c), 2013). Initial stress state is given by the INISTATE command

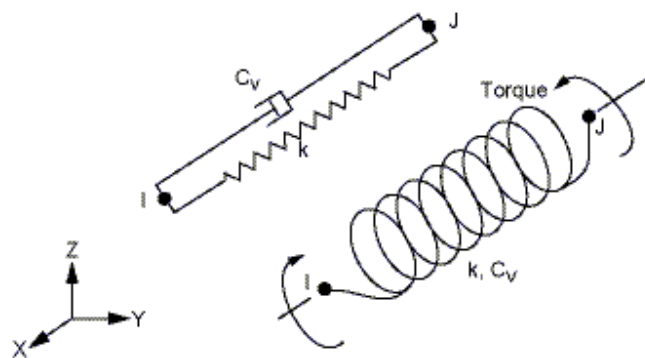
Relevant assumptions and restrictions for the LINK180 element (ANSYS Inc. (b), 2013)

- The spar element assumes a straight bar, axially loaded at its ends and of uniform properties from end to end.
- The length of the spar must be greater than zero.
- The cross-sectional area must be greater than zero.
- The displacement shape function implies a uniform stress in the spar.
- To simulate the tension-/compression-only options, a nonlinear iterative solution approach is necessary.

### 5.2.3 COMBIN14

The combin14 is a spring/damper element (ANSYS Inc. (b), 2013). It is used as a damper to tune decay tests. "COMBIN14 has longitudinal or torsional capability in 1-D, 2-D, or 3-D applications. The longitudinal spring-damper option is a uniaxial tension-compression element with up to three degrees of freedom at each node: translations in the nodal x, y, and z directions. No bending or torsion is considered. The torsional spring-damper option is a purely rotational element with three degrees of freedom at each node: rotations about the nodal x, y, and z axes. No bending or axial loads are considered." (ANSYS Inc. (b), 2013)

**Figure 14.1 COMBIN14 Geometry**



2-D elements must lie in a  $z = \text{constant}$  plane

### 5.2.4 MASS21

The mass21 is a mass element for modelling of point masses (ANSYS Inc. (b), 2013). It is a single node element with up to six degrees of freedom. In this thesis it is used to model the masses of the mooring points on the prototypes.

## 5.3 Assumptions and Simplifications

The mooring brackets are not modelled to be subject of ocean loads. Since the anchor point two, three, five and six on each side of the xz-plane is likely to be positioned in a unsymmetrical in the experiment, this may cause torque on the model and create yaw rotation.

The mooring lines has been set up as one element to avoid buckling of the mooring line when the load changes. The use of the link element does not allow bending in the element, but the there should be minimal bending of the element since it will only be created by drag forces in the water.

The lines are also unsymmetrically positioned around the xz plane. The drag in the lines will create a torque around the z axis of the prototype. These effect will not be found in the simualation because there is no ocena loading on the brackets or mooring lines.

The lines end at a anchor point, whereas the experimental lines end in a pulley. If the model twist this will cause bending torque on the axis of the pulley. This may cause friction in the experiment which we will not be able to replicate in the experiment with this setup.

The effect of the above mentioned simplifications are assumed to be minimal, so the simplifications are allowed.

The Numark implicit scheme has been applied with Newton Raphson option to solve the finite element model. Large deflection have been allowed and the model has been solved with forces and deflections as convergence parameters. The tolerance level has been set automatically by ANSYS.

### **5.3.1 Constraining the model and choices**

The model is constrained at six points, and in three degrees of freedom at each point. The model is constrained at the end of each mooring line, in x, y, and z direction.

Three linear dampers has been put on the model. One damper is placed on the bottom node to damp the heave motion. A pair of dampers has been put on the model below the waterline to damp the surge/pitch motion and sway/roll motion

## **5.4 Modelling the three simulation models:**

### **5.4.1 TLB Simple:**

The TLB S is a reference prototype that can be easily modeled in a Finite Element Analysis (FEA) program. It is also convenient that it is easier to do hand calculations on it. Controlling the forces in the mooring lines is difficult, if not impossible in hand calculations, but controlling the forces from the waves on the model is a way to ensure that the FEA code applies the forces properly. There are inertia forces from vertical movement of the waves on the TLB S due to the bottom lid. There are also small vertical drag forces on the side of model from its movement up and down in water. This means that there are fewer variables to explain and understand on the TLB S. This gives a good way to find explanation variables on the two other prototypes.

All of the models are set up as line models. The structure of the modelling is as follows:

1. Create a key point after the given geometry
2. Make lines between key points
3. Mesh lines with material properties and section properties.

The TLB S is modelled in five pieces. The large PVC pipe is the main part. The lid is modeled in two pieces because it has two diameters. The smaller diameter is inside the pipe (section 2 and 4) so it the total diameter of these sections is the same as the larger diameter of the lid. The exact mass of the parts is known, but not the exact density. The mass is divided by volume in the input data for ANSYS to have the right density. The difference in part weight and total weight is tape and glue.

The table above shows material properties and section properties for each part in the model. The data in the table comes directly from the measured geometry and masses. Young's modulus is as given in the data sheet from the vendor. (FinnLøkenAS, 2012)

The sections with outer and inner diameter are used with beam elements. (PIPE288)

The Brackets are elements with high stiffness. They are made to replicate the radius of the mooring points around the radius of the center. The material used together with these elements are the "bracket material". This material has extra high young's modulus and no mass density.

The section properties of the mooring lines are given as areas instead of diameters because the mooring lines are rod/link elements (LINK180).

#### **5.4.2 TLB B**

The TLB B consists of three pipes with two transition pieces between them and a weight on top to imitate the nacelle.

It is not possible to make tapered sections with PIPE288 elements, and it is not possible to choose another element because only PIPE288 and PIPE289 is compatible with the OCEAN commands. The solution is to make many sections with increasing diameter from top to bottom of the tapered section. With higher number of subsections in this area, the volume and area gets closer to the real measures. The inner diameter of all the sections are the same as it is on the tapered section. The weight of the brackets is included as point masses at the top of the simulated brackets.

The tapered section (section 9) is not possible to model in ANSYS if ocean forces is to be applied on it. The section is instead modelled as several pipes with increasing diameter. This gives a relatively good imitation of the area perpendicular to the wave propagation direction and the volume of the section.

A source of uncertainty is how ocean forces are applied to the top of each section. Since there are vertical forces working on the prototype in this area, this creates some uncertainty. This might be a source for the error in the UZ movements.

#### **5.4.3 TLB X3**

The TLB X3 is as the TLB B built in three sections with the nacelle on top. The TLB X3 has a thinner, but higher bottom part than TLB B to provide the buoyancy. The middle section consists of three columns in a triangle to support the tower above. It is this three column section that breaks the water line and this minimizes the force from waves on the prototype, because the area orthogonal to the wave propagation direction is minimized. This prototype loses some of its strength but it is interesting to see what can be gained from having this type of geometry. To model the three columns, six brackets had to be made in the horizontal plane. They connect and position the X3 columns correctly to the rest of the line model. The six brackets are modelled as stiff elements to avoid deflection in these elements.



Figure 60: Illustration of the modelling of X3 columns in ANSYS

The tower and nacelle is identical to the tower and nacelle on TLB B. The mooring points are located at the same height as on the TLB B.

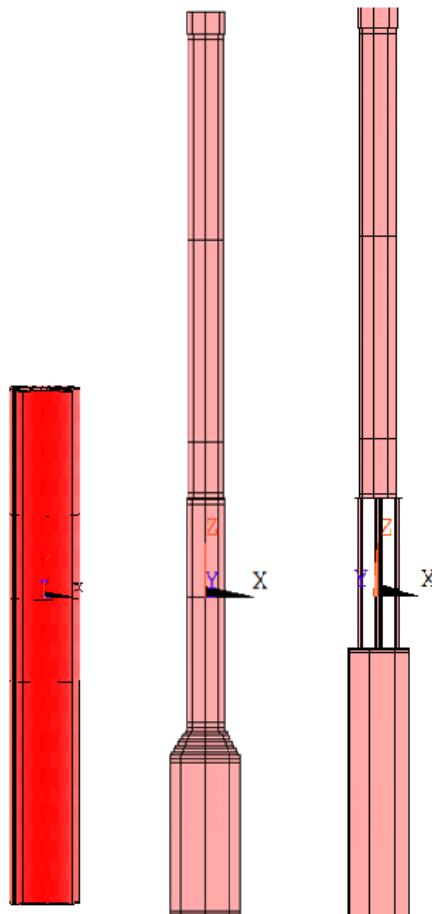


Figure 61: Illustration of the three computational models

## 6 Calibration and control of the simulation models:

The following chapter includes the measures that has taken place to calibrate the simulation model. To make sure that the model is working and giving correct results the geometry has been checked. To make sure that solution of the time steps and element size is correct, two convergence analyzes has been done. The eigen periods has been controlled and the damping parameters has been adjusted to fit the experiment.

To be sure that of having a working FEM model for transient analysis the following points must be in place:

1. Make sure to have the right geometry and material data
2. The time step must be short enough to catch up small variances in forces and loadings.
3. The element size must be small enough to replicate the real world physics of the model.
4. The parameters such as fluid coefficients and damping parameters must replicate the real world.

### 6.1 Controlling the geometry:

To be sure of having the right geometry in the simulation models, the models has been carefully measured to be make sure that they correspond in experiment and simulation. The masses, forces in lines, and Eigen periods in ANSYS and 3DFloat were compared.

### 6.2 The figures for pretension in the lines were measured during the experiment:

Table 17: Pretension in the lines (Myhr, 2013)

	TLB S [N]	TLB B [N]	TLB X3 [N]
Line 1	185	189	150
Line 2	178	184	148
Line 3	180	179	143
Line 4	201	165	186
Line 5	195	164	180
Line 6	197	160	173

The pretension in the mooring lines are the forces present in the lines when the prototypes were launched and positioned correctly in the wave tank. These figures are used to model the mooring lines correctly in ANSYS. Pretension of mooring lines

The **INISTATE command in ANSYS** (ANSYS, inc., 2012) was used to put pretension in the lines. The pre stress command requires that each line is a separate material. The pretension is given in  $N/mm^2$ . Since the pretension from the experiment is given as a force, the stress must be applied as a function of the cross sectional area of the mooring line.

### 6.3 Convergence analysis:

The control the required amount of time steps per second of simulation. This is to secure reliable results from the simulation. When size of the time step is known, it is possible to do an element size convergence analysis to find the needed element size.

### 6.3.1 Time convergence analysis:

The time resolution means how many time steps there is in a load step. If a load step lasts for 10 seconds, and there is 200 sub steps in a load step, the time resolution will be 200 sub steps divided by 10 seconds. This is 20 sub steps per second. In each sub step the solver checks among other parameters:

- What is the speed and height of the wave at this instant
- What is the position and speed of the floating object

A low resolution will cause a loss in information and the results from the simulation will be poorer if not wrong. It is important that the time resolution is fine enough to capture the effects of the Eigen periods.

The convergence analysis answers the question of how fine the resolution must be to give satisfactory results. The same analysis is conducted several times with increasing time resolution. The time resolution is satisfactory when the results from the chosen parameters stabilizes or converges.

The convergence analysis is conducted with a wave height of 0.4 meters and a wave period of 2 for all the models. All the input files for the convergence analysis can be found in the appendix. This is also the final files that are used for the final simulations.

The parameters that are measured in the convergence analysis is:

1. The force in line four (the top line in the wake of the prototype)
2. The force in line two (The bottom line in negative x and negative y direction)
3. The vertical movement of the node in the waterline
4. The rotation of the node in the waterline.

The maximum, minimum and average value of these four parameters are found for the last to wave periods in the 10-second simulation. The results from the three first periods are not used because they include some disturbances from the first wave meeting the prototype that stands still in the water.

To have comparable values for all parameters they have been divided by their own mean value. The y axis in the plot is either N/N or mm/mm. The number of sub steps per second is how many iterations ANSYS will make within each second. 500 sub steps per second means that each second is divided into 500, and ANSYS calculates every 0.002 second.



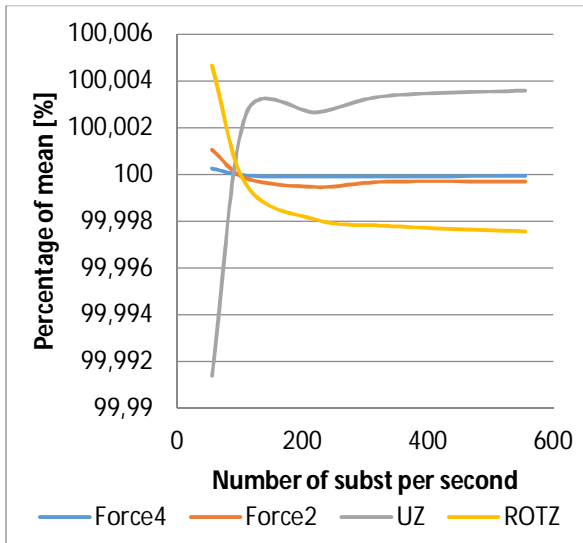


Figure 62: TLB S time convergence max

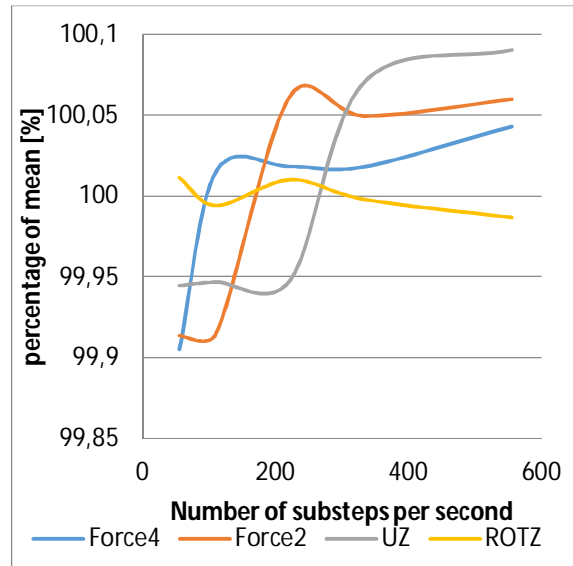


Figure 63: TLB B time convergence max

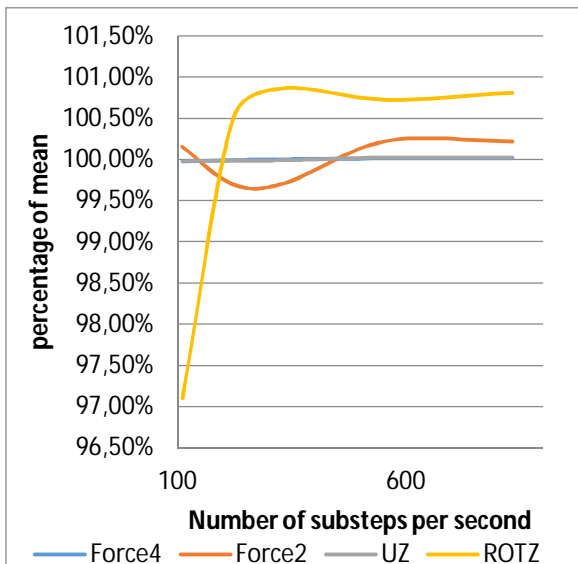


Figure 64: TLB X3 time convergence max

Figure 62 shows that a time resolution of more than 400 sub steps per second does not give significantly better results, so 400 sub steps per second is satisfactory for the simulation of the TLB S. Higher time resolution will only acquire more time and computing power.

Figure 63 shows that 400 sub steps per second is needed for the simulation of TLB B. The average value of the vertical deflection continues to increase slightly, but this is too little to be considered as significant.

Figure 64 shows that the TLB X3 is more complex than the other two model. It requires 600 time steps per second before it delivers steady and reliable results. The force in line 4 lies exactly under the line UZ.

### 6.3.2 Element size analysis

The right size of the time step is required to run a proper element size analysis. This is the reason why the element size analysis comes after the time step analysis.

The element size analysis has been done the same way as the time resolution analysis with the same parameters. The only difference is that the analysis is conducted with an increasing number of elements. The element length is the length of the elements in the model, from the bottom of the floater to the top

of the nacelle. Shorter element length gives more accuracy in the simulation, but takes longer time to calculate.

From 0.3 m below the water line to 0.3 meter above the water line, the element length is 1/10 of the length of the elements in the rest of the model. This is because an extra high accuracy concerning the waves meeting the prototype is desirable. It is desirable because the forces from the waves are transferred to the model on the nodes. More elements means more nodes and therefore more accuracy

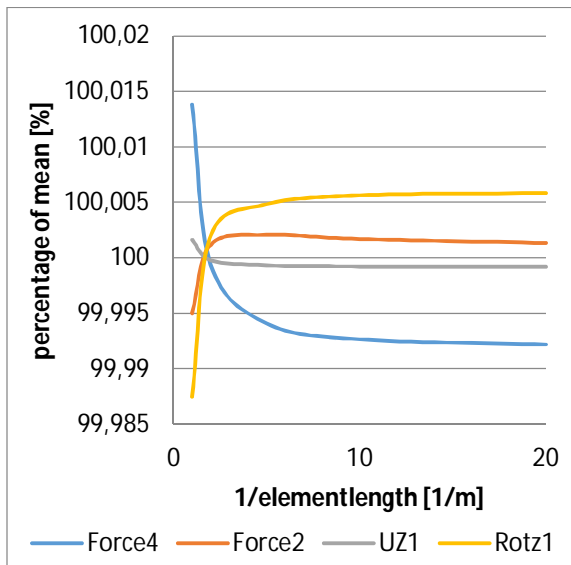


Figure 65: TLB S element convergence max

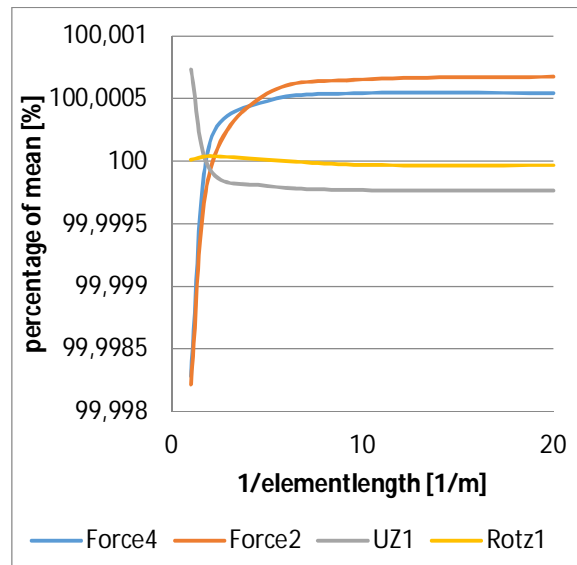


Figure 66: TLB B element convergence max

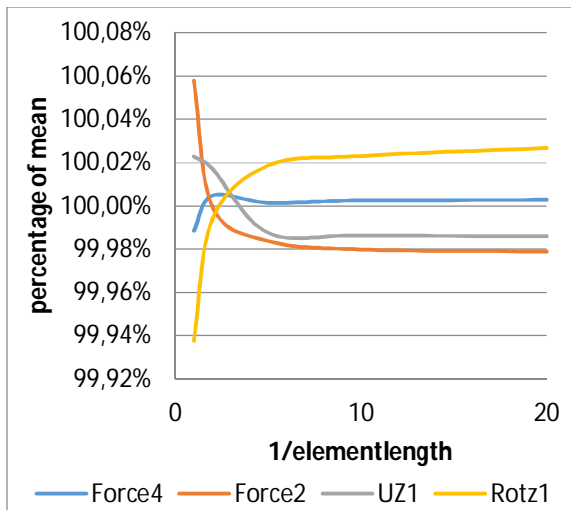


Figure 67: TLB X3 element convergence max

The element size of the TLB Simple should not be longer than 0.1 meters ( $1/10=0.01$ ) All values are fully converged with this element length.

The element length of B should not be longer than 0.14 meters generally and 0.014 meters in the region of the water level.

The element length of TLB X3 should not be longer than 0.125 meters generally and 0.0125 meters in the region of the water level.

## 6.4 Drag and Inertia coefficients

The values of the drag coefficient and inertia coefficient has partially been found through literature and partially through testing and comparing simulation with experiment.

Setting the drag parameter is not an exact science since it will vary with the Reynolds number and Keulegan Carpenter number which in turn varies with wave period and diameter of the floating object. The exact drag parameter is in the range between 0.8 and 1.5. The coefficient of inertia is close to 2.0. To see how much these parameters affect the model, several test simulations has been conducted to see the effect of changing parameters. For all the models that have been tested, values for Cd is between 0.8 and 1.6 and for Cm between 1.6 and 2.2. The results differ for each model because they have different geometry. There are also other variables that matters; for example the TLB Simple have different coating layer as TLB B and X3. This means that each model may require different values for Cd and Cm.

According to the earlier studies of the drag coefficients should be in the area between 1 and 1.5 and the inertia coefficient should be around 2. (Det Norske Veritas RP-C205, 2010). Sarpkaya and Isaacson suggests that the  $C_d < 1.0$  for  $KC < 4$ .

The coefficient testing was done through running the simulation of each model several times and collect data to compare with the experiment. The coefficients that gave results closest to the experiment were chosen. More important than a fitting curve is maximum and minimum amplitude of the measured parameter.

Figure 68 to Figure 73 are plots of the UX movement of the wind turbine in 0.3 meter, 1.58 second period waves. The plots show that neither the drag coefficient or the inertia coefficient has very large impact on the movement of the wind turbine.

Table 18: Table of tested coefficients in drag/inertia coefficient test

Drag coefficient test		Inertia coefficient test	
Drag coefficient	Inertia coefficient	Drag coefficient	Inertia coefficient
0.8	2.0	1.3	1.6
1.0	2.0	1.3	1.8
1.2	2.0	1.3	2.0
1.4	2.0	1.3	2.2
1.5	2.0		
1.6	2.0		

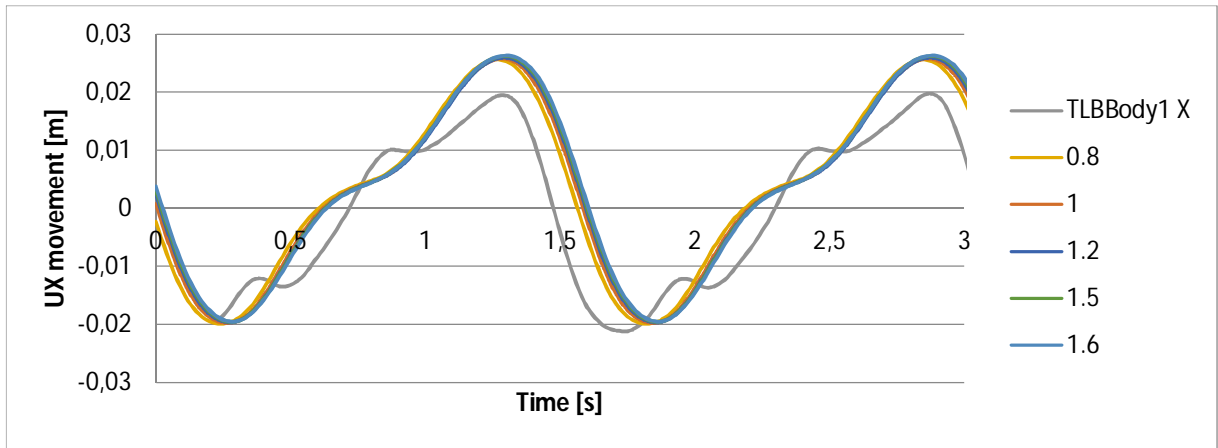


Figure 68: Drag parameter testing TLB S (tested with  $C_m = 2.0$ )

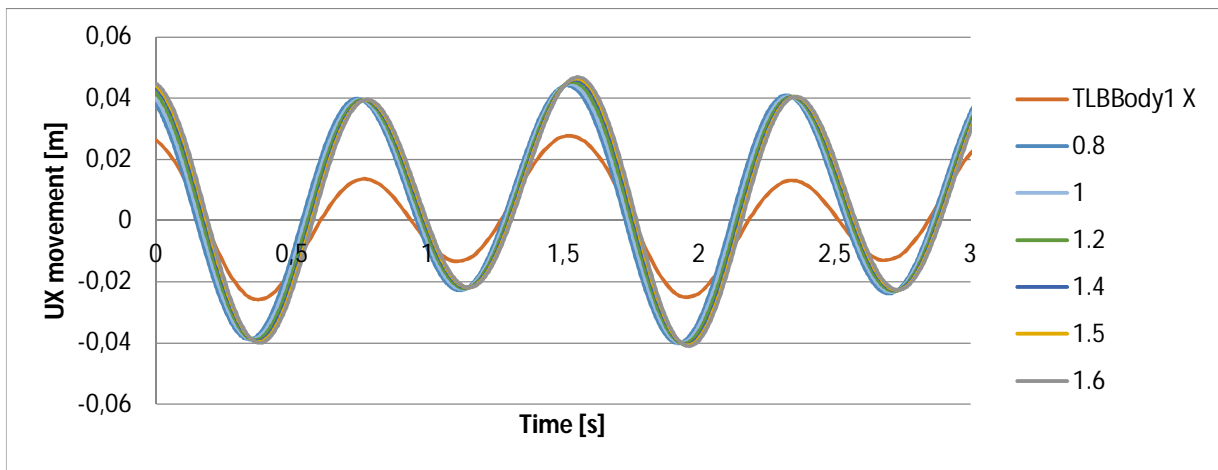


Figure 69: Drag parameter testing TLB B (tested with  $C_m = 2.0$ )

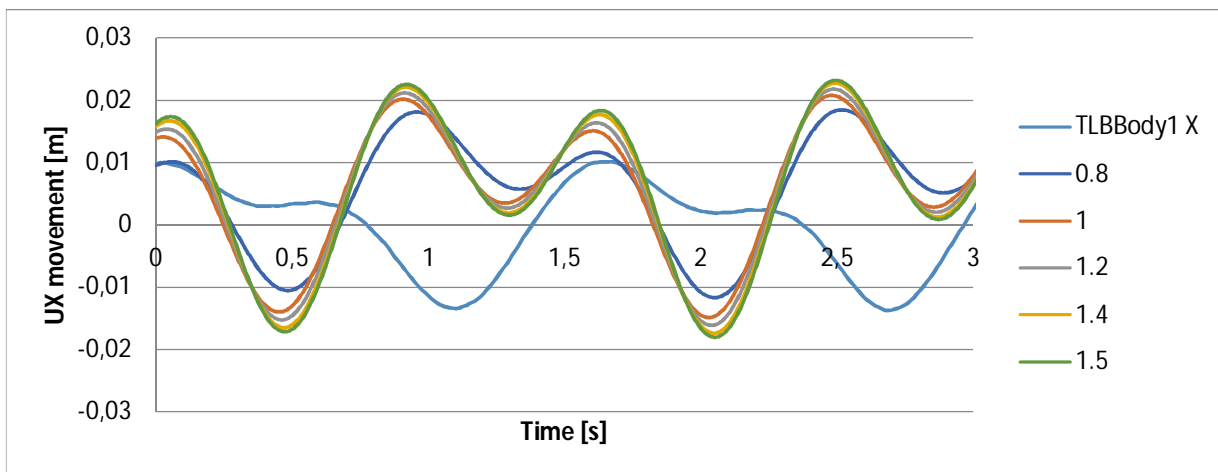


Figure 70: Drag parameter testing TLB X3 (tested with  $C_m = 2.0$ )

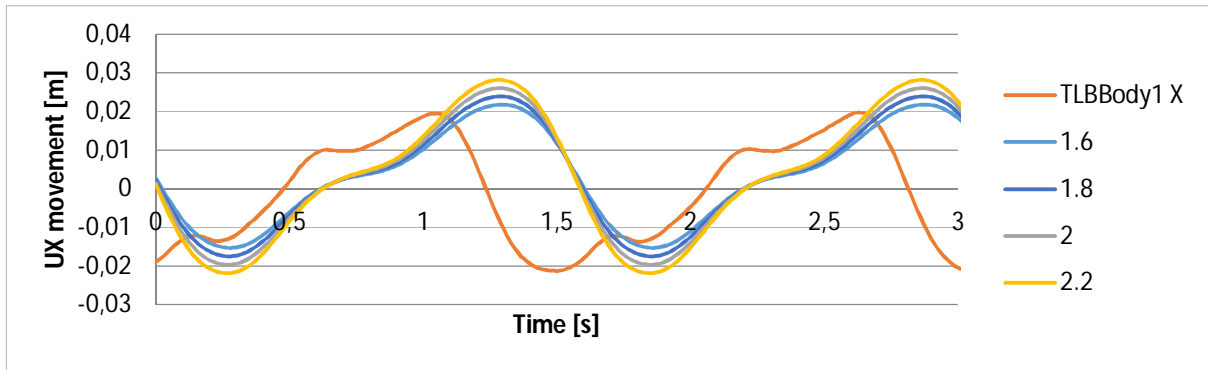


Figure 71: Parameter testing of coefficient of inertia on TLB S (tested with  $C_d = 1.3$ )

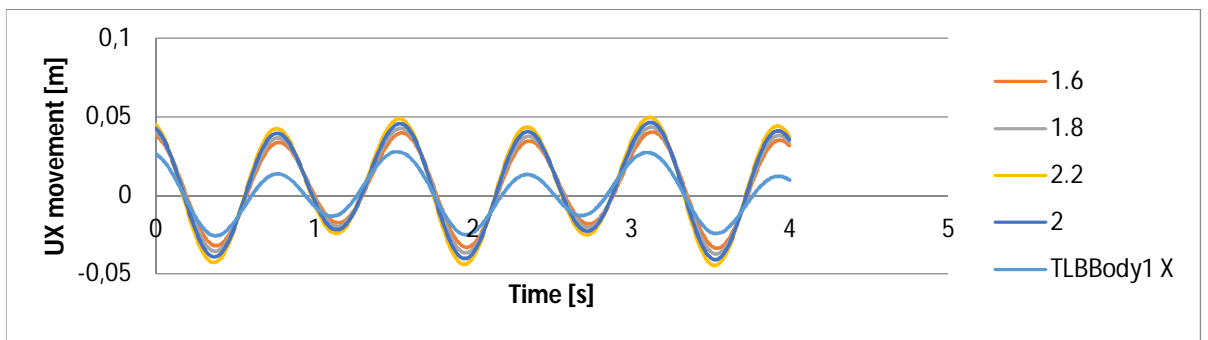


Figure 72: Parameter testing of coefficient of inertia on TLB B (tested with  $C_d = 1.3$ )

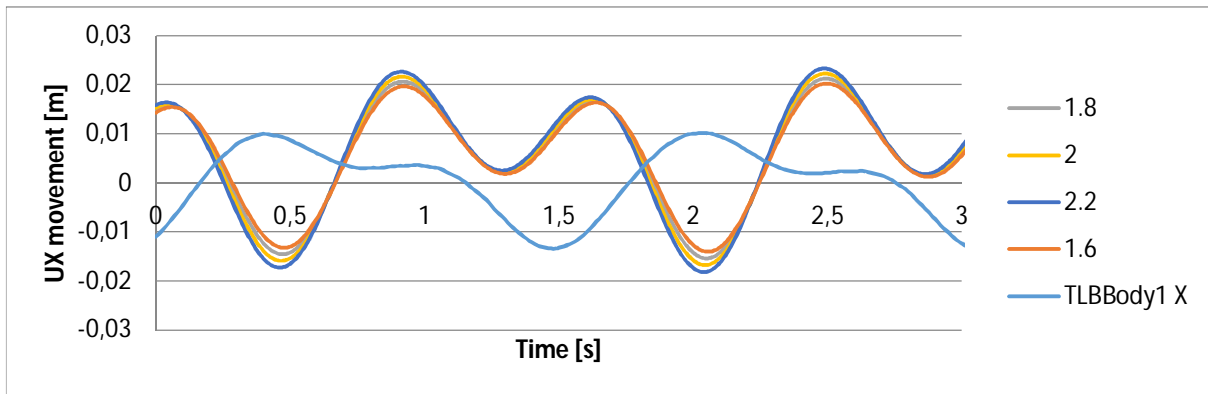


Figure 73: Parameter testing of coefficient of inertia on TLB X3 (tested with  $C_d = 1.3$ )

The parameter study of the drag coefficient and inertia coefficient reveals that they have an effect on the results. They do not have large enough effect to bring the results from the experiment and simulation together. By changing the coefficients significantly we might be able to come close to the experimental results, but that would not comply with the authorities on the field (Det Norske Veritas, 2010) (Sarpkaya & Isaacson, 1981) There are other sources to this difference. The parameter test does not approve or disprove any of the parameters.

Table 19: Coefficients of drag and inertia shows the values for the drag coefficient and inertia coefficient that is used for the further simulations. 1.3 is chosen as Cd parameter because it is in the middle of what is recommended by DNV. (Det Norske Veritas, 2013) Cm is set to 2.0 because it is recommended by DNV.

Table 19: Coefficients of drag and inertia

	Cd	Cm
TLB Simple	1.3	2
TLB B	1.3	2
TLB X3	1.3	2

## 6.5 Eigen periods:

All of the Eigen periods are below The Eigen modes from the three models are of the same modes, but they have different values. These figures are extracted from ANSYS with the modal analysis solver. They are extracted without the damping effect of water and therefore not directly comparable with the eigen periods from the experiment. The eigen values for yaw and bending are not included in the table.

Table 20: Eigen periods calculated in ANSYS

	TLB S	TLB B	TLB X3
Surge	0.63	0.73	0.75
Sway	0.63	0.73	0.75
Heave	0.35	0.54	0.54
Pitch	0.26	0.68	0.69
Roll	0.26	0.67	0.68
Yaw			

The Eigen periods mainly a result of the mooring line stiffness, but they are also sensitive to changes the anchor height and the anchor line angle. It seems like a 45-degree angle from the anchor point to center of gravity gives the highest Eigen period/lowest Eigen periods. The yaw Eigen period varies from 0.4 to 2 sec. To find the exact Eigen periods anchor depth needs to be exact. Table 20: Eigen periods calculated in ANSYS does not deliver the yaw eigen period values properly so they must be calculated separately.

### 6.5.1 Yaw eigen period

Because of numerical errors, the yaw Eigen period cannot be found just by a modal analysis in ANSYS. The stiffness from the lines does not have an effect before the model has rotated a certain angle. The modal analysis assumes that there is just a small rotational stiffness in the model and overestimates the yaw Eigen period. To solve this problem, springs with a constant rotational stiffness must be applied. For the yaw Eigen period test there is no waves involved. The stiffness of the spring, or spring constant is found through three steps:

1. Find the rotation of the node in the water line for each model without any applied force in order to find how much the model rotates by itself.

2. Afterwards a torque of 0.002 Nm is applied at the same node and rotation is found again.
3. The spring constant is the applied torque divided by the change in rotation

$$\tau = -k \times \Delta\theta \rightarrow k = -\frac{\tau}{\Delta\theta} \quad \text{Equation 16}$$

Where:

- k is the spring constant
- $\tau$  is the applied Torque
- $\theta$  is the change in rotation (angle of rotation from applied torque)

Table 21: Finding and controlling yaw Eigen periods

Rotation of:	Without Force	with Force	difference
TLB Simple (node 12)	-0.00098105	-0.000969	-1.20E-05
TLB B (node 32)	-0.0022942	-0.00228	-1.42E-05
TLB X3 (node 48)	-0.0016349	-0.001618	-1.66E-05
Torque [Nm]			0.002
Spring constant K for Eigen period analysis			
TLB Simple			-167.36
TLB B			-140.85
TLB X3			-120.48
Eigen period Yaw		Decay test	ANSYS
TLB Simple			0.17
TLB B		0.21	0.22
TLB X3		0.21	0.23

There is a difference between the observed experimental yaw Eigen period and the calculated. The difference is around 0.01 s for both TLB B and X3.

Table 22: Difference in eigen periods between experimental decay tests and simulated decay test results

	TLB S	TLB B	TLB X3
Sim Heave	0.35	0.49	0.55
Sim Pitch	0.28	0.80	0.80
Exp Heave	0.35	0.53	0.57
Exp Pitch	0.25	0.71	0.74
Difference Heave	0 %	7 %	3 %
Difference Pitch	-12 %	-13 %	-8 %

Table 22 shows other values for the eigen period of the simulated eigen periods than the modal analysis Table 20. This is because the decay test results include the water, while the modal analysis does not. There are uncertainties in these figures, but they illustrate variation that can be seen in the eigen values, and that they will affect the results in the comparison. Figure 51 to Figure 54 shows that the prototypes are more responsive to waves close to their eigen periods. If the eigen period is different it will effect the response to a slightly different range of wave periods and therefore change the results.

## 6.6 Calibrating simulated damping parameters

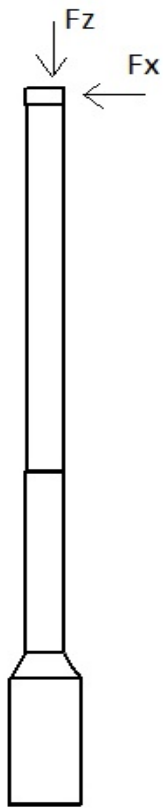


Figure 74: Illustration of decay loads

The decay tests from the experiment is used to calibrate the damping parameters in the simulation. The purpose is to make the damping in the simulation equal in its progress. That involves making the simulation and experiment have the same amplitudes and decay fully at the same time. The simulation models has been set up with a pitch damper and a heave damper to adjust the movement to the experimental decay in the best possible way. The decay experiments were done on the Surge/Pitch motion and on the heave motion. The model was pushed three-four times for each model to be sure that the test provided proper results. The force of about 35 N in the x-direction induces a surge/pitch motion. The top node was pushed with a force of about 15 N in the negative z direction to start the heave motion. Attempts were made to create a yaw decay test as well, but these results includes a lot of disturbance and were not used to tune the damping.

The results from the calibration of the models are the best fits after a long series of parameter testing for each decay test



### 6.6.1 TLB S

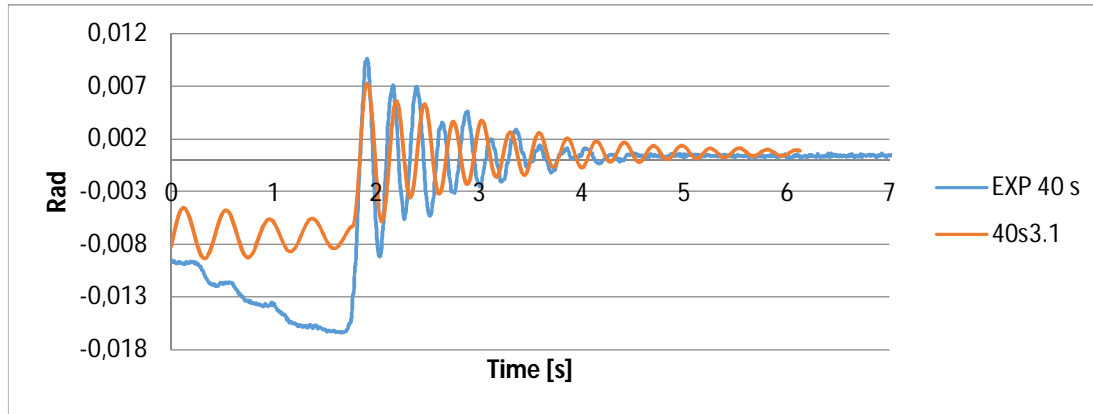


Figure 75: Decay pitch/ROTY

Table 23: Best fitting parameters for the TLB S decay test

	Fz	Fx	ALPHAD	BETAD	Cd	Cm	Heave-damp.	Pitch-damp.
Test 40h4.4	-15	-	0.18	0.0018	1.3	2	10	70
Test 40s3.1	-	-35	0.18	0.0018	1.3	2	10	70

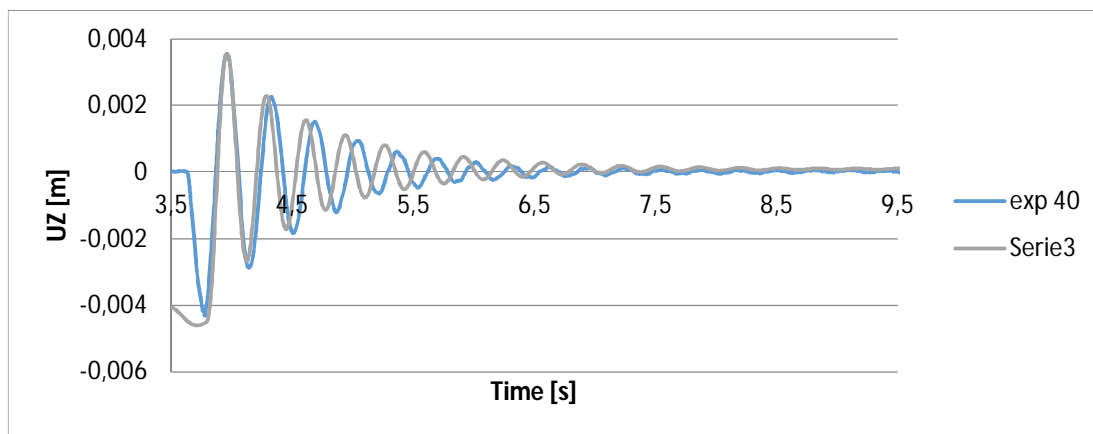


Figure 76: Simple decay heave

There is much disturbance in the experimental pitch decay for TLB S and so also for the simulation. This is likely because the prototype is very light and the pitch movement is under influence of the surge movement. This is not a very good and reliable test for this prototype.

The heave movement is much tidier and the decay is similar in experiment and simulation except for the period.

In both the pitch decay it can be observed that eigen period is shorter for the experiment than the simulation. This is consistent with deviation in eigen periods from Table 22.

## 6.6.2 TLB B

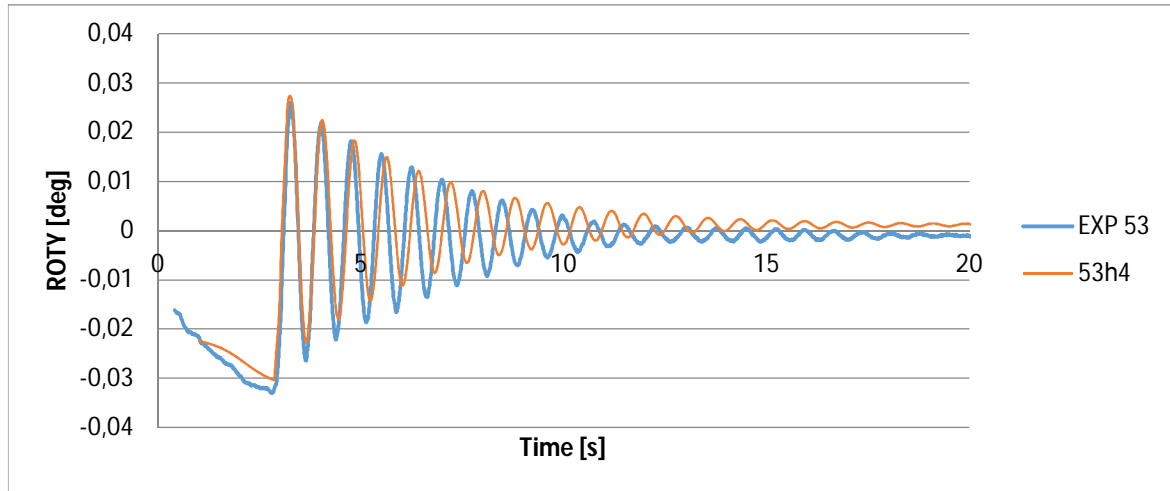


Figure 77: Test 53: TLB B Decay pitch

Table 24: Best fitting parameters for the TLB B decay test

	Fz	Fx	ALPHAD	BETAD	Cd	Cm	heave-damp.	Pitch-damp.
Test 53heave1	-13	-	0.18	0.0018	1.3	2	12	25
Test 53h4	-	-35	0.18	0.0018	1.3	2	12	25

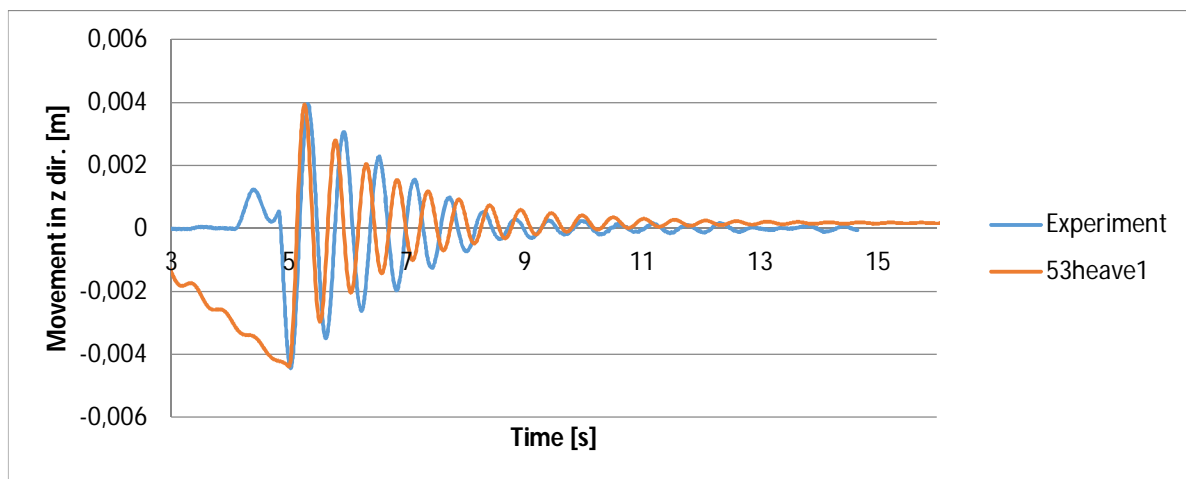


Figure 78: Damping of heave motion (UZ)

The damping is a little too high early in the damping progress for both heave and pitch decay, but the difference between experiment and simulation evens out later. There are differences in the eigen period between experiment and simulation as seen in the TLB S decay plots also.

There is less disturbance in the TLB B decay tests than for TLB S. This indicates stable and reliable results from the decay test.

### 6.6.3 TLB X3

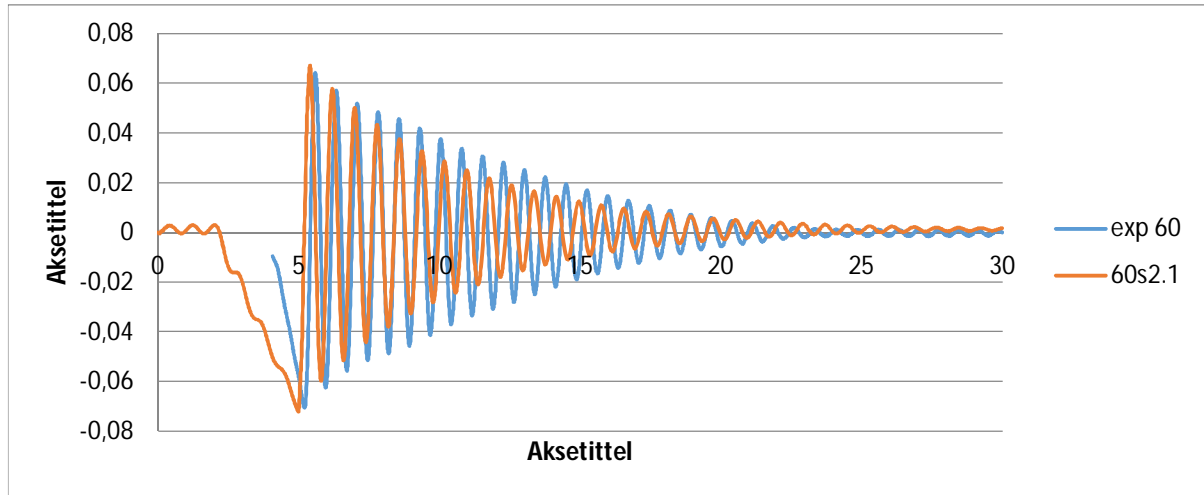


Figure 79: TLB X3: Decay pitch

Table 25: Best fitting parameters for the TLB X3 decay test

	Fz	Fx	ALPHAD	BETAD	Cd	Cm	Heave-damp.	Pitch-damp.
Test 60h2.2	-8	-	0.18	0.0018	1.3	2	12	10
Test 60s2.1	-	-80	0.18	0.0018	1.3	2	12	10

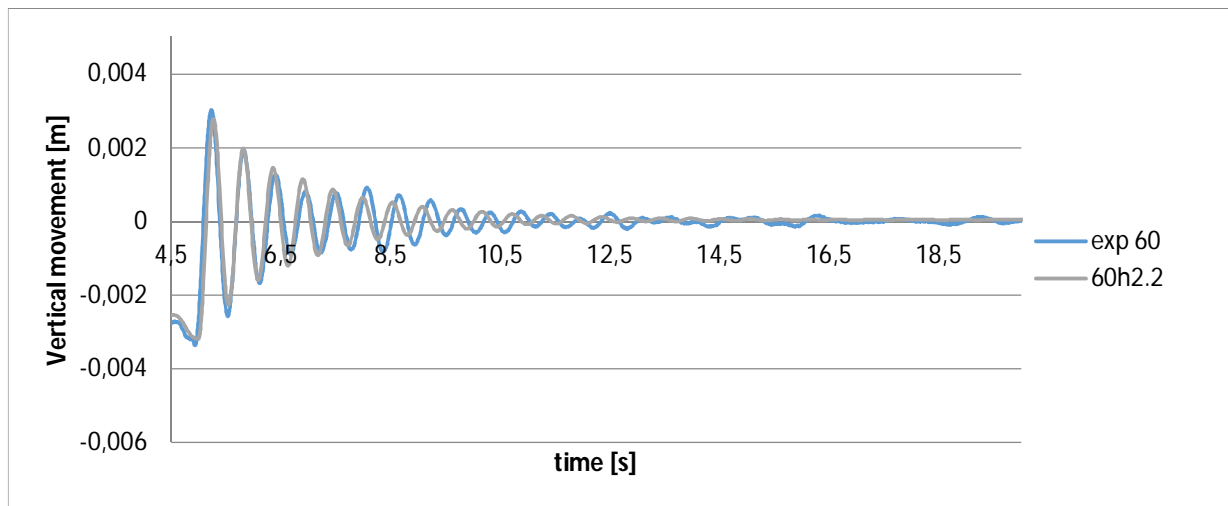


Figure 80: TLB X3: Heave decay (UZ)

The pitch movement in the experiment decays faster in the first part while the simulation catches up towards the end. The movement dies out simultaneously.

The calibration of the damping reveals that there is a difference in the period of decay in the experiment and in the simulations for all Eigen period modes. This indicates that the simulation models does not have the right eigen periods.

After adjusting the damping parameters to fit the decay tests, the parameters for the models are set to:

Table 26: Damping parameters all models

	ALPHAD	BETAD	Heave damping	Surge/Pitch damping
TLB Simple	0.18	0.0018	10	70
TLB B	0.18	0.0018	12	25
TLB X3	0.18	0.0018	12	10

The parameters have been tested against the decay experiments.

The surge decay test included some disturbance on the surge/pitch experiment that cannot be seen in the other experiments. There is some of the same disturbance in the simulation of the same case. It is possible that the TLB S are on the edge of being too light, compared to its size.

None of the models is especially sensitive to changes in the Alpha damping and the Beta damping. Attempts on the decay tests with ALPHAD = 0.28 and BETAD = 0.0035 were made and it gave very similar results as with 0.18/0.0018. 0.18 and 0.0018 was chosen because scaled versions of them has been used for the full-scale simulations. (0.0018/0.018)

These values has proven to be right for the decay tests, but they do not give exact results on the wave simulations. This is probably a result of model errors and friction in the experimental system. The difference in the parameters between the models is a result of the different mass and geometries of the model. The simple has a higher surge/pitch damping because it has a large diameter compared to its mass. It is closer to over damped. The TLB X3 has a small diameter in the range of the waves because of its three column construction. This means that it moves easier sideways in the water. The heave damping is almost the same for all models because of the area at the bottom of each model are close to similar.

The experiment seem to have a longer eigen period than the simulation, since the period of the decay motion is longer for the experiment than for the simulations. The same deviation can be seen in both the TLB S decay test and the decay test of TLB X3. The reason can be a difference in mooring line stiffness or pretension in the mooring lines.

## 6.7 Control of wave loads in ANSYS

This is a test with deep water Airy waves used on the TLB S to control that hand calculations and ANSYS gives the same results. This will indicate that the model is right. To do the hand calculation Morison's equation is used with Airy wave theory as found in DNV-RP-C205. I have chosen wave height, period and depth of the sea in order to come close to the domain of the Airy theory (see figure with ranges of validity of wave theories)

The model has been tested with a drag coefficient = 1 and wave height = 0.1 m. This is not necessarily the same as in the simulation and experiment, but what is important is that the same parameters are used in both the hand calculation and FEM code in the test.

Table 27: Input values for the hand calculation

Control parameters		Input for calculation		ANSYS
Wave length	$\lambda$	25.48	m	
Wave number	$k$	0.25		
water density	$\rho$	1026.00	kg/m3	
Coefficient of drag	$C_d$	1.00		
coefficient of inertia	$C_m$	2.00		
Diameter of cylinder	$D$	0.25	m	
Height of waves	$H$	0.10	m	
length of cylinder	$z$	-1.09	m	
Period of waves	$T$	4.04	s	
Max force of inertia		11.69	N	11.762
Max force of Drag		0.66	N	0.772

$$dF = dF_M + dF_D = C_M \rho A \ddot{x} dz + C_D \rho \frac{D}{2} |\dot{x}| \dot{x} dz \quad \text{Equation 17}$$

$$\ddot{x} = \frac{2\pi^2 H}{T^2} e^{kz} \sin \theta \quad \text{Equation 18}$$

$$\dot{x} = \frac{\pi H}{T} e^{kz} \cos \theta \quad \text{Equation 19}$$

$$\int dF = \int F_M + dF_D dz \quad \text{Equation 20}$$

$$F_M = C_M \rho A \frac{2\pi^2 H}{kT^2} (1 - e^{-1.094k}) \sin \theta = 11,688 \sin \theta \quad \text{Equation 21}$$

$$F_D = C_D \rho \frac{D}{2} \frac{\pi^2 H^2}{2kT^2} (1 - e^{2*1.094k}) \cos^2 \theta = 0,656 \cos^2 \theta \quad \text{Equation 22}$$

Equation 21 states that  $F_M$  is at largest, when  $\sin(\theta) = 1$ ,  $\cos^2(\theta) = 0$  and  $F_D = 0$ . The maximal force from the waves working on the TLB S is 11,688 N in the horizontal direction. The result from the test in ANSYS gives reaction solution in the anchor points. The sum of forces in the wave propagation direction is 11,77 N. This is very close to the hand-calculated result of 11.69 N. The hand calculation verifies the results of the TLB S. The applied horizontal force on the TLB S is very similar to the hand calculated force. The wave theory used for the calculation is not the one that will be used in the further simulation and the calculation is only conducted for the TLB S.

The TLB S returns good results when compared to the hand calculated results. This indicates that the sum of forces exerted on the simulation model is approximately right, but the forces are uncorrectly distributed on the nodes. It is more likely that the vertical forces are miscalculated by ANSYS than the horizontal forces because the lids in the horizontal planes are not modelled to absorb ocean loads.

## 7 ANSYS APDL Results

The following simulations has been conducted with Stokes 5. Order wave theory. Tests with Airy wave theory have also been done, but with no significant difference in results. The chapter shows result from three simulations, one for each prototype. When something has been unclear other simulations has been used to clarify. The effects that is commented in these simulations has been checked in other simulations. If the effects can be seen in other experiments on the same prototype, but not the other this is considered a prototype specific effect. If it is only seen in one or a few experiments, another explanation variable must be found.

To avoid noise and disturbance it has been decided to analyze the wave cases with a minimum of problems. The three simulations that has been subject to further analysis in this chapter is simulation 37, 45 and 67. They are chosen because they show a smooth movement.. The probability for successful simulation is higher for these load cases than for the other. This is also because of the simplicity of the TLBS. Load case 45 and 67 is also picked for closer examination because they hav a wave period and wave height that is moderate.

Table 28: Table of experiments used for the analysis

Simulation	corresponding experiment	Wave period	Wave height
37	37	2.5 s	0.5 m
45	45	1.58 s	0.3 m
67	67	1.58 s	0.3 m

### 7.1 Simulation 37: TLB S, 2.5 sec, 0.5 m

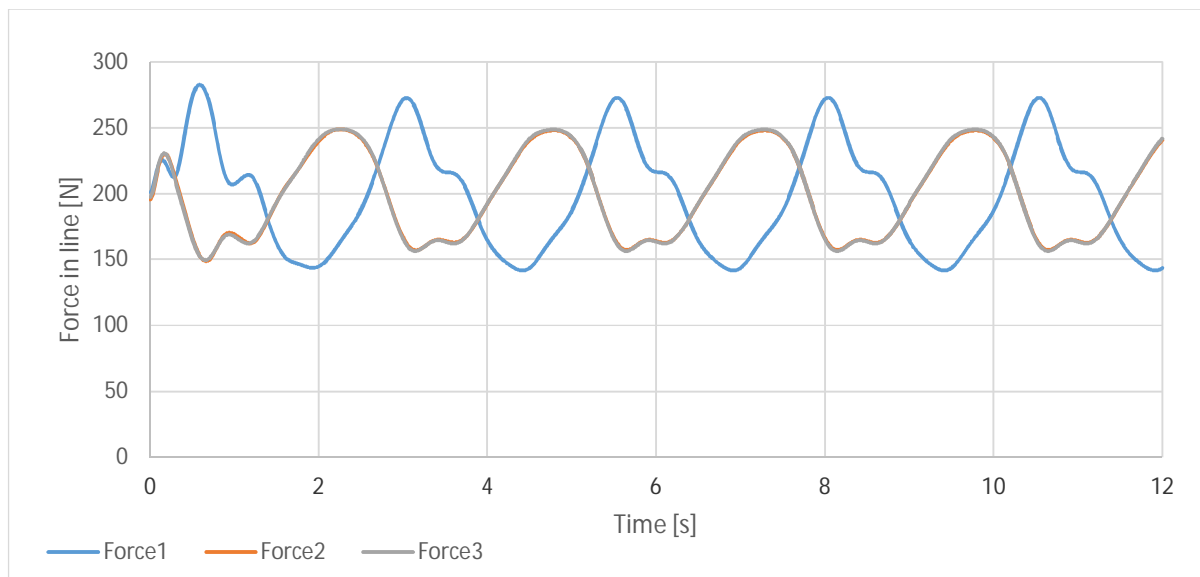


Figure 81: Forces in lower lines load case 37

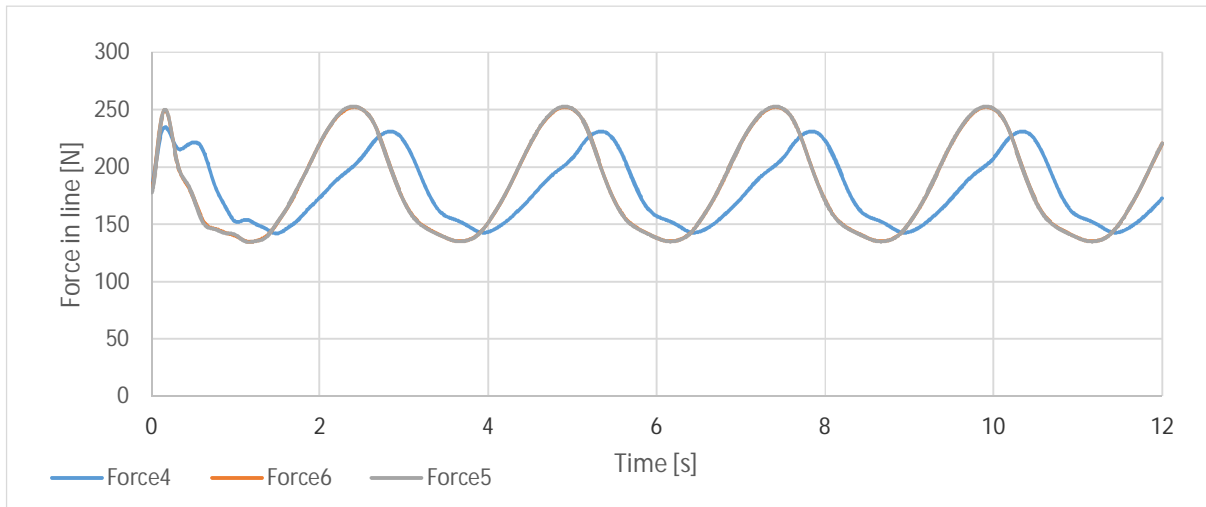


Figure 82: Forces in upper lines load case 37

The force in line 2,3,5,6 is at their maximum at the same time. This is the same time as the x and z translation is at their top.

There is a smaller phase offsets in the upper lines than lower because the heave movement induces loads in all the upper lines at once, while the lower lines are less affected by the heave movement. This is a sign of the model working properly.

The forces in line one and four is at their maximum when the x movement is at its lowest. This makes sense, since the prototype is furthest away from the mooring point of one and four at this stage. Line one and four has pointier tops and bottoms than the other lines.

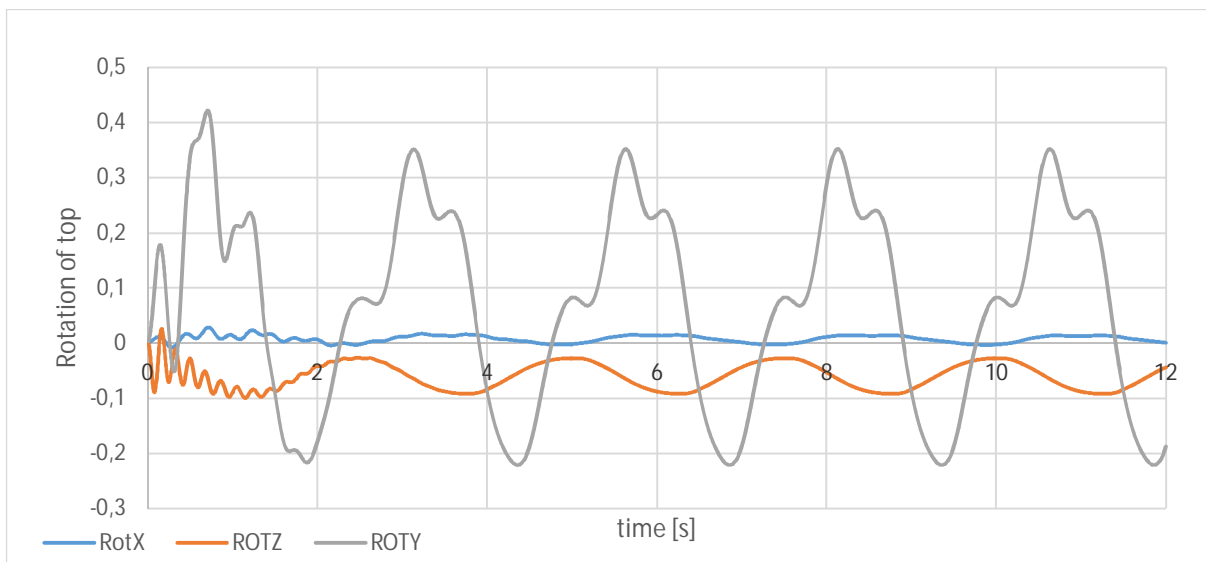


Figure 83: Rotational movement load case 37

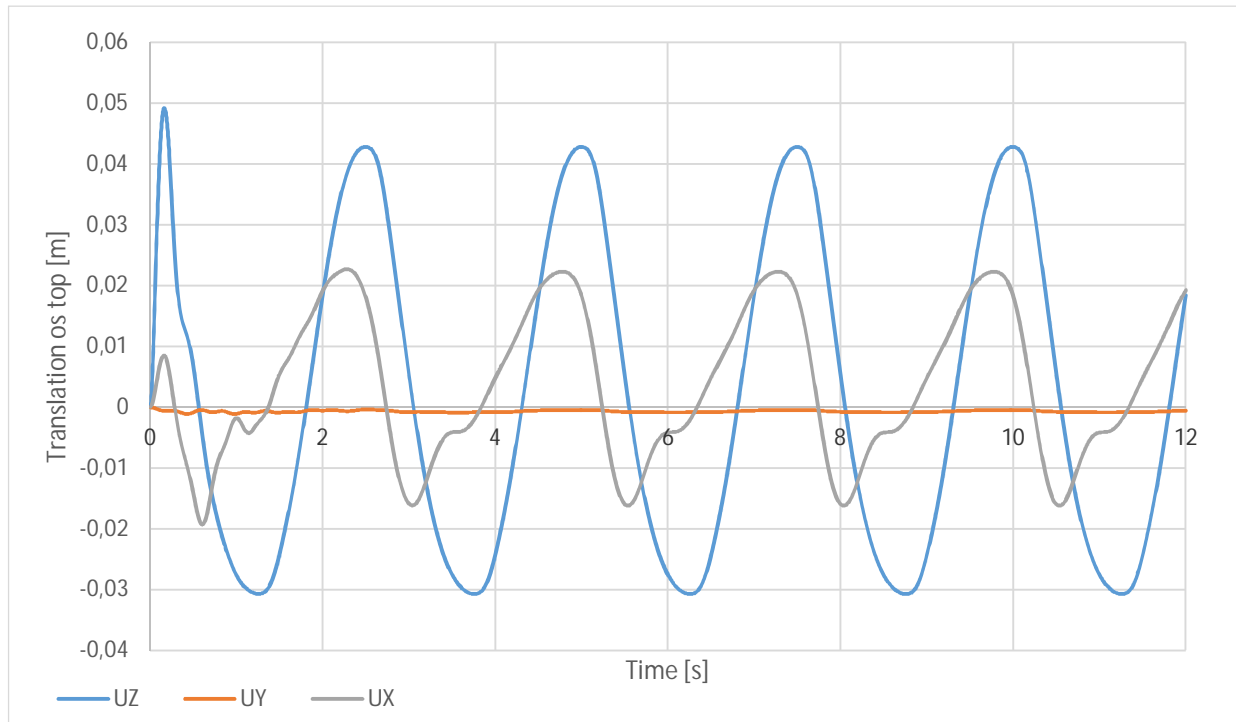


Figure 84: Translational movement load case 37

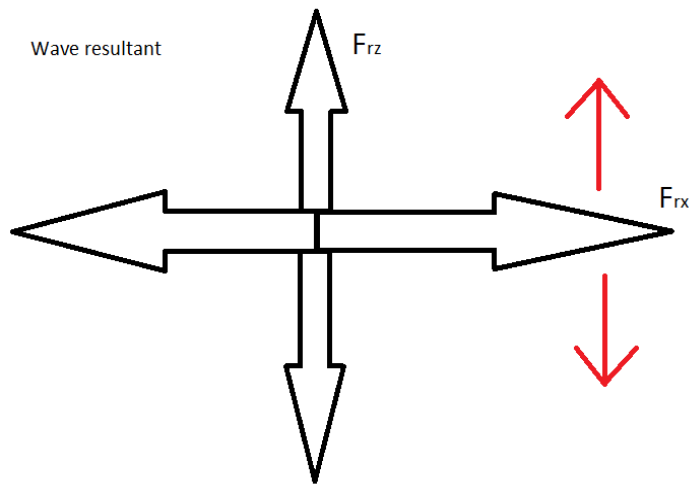
There is almost no roll in the simulation. This is good sign because no forces is applied in the direction perpendicular to the waves. This is also an indication that the model is stable.

The transient movement stops after about three seconds, and becomes harmonic. This is important because it leaves with little disturbance in the results.

One of the most interesting observations is that the pitch movement is out of phase from the UX translation. This is likely to have something to do with the resultant force of the wave. Closer to a wave trough the resultant force is deeper and it does not apply a moment around a center of rotation. When the resultant force is below the center of rotation a positive surge motion and a negative pitch motion is observed. When the resultant force is above the center of rotation, a positive surge/positive pitch is also present.

The center of rotation changes with the angle of the lines and the forces in the lines in addition to the position of the turbine relative to the wave resultant. The vertical wave resultant works on the prototype on the same point at all times, the point of buoyancy. The horizontal resultant force oscillates in the z direction depending on the wave height. This changes the momentum around the prototypes center of rotation and forces it to rotate around its y axis (pitch movement). This is the reason why the surge motion is followed by a pitch motion as the wave rises. When the prototype moves back again from its surge movement, the prototype stay in a positive pitch until rotates back again when the positive surge movement has started once more. The movement can look a little like a slow whip.





The prototype moves very fast backwards after the top in x translation. This means that when the force from the wave disappears and goes negative in x direction the prototype is subject to two negative forces. The the force from four stretched lines (2,3,5 and 6) plus the negative wave force. This makes it move backward more then twice as fast as it moves in the positive x direction. This observation cannot be seen in cases with lower waves where the movement is more sinusoidal.

Figure 85: Wave resultant working on the model

The results from loadcase 29 have been checked to control the findings in load case 37. The same movements and the same force variations is present in experiment 29 as they are seen in experiment 37. Force in line 1 is phase shifted from force in line 2 and 3 the same amount of time as in sim37. The only difference is that the curves are more sinusoidal in their shapes in sim29. This can especially be seen in the UX translation.

## 7.2 Simulation 45: TLB B, 1.58 sec, 0.3 meter

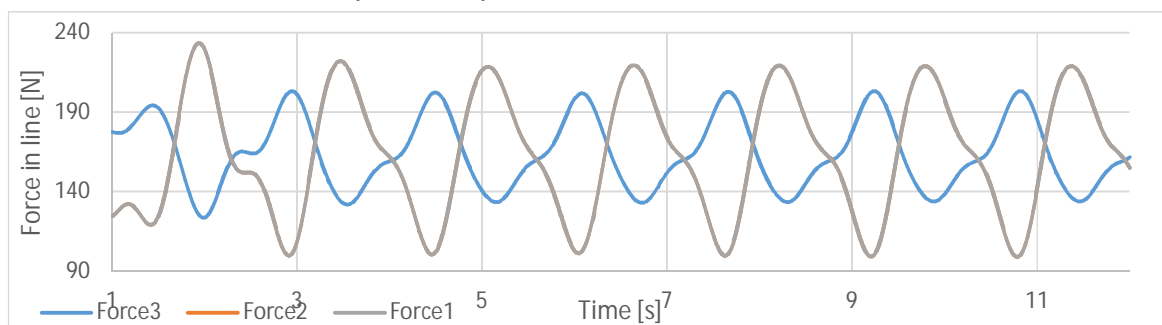


Figure 86: Forces in lines load case 45

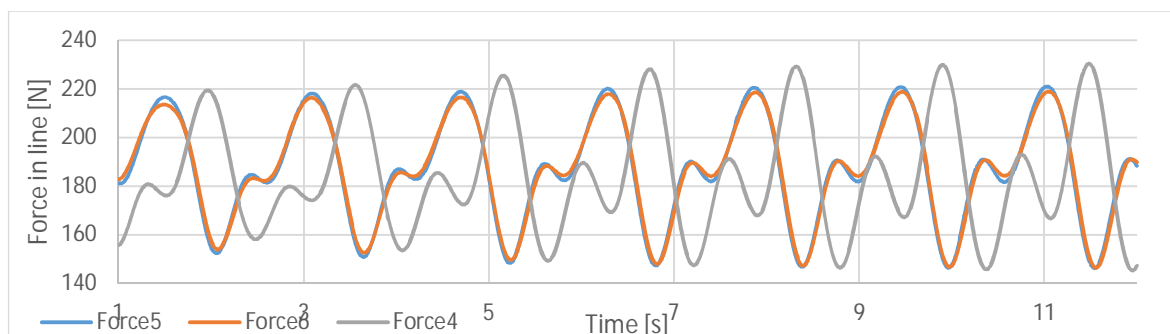


Figure 87: Forces in upper lines load case 45

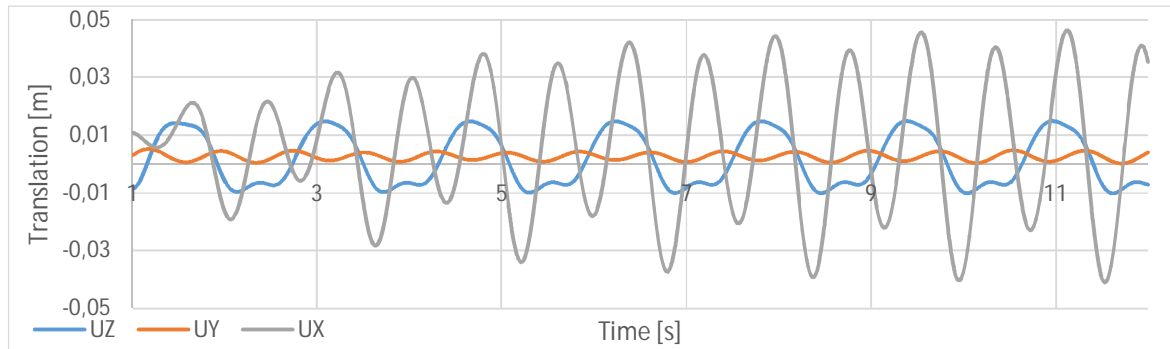


Figure 88: Translation in load case 45

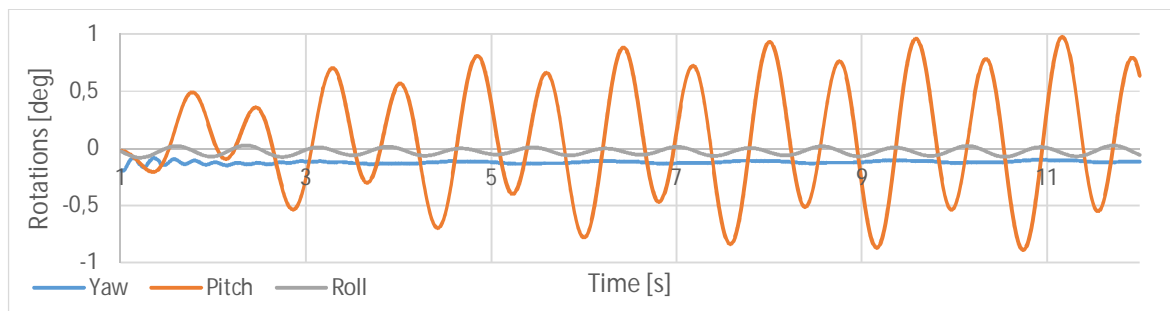


Figure 89: Rotation in load case 45

The first thing to observe from simulation 45 is that line one has almost twice as large amplitude as line two and three. The translation chart provides the explanation. There are large x translation and smaller z translations. Line one and four is alone in taking up forces in x direction on one side of the floater, while line two, three, five and six share the force on the other side. Since the amplitudes in the upper tide is relatively similar this is also an indication that the lower lines takes up much of the surge movement and the upper lines takes up heave and pitch movement.

Another thing to observe is the coincidence of the pitch and UX movement. They look like they follow each other almost perfectly. The reality is that the UX translation is the sum of the pitch plus surge movement in the entire prototype. The UX translation has its deeper bottoms at the same time as the pitch has its shallow bottoms and vice versa. The UX has its highest tops at the same time as the pitch is at its tops. It cannot be told from just the UX translation what the surge movement is. The pitch must be compensated for. What this also tell is that the attack point of the wave is above the balance height of the TLB B. The TLB B could be made more stable against pitch be changing the height of the mooring points.

### 7.3 Simulation 61: TLB X3, 0.95 sec, 0.13 m

The X3 turns negatively around the z axis and positively around the x and z axis in the load case 61 with 0.13 m/0.95 sec wave motion. It simply tips a bit over forward and against left if the wind turbine is seen from upstream. The reason is that line three and six has 10 N less of pretension. The pretension numbers is the same as measured in the experiment and they are likely to influence the results in the experiment as well.

### 7.4 Simulation 67: TLB X3, 1.58 sec, 0.3 m

Simulation 67 is a 1.58 sec and 0.3 meter wave case of the TLB X3

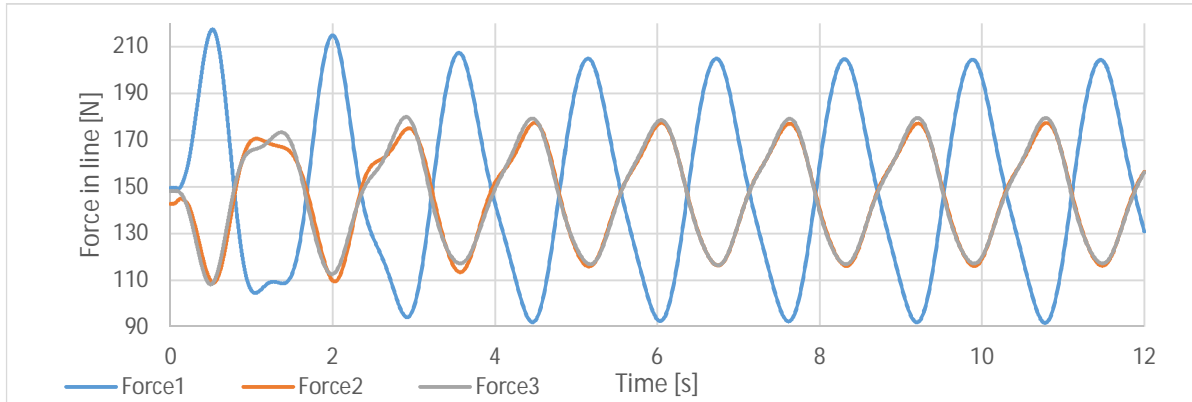


Figure 90: Forces in lower lines simulation 67

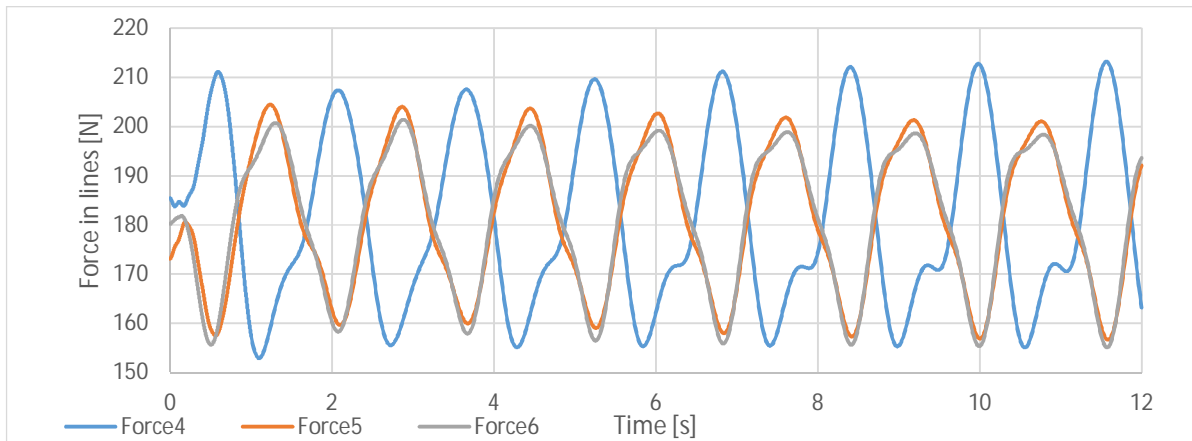


Figure 91: Forces in upper lines simulation 67

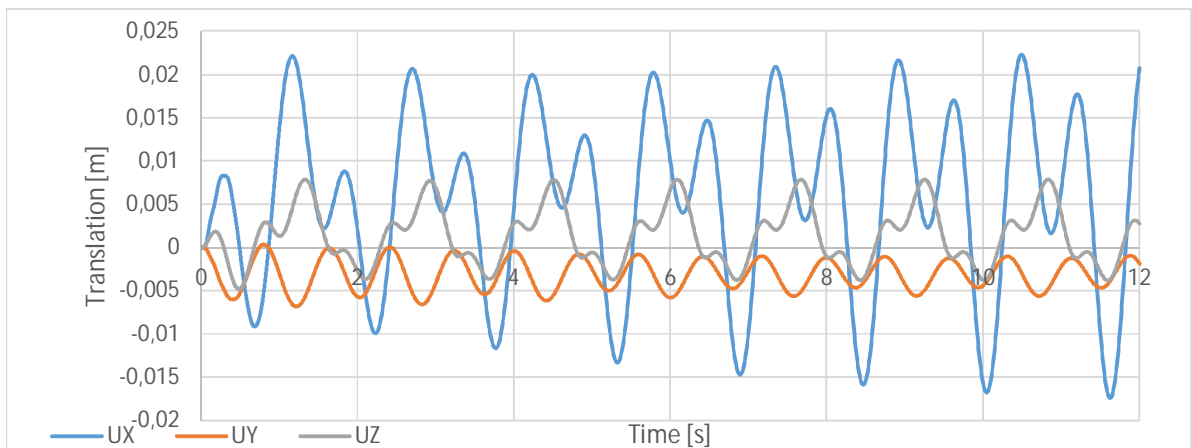


Figure 92: Translation in simulation 67

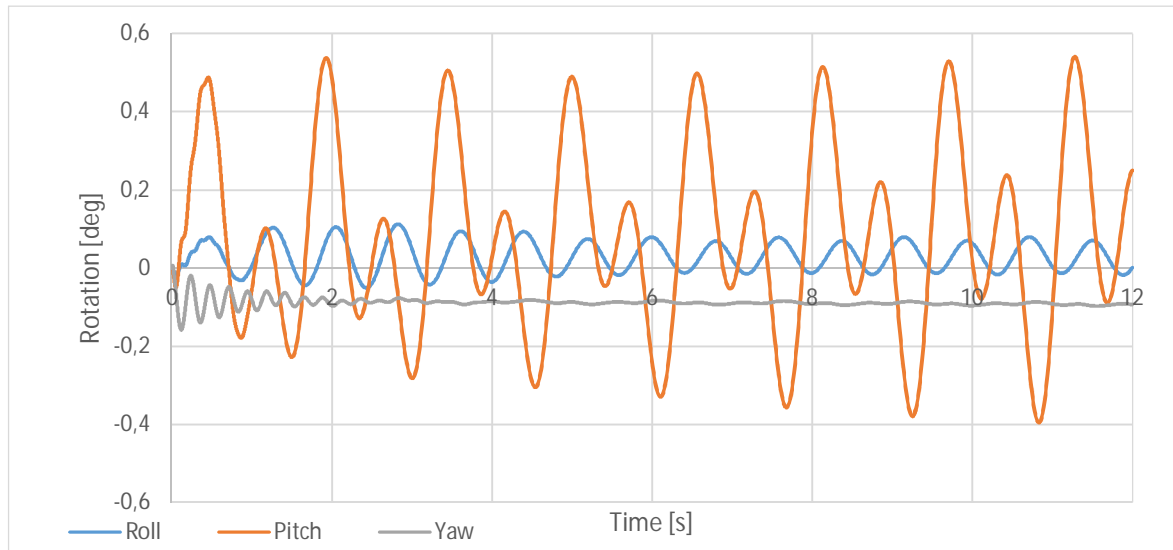


Figure 93: Rotations in simulation 67

The force in line one and four is countercyclical to the other lines. Both line one and four is at their maximum when UX is at its minimum. The highest tops in UX is at the lowest tops of pitch. The lower tops in UX is at highest tops of pitch. This means that the UX movement is more pitch independent in the TLB X3 than the TLB B. This is good considering because it keep the nacelle from moving too much.

The heave translation amplitude is 0.5 cm. This is 3.3 percent of the wave amplitude which is very little.

## 7.5 Summarizing discussion of simulation results

The UX translations is about half of what is seen in simulation 45. This is not the result of a smaller area because there are perpendicular to the wave propagation direction is  $0.29 \text{ m}^2$  on both models. Instead it's the fact that the area is deeper under sea level on the TLB X3. The wave theory states that the horizontal force of waves decreases with depth below sea level. Because of this the resultant force from the waves is moved deeper and will be smaller on the TLB X3 than TLB B.

In the rotation chart, some roll movement can be seen on the negative side of zero. This indicates an instability in the model that forces the TLB B top tip over slightly. This instability is strengthened by a constant negative yaw.

Drag parameter: There is uncertainty about the drag parameter. It is possible that it should be lower than 1.0 (Sarpkaya & Isaacson, 1981). If we look to DNV (Det Norske Veritas, 2010), they say it should be between 1.0 and 1.5. while princeton.edu suggests a  $C_d$  around 1.5. A drag parameter of 1.3 gives the better fit to the experiment.

There is also uncertainty around the  $C_m$ . Sarpkaya and Isaacson says that it is higher than 2.0 for Keulegan Carpenter numbers smaller than 4.0. DNV says that it should be 2.0. (Sarpkaya & Isaacson, 1981). We have chosen to use  $C_m = 2.0$ . Some of the difference in experimental simulated results are likely to be caused by drag and inertia coefficients being different for different wave cases and also between models.

### 7.5.1 Separating surge movement from pitch movement

It is in the interest of the analysis to separate the movement in UX direction and pitch rotation because this gives a high velocity at the top of the nacelle. This high velocity will cause extra problems for the turbine when it produces power and it does add extra stress to the mooring lines and construction as a whole. It seems like the TLB S is better at separating the surge and pitch movement. One reason for this might be that the TLB B has its eigen period in both pitch and surge direction in the wave specter of test 45. It might be different in other cases. It might also be because the TLB S is better balanced. This might be an unfair comparison since the TLB S is just a pipe in the water and not close to be an imitation. Nevertheless, it should be a goal to grasp for the TLB B and X3.

The forces in the upper lines Has an extra top more visible on line four than line five and six. This is a result of the double movement of the pitch rotation. If it were the surge movement, it would be more prominent in the bottom lines. This will cause extra fatigue in the mooring lines and anchors.

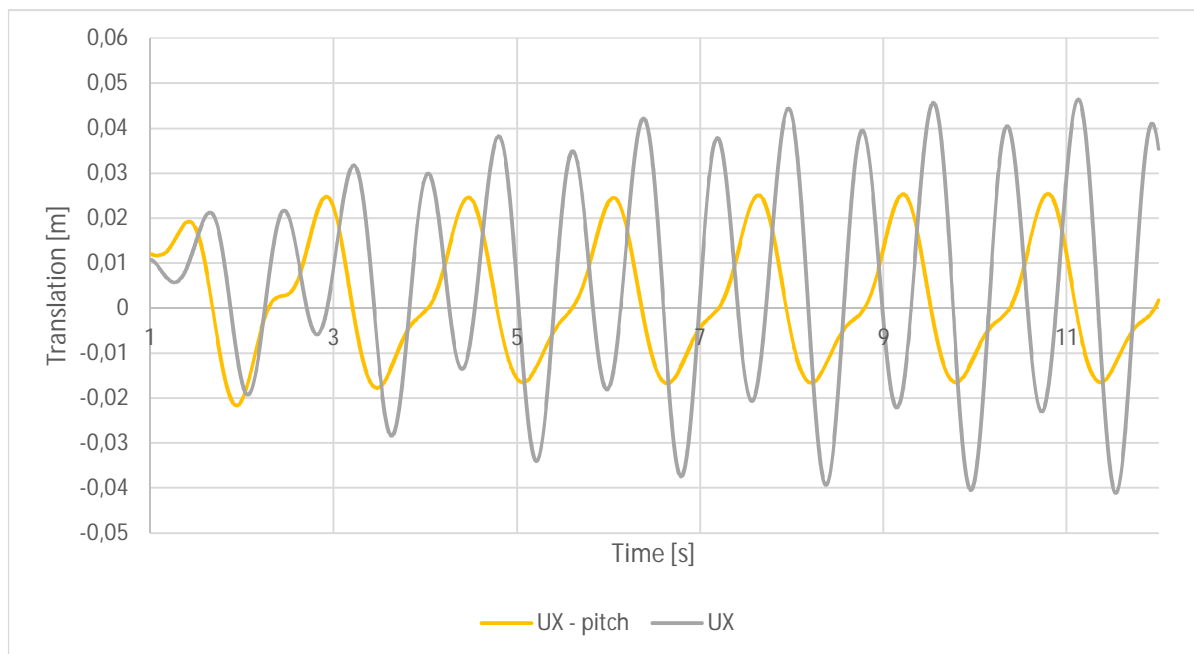


Figure 94: Load case 45, UX movement in top node and UX movement corrected for pitch movement

The UX – pitch is a scaled pitch movement subtracted from the UX translations. The scaled pitch movement is scaled by fitting the tops of the pitch movement the tops of the UX movement. This provides an image of what the underlying UX translation look like. It has a shape quite similar to the forces in line one to three. This is another indication that the lower lines takes up the surge movement.

## 8 Comparisons and discussion of experimental and simulated results

The purpose of the following chapter is to compare the experimental results with the simulated results and analyze the differences between them. The same wave cases as in the previous chapter have been chosen.

The measured variables in the experiment will be compared with simulation by looking at the difference between them. Attempts to explain the deviations will be done when they deviate.

The initial z-position in the experiment is the height of the prototype above water level. In ANSYS, the results return only the deflection about its initial position. The results of the z-position from the experiment have been modified to show displacement around an initial position. This has been done by subtracting the average of the z results from the the results, and we have the movement around zero.

### 8.1 Load case 37: TLB S, 2.5 sec, 0.5 m

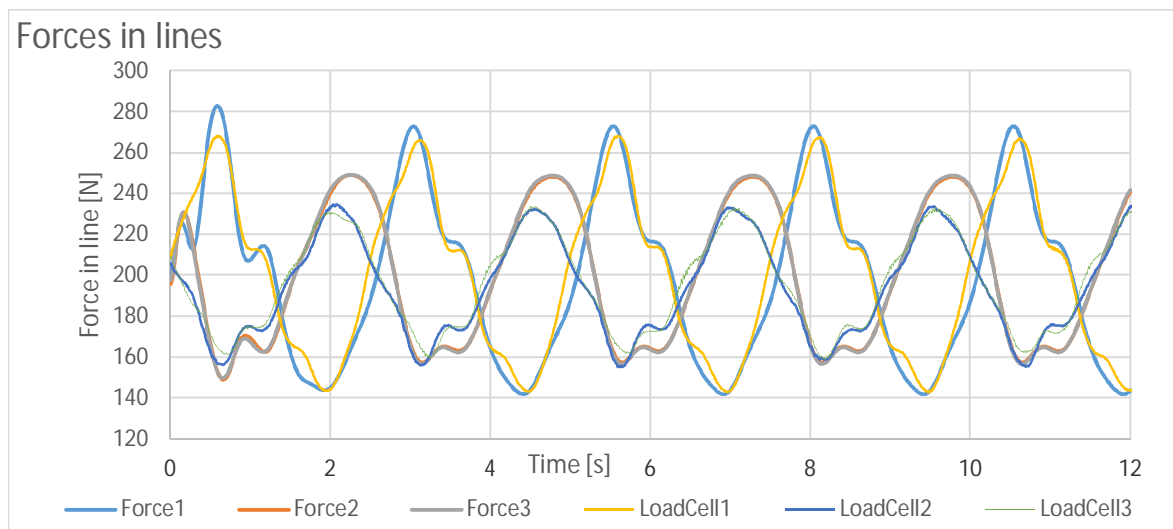


Figure 95: Comparison of forces in lower lines case 37

Smaller amplitudes on all forces in the experiment compared to the simulation. The reason might be friction somewhere in the system. It might also be difference in how much forces the waves place on the TLB.

The results of the experiment and simulation have the same shapes. The experimental results seem to have sharper tops and edges, but they have the same small plateaus and double top tendencies.

Some small phase offsets are seen when the simulation and experiment is compared. The phase is set after line one and the small plateaus on line two and three. The same reference time is used to compare the rest of the variables.

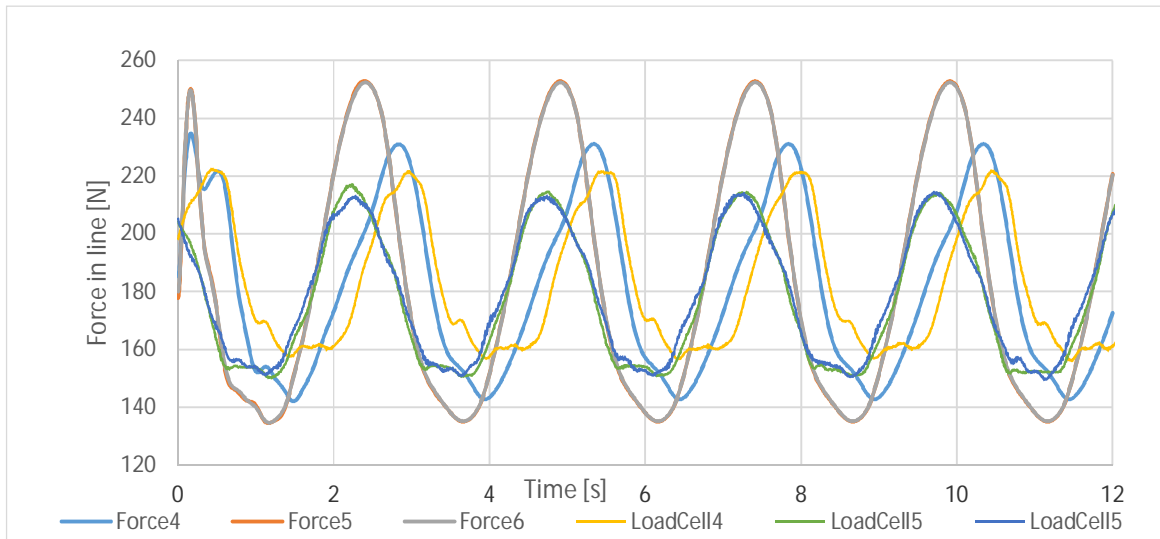


Figure 96: Comparison of forces in upper lines case 37

The phase offset seen in the lower lines can be seen in the upper lines as also. The amplitudes are also smaller in the experiment than the simulation. As for the lower lines the shapes are the same for experiment and simulation. The experiment seems to cut off of the troughs a little and that causes the amplitude to be smaller. The answer can be found in the pitch movement which has the same tops in the experiment as simulations, but the experiment does not have the same troughs in its shape. The UY and UZ translation is relatively similar, but the UX translation has a smaller amplitude in the experiment.

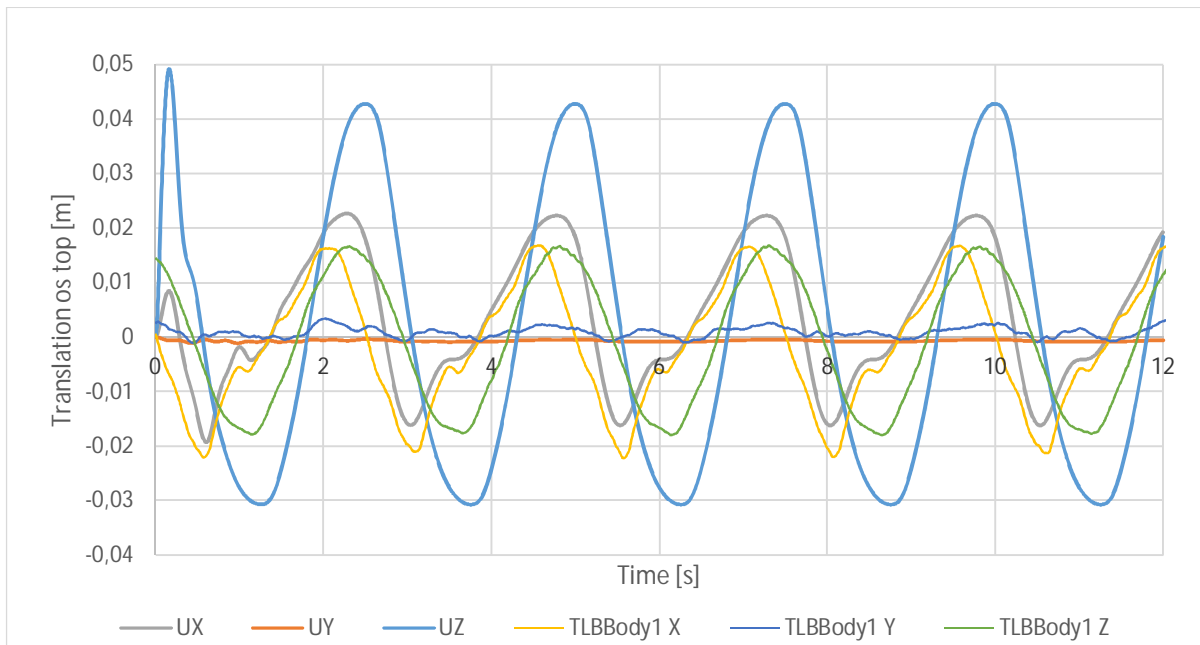


Figure 97: Comparison of translation in load case 37

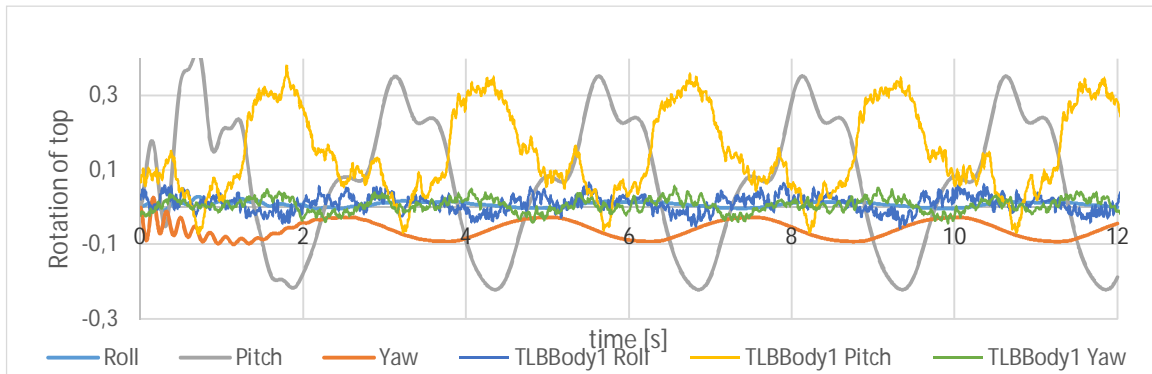


Figure 98: Comparison of Rotation movement case 37

The roll and yaw are all relatively similar in magnitude for experiment and simulation, but they do have different shapes. The experimental yaw has two tops within a period, while the simulated has a sinusoidal curve. This might be caused by noise and disturbance in the water. The same can be said about the roll. The pitch has the same shape with small plateaus on each side of the top. The top in the experiment seems to be more stretched out in time, and that leaves less time for the prototype to reach the bottom of the pitch movement.

It's interesting to see that there is an offset in the tops in pitch and UX translation. In the simulation, the pitch top is found after the UX top. In the experiment, the top in pitch is found before the top in UX translation.

Load case 37 is the one that is the least difficult to simulate. It is the TLB S, which is the easiest prototype to simulate, and the case has a long wave period. The following load cases are likely to have larger differences between experiment and simulation, but they may indicate why there are differences in results.

## 8.2 Load case 45: TLB B, 1.58 sec, 0.3 m

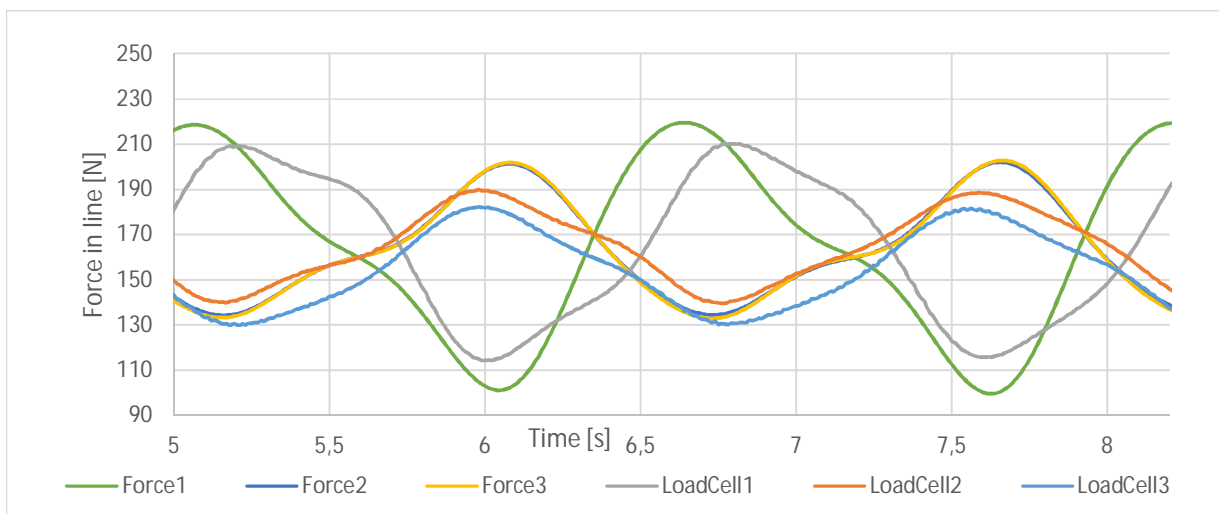


Figure 99: Comparison of forces in lower lines case 45



The forces in the lines have relatively similar magnitudes, the experiment having just a little smaller sizes. This is the same observation as made in load case 37. There is no sign of the simplified modelling of the tapered section in the line forces, but it might be one of more reasons for differences in results.

Line 4 is interesting because it looks like either the experiment or simulation is recorded backwards. This is not the case, it's the bottoms on each side of the small top that is deeper before the small top in the simulation, while its deeper after the small top in the experiment. This effect is likely to be connected to the phase offsets seen between experiment and simulation in motions.

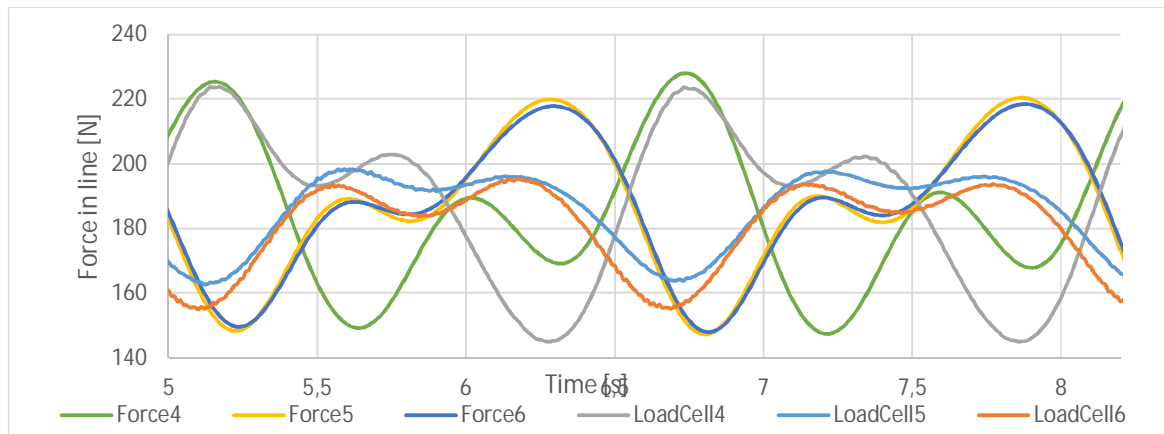


Figure 100: Comparison of forces in upper lines in load case 45

Since there is only one top per wave period it is reasonable to assume that the surge movement follows the wave period. The UX, pitch and also forces in the upper lines has two tops within one period. This might be interference from pitch eigen periods and deviations in eigen period and damping coefficients between experiment and simulation. Interference from the surge eigen period should perhaps have been seen as well, because it is in close to the pitch value. The high influence of pitch in the measured UX may have overshadowed the surge movement in the UX value, or it is simply not present.

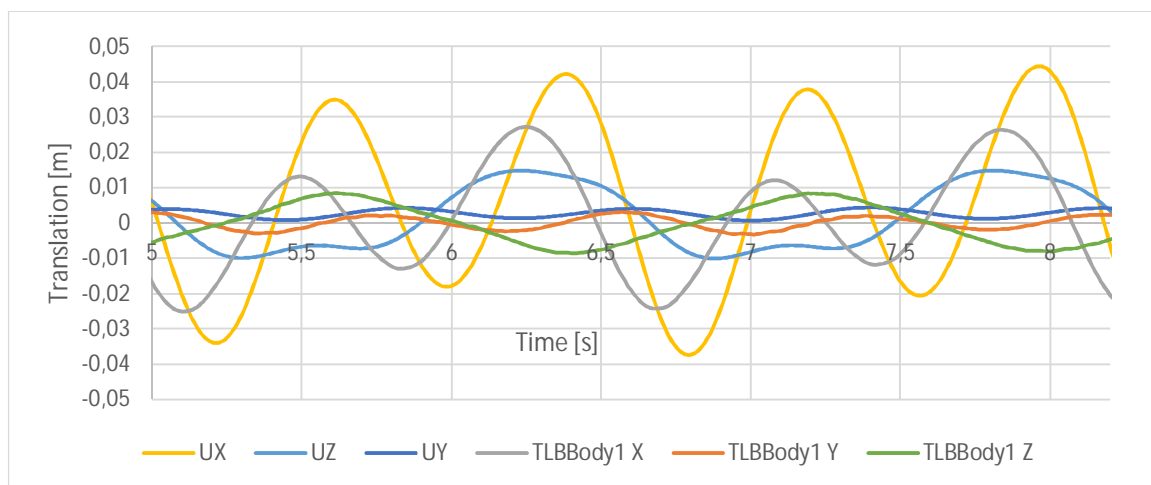


Figure 101: Comparison of translation in load case 45

It is interesting to see the shape of the UX results being so similar in shape. There are offsets in phase and amplitudes, but it might be possible to close this gap with a more sophisticated modelling tool. The gap can also be made smaller by further tuning of the damping and drag parameters on the existing model.

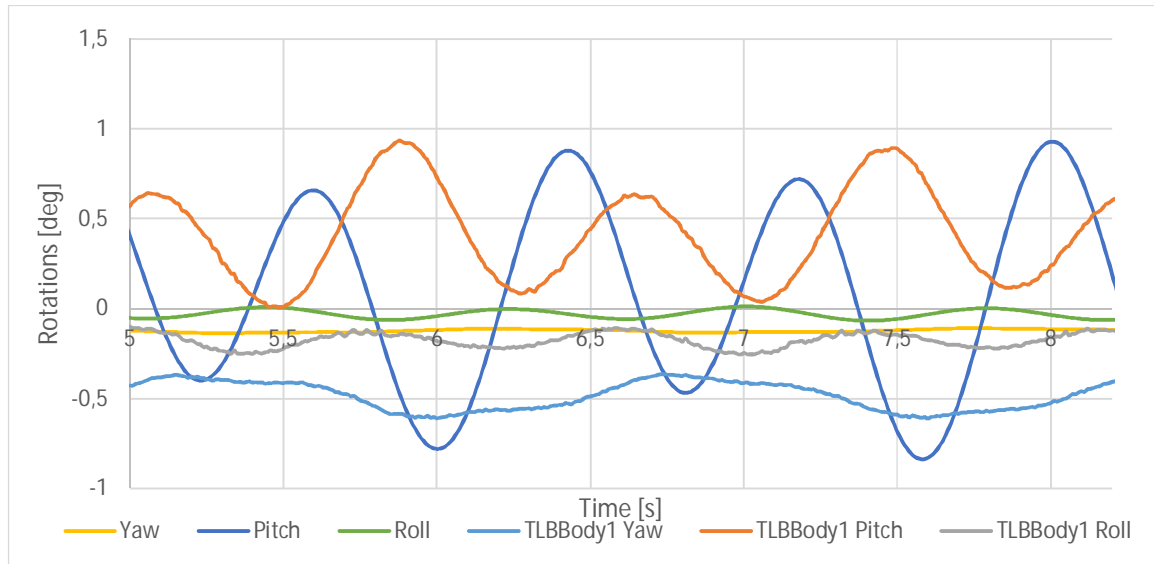


Figure 102: Comparison of Rotation movement in load case 45

The roll rotation is similar in experiment and simulation, both of the slightly negative. They are 90 degrees out of phase with each other, but this is likely just disturbance. No yaw movement is seen in the simulation, as in the experiment. There is a yaw damper in the simulation that has damped the yaw movement. The yaw movement in the experiment can be a result of moments caused by the lines and brackets. The lines are not exactly symmetrically placed around the floater, so it is likely that this has an effect. If this is the cause, it will not be seen in ANSYS since the bracket do not take up forces from the waves.

The pitch has similar shape both in experiment and simulation with two tops and bottoms in each wave period. The larger bottom comes before the larger top in both experiment and simulation. The magnitude of the experimental pitch rotation is about half of what is found in the simulation. The experimental mean level is above zero degrees while the mean of the simulation is about zero. The experiment prototype leans more forward and is subject to less torque around its center of rotation than the simulation. This is likely because the resultant force is lower in the water in the experiment, or the prototype floats higher in the water. If this is the case, it should be possible to see it in the ratio of surge translation and pitch induced translation in the UX value in the experiment. The simulation has relatively more pitch induced translation in its UX movement compared to the experiment. It is hard to verify this hypothesis since there is no tracking on the prototype at its center of rotation. The only thing possible to see is that the UX movement is more detached from pitch rotation in the experiment because the phase offset are larger here. The phase offset is smaller in the simulation indicating that the UX movement is closer related to the UX movement.

### 8.3 Load case 67: TLB X3, 1.58 sec, 0.3 m

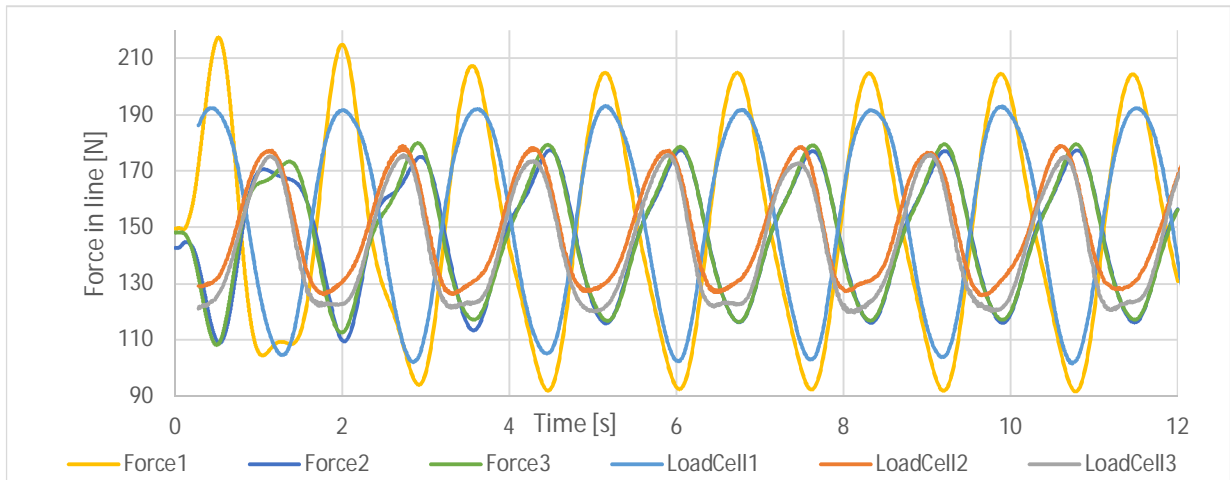


Figure 103: Comparison of forces in lower lines

In the lower lines it can be seen that the forces are in phase, but that is because all the parameters has been adjusted after them. It has been chosen to adjust after the lower lines because they are mainly subject to the surge movement. They are the most stable results in the load case and do not have many irregularities. The forces in the simulation have a larger magnitude than the experiment.

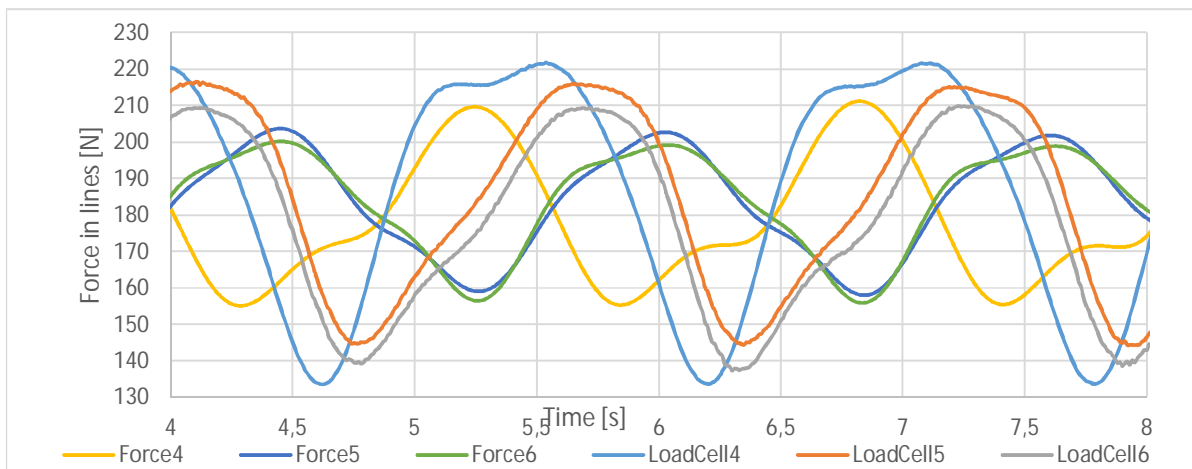


Figure 104: Comparison of forces in upper lines

The largest amplitude is in the experimental line four. The experimental line five and six is also larger than the forces in the simulation. This is a result of the large heave movement in the experiment. The experimental line four has a slightly larger amplitude than the line five and six. The same observation can be done in the simulation. There are traces of the same shapes when line four in the exp and sim is compared. They both have a plateau on the way up to the top, but it is much lower in the sim. A small phase shift in Force4-6 can also be seen when experiment and simulation is compared.

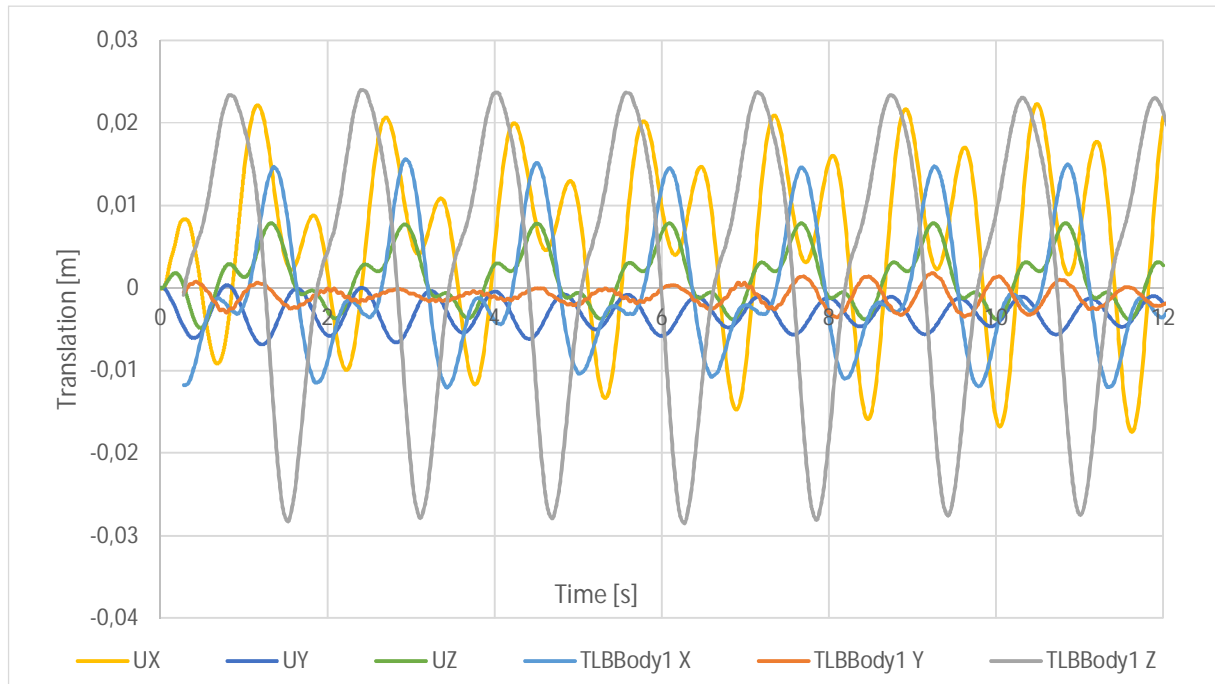


Figure 105: Comparison of translation

The experiment has a very large Z amplitude. The same large z amplitude is found in the other experiments on the TLB X3 also. It is different from the TLB S and B, and it is only found in the experiment. It is assumed that it might be caused by an end cap effect that is impossible to simulate in ANSYS. If a wave passes X3 and puts more weight on the transition piece between floater and three columns, it will push the X3 down. The effect has been seen when the UZ translation is plotted against the waves. The X3 goes down when a wave passes. In some of the plots with translation over wave height, the same effect is found on the TLB B. The difference is that the effect is about three times larger on the X3 in all experiments. This indicates that there is two effects pulling X3 down under a wave top and one effect pulling the TLB B down. A hypothesis for this behavior is that it is the lines pulling the TLB B down when it has a surge movement. The lines pull down the X3 and additionally the pressure on the lid of the floater pushes it down. When the extra pressure and the pull from the lines disappear, the TLB X3 comes up again. It has a higher upward velocity when it comes to its normal level so it continues until it is decelerated down by the mooring lines.

From the video from the experiments it is clearly seen that the X3 moves down under the pressure of the wave top. This verifies that the result are sampled correctly and it does not exclude the above-mentioned hypothesis about the TLB X3 movement.

There are tendencies of a double top in both the experiment and simulation, but less developed in the simulation. This is probably related to the large pitch movement in the simulation, which is not found in the experiment.

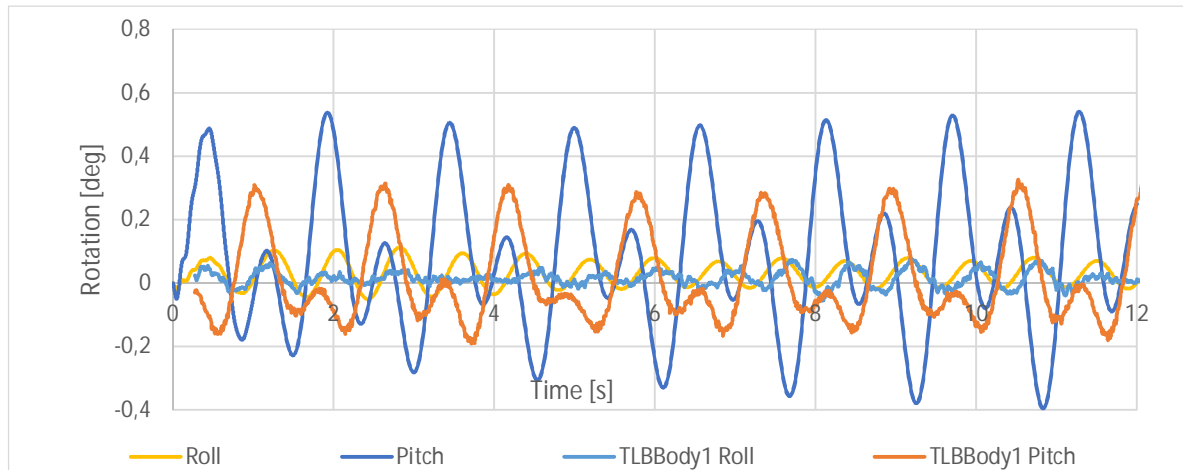


Figure 106: Comparison of Rotation movement

#### 8.4 Summarizing discussion of results from comparison

There are many similarities between the experiment and simulation. Many of the same shapes can be observed in both. Double tops and bottoms within a wave period is often seen in experiment and simulation, but with variations in long time it takes from top to top. This can be caused by the variations in eigen periods. The simulated results deviate from the experimental results in some of the parameters, but shapes, overall amplitudes and mean values of the experiment and simulation is relatively similar.

The amplitudes in forces are similar for many load cases, which means that the load applied to the prototypes is relatively equal in experiment and simulation.

Four main causes for the difference in results between simulation and experiment seems probable:

1. The lack of correct damping parameters
2. The deviations in eigen periods between experiment and simulation.
3. The lack of ability in ANSYS to model lids/end caps on pipe elements
4. The height of the wave force resultant is different in experiment and simulation

Even if we cannot simulate the forces and movements exactly we can do rough estimations. This makes it possible to turn the morning lines around to analyze what happens when wave attack from different angles. Approximate analysis on the floater and tower is also attainable .

It has been verified that the ANSYS model and the 3DFloat model returns the same eigen frequencies and that they have the same geometry. It does not return the exact eigen values as we find them in the decay tests. This means that we have small differences between the simulated and the experimental model. These differences may be one of the cause of deviating results. We do not know if the damping in the roll direction is correct.

## 9 Conclusion:

The experiment was conducted as planned in January and it generated a large set data material. The data material has been analyzed and there is no signs of major error in the sets. There are no insurance from errors in such experiments and there are uncertainties but the studies of the material so far, concludes experiment can be considered successful. It returned useful results that puts light to the behavior of the TLB prototypes and can be valuable in further studies.

Three simulation models is built for ANSYS and simulations have been conducted. The results from the simulation delivers results that are very close to the experimental results in some wave cases and further away in other cases. The results from the simulation of TLB S are in general better fits to the experiment than for the other two prototypes. The causes for the deviating results may be wrong damping parameters in addition to wrong choice of drag and mass coefficients. The simulation model is promising, but still lack tuning to deliver optimal results.

The TLB B and X3 prototypes show similar behavior in the experiment. The X3 is more responsive in the heave direction while the TLB B is more responsive in the pitch/surge direction. There are no significant signs of greater instability in the TLB X3 than TLB B. The TLB S has a little different behavior, mainly because of its weight and mass momentum around x and y-axis.

The qualitative analysis of the plots concludes that the experiment and simulation delivers satisfactory results. Many of the parameters have the same shapes and amplitudes. There are offset in phase and magnitude, but similarities are too strong to reject the experimental results in any way. If the similarities were weaker, it would more likely be caused by errors in the model, not the experiment.

The goals of the thesis have been met.

## **10 Further work:**

Both regarding the experiment and the simulation models there are further work to be done.

Further studies on the uncertainties in the experiment should be conducted to uncover the uncertainty in each of the measured parameters. With more certain and quantified uncertainties it would be possible to state whether a simulation model can be accepted or must be rejected in later stages.

Several load cases in the experiment are not fully analyzed. It is likely more to gain from studying all of the parameters in the load cases closer.

More information and understanding indicates that further studies should be conducted on the damping parameters. The mooring lines should be set up with its own structural stiffness damping. It should also be attempted to decrease the difference in eigen period between the experiment and simulation. The wave response plots shows that the models are more sensitive to the waves when the wave period is close to the eigen periods of the prototypes. The drag and mass coefficients should be set again after the damping parameters have been optimized.

The wave gauge results show that the wave heights that is recorded is not exactly equal to what the table of load cases indicate. The actual wave height are smaller in the cases controlled. The simulations should be attempted with the measured wave height instead of input wave height to come closer to the experiment.

## 11 Bibliography

- ANSYS Inc. (b). (2013). ANSYS APDL Mechanical, release 14.5 help system, Element Reference Guide.
- ANSYS Inc. (c). (2013). ANSYS APDL Mechanical, release 14.5 help system: Command references.
- ANSYS Inc. (d). (2013). ANSYS APDL Mechanical, release 14.5 help system: Advanced Analysis Guide.
- ANSYS, inc. (2012). ANSYS APDL Mechanical, release 14.5 help system. Canonsburg, USA.
- Blue H group. (2013, May). *Blue H group*. Retrieved from <http://www.bluehgroup.com/product/index.php>
- Butterfield, S. M. (2005). Engineering Challenges for Floating Offshore Wind Turbines. *2005 Copenhagen Offshore Wind Conference* (pp. 26-28). Copenhagen, Denmark: Copenhagen Offshore Wind Conference.
- Chakrabarti, S. K. (2005). *Handbook of offshore engineering, 1.ed.* Illinois, USA: Elsevier Ltd.
- Det Norske Veritas. (2010). *Recommended Practice DNV-RP-C205: Environmental conditions and environmental loads*. Oslo: Det Norske Veritas.
- Det Norske Veritas. (2013). *Offshore Standard DNV-OS-J101*. Oslo: Det Norske Veritas (DNV).
- Det Norske Veritas AS. (2012). *Tecnology Outlook 2020*. Oslo: Det Norske Veritas AS.
- Det Norske Veritas RP-C205. (2010). *DNV Recommended practice DNV-RP-C205 Environmental conditions and environmental loads*. Oslo: Det Norske Veritas.
- EDR-Medeso. (2013, February). Email correspondence with ANSYS supplier EDR Medeso. (J. Berg, Interviewer)
- FinnLøkenAS. (2012, Jan.). *Plast halv fabrikata*. Ås, Norge: Finn Løken A.S.
- Flintec sensor solutions. (2013, May 2.). *Flintec sensor solutions*. Retrieved from [http://www.flintec.com/hres/a18\\_rev7\\_gb%20sb6%20data%20sheet.pdf](http://www.flintec.com/hres/a18_rev7_gb%20sb6%20data%20sheet.pdf)
- Huebner, K., Dewhirst, D. L., Smith, D. E., & Byrom, T. G. (2001). *The finite Element Method for Engineers*. New York: John Wiley & Sons.
- IFREMER. (2013, May). *IFREMER: Marine Environment Tests and Research Infrastructure*. Retrieved from IFREMER: [http://www.ifremer.fr/metri/pages\\_metri/infrastructure/brest\\_basin.htm](http://www.ifremer.fr/metri/pages_metri/infrastructure/brest_basin.htm)
- International Energy Agency. (2010). *World Energy Outlook 2010*. Paris: OECD/IEA.
- Keulegan, G. H., & Patterson, G. W. (1940). Mathematical theory of irrotational translation waves. *National bureau of standards volume 24.*, 48-100.



- Knapp, D. -I. (2012). *Ocean and Wind energy - Harvesting renewable energy potentials*. München: Lehrstuhl und Versuchsanstalt für Wasserbau und Wasserwirtschaft Technische Universität München.
- LINAK (a). (2013, May 2). *LINAK*. Retrieved from LINAK:  
[http://www.linak.com/corporate/pdf/ENGLISH/DATA%20SHEET/Linear%20Actuator\\_LA23\\_Data%20Sheet\\_Eng.pdf](http://www.linak.com/corporate/pdf/ENGLISH/DATA%20SHEET/Linear%20Actuator_LA23_Data%20Sheet_Eng.pdf)
- LINAK (b). (2013, May 2). *LINAK*. Retrieved from LINAK:  
[http://www.linak.com/corporate/pdf/ENGLISH/BROCHURE/TECHLINE\\_Product%20Overview\\_Brochure\\_Eng.pdf](http://www.linak.com/corporate/pdf/ENGLISH/BROCHURE/TECHLINE_Product%20Overview_Brochure_Eng.pdf)
- Lohmann, K. C. (2013, May 3). *The University of Michigan: Kyger C Lohmann*. Retrieved from Geological sciences 100, Coral reef mini course:  
<http://www.earth.lsa.umich.edu/~kacey/ugrad/coral7.html>
- Myhr, A. (2013, March). Pretension in the mooring lines during experiment. (J. Berg, Interviewer)
- Myhr, A. (2013, April 26). Response plots from MARINET experiment. Ås.
- Myhr, A., & Moss, D. W. (2009). *Concept for installation of floating wind turbines*. Ås: Institutt for matematiske realfag og teknologi ved Universitetet for Miljø og Biovitenskap.
- Myhr, A., & Nygaard, T. A. (2012, June 17-22). Load Reductions and optimizations on a tension legged buoy offshore wind turbine platforms. *The proceedings of the twenty-second international offshore and polar engineering conference, Rhodes, Greece*, p. 8.
- Nygaard, T. A. (2013, April). Evaluation and guidance lesson. (J. Berg, Interviewer)
- Palmer, A. C., & King, R. A. (2008). *Subsea pipeline Engineering*. Tulsa, Oklahoma: PennWell Corporation.
- Petersen, E. L., & Troen, I. (2012, September/October). Wind Conditions and Resource Assesment 1. *Wires Energy and Environment*, pp. 206-217.
- Principle power inc. (2013, May). *Principle power inc*. Retrieved from Principle Power inc.:  
<http://www.principlepowerinc.com/products/windfloat.html>
- Reynolds, O. (1883). *An experimental investigation of the circumstances which determine whether the motion of water shall be direct or sinuous, and of the law of resistance in parallel channels*. London: The Royal Society.
- Sarpkaya, T., & Isaacson, M. (1981). *Mechanics of Wave Forces on Offshore Structures*. New York: Litton Educational Publishing, Inc.
- Smits, A. J. (2013, March 15). *Drag of Blunt Bodies and Streamlined Bodies*. Retrieved from Princeton University: [http://www.princeton.edu/~asmits/Bicycle\\_web/blunt.html](http://www.princeton.edu/~asmits/Bicycle_web/blunt.html)

Spæren, A. (2013). *Development and construction of floating wind turbine models and test rig for wave tank test*. Ås: Norwegian University of Life sciences.

Statoil ASA. (2013, May). *Statoil*. Retrieved from Statoil - technology and innovation:  
<http://www.statoil.com/no/TechnologyInnovation/NewEnergy/RenewablePowerProduction/Offshore/Hywind/Pages/HywindPuttingWindPowerToTheTest.aspx?WT.srch=1&gclid=CMXk2t7Ai7cCFfQZtAodBXOAPg>

Tipler, P. A., & Mosca, G. P. (2007). *Physics for Scientists and Engineers with Modern Physics, sixth ed.* Michigan: W. H. Freeman.

Twidell, J., & Weir, T. (2006). *Renewable Energy Resources 2. ed.* New York, USA: Taylor & Francis Ltd.

Volden, B. I., & Sanden, I. L. (2010). *Life cycle analysis of floating wind turbines with regard to internal and external factors compared with bottom-fixed wind turbines*. Ås: Institutt for matematiske realfag og teknologi ved Universitetet for Miljø .

## **12 Appendix**

1. Appendix I: Figure list
2. Appendix II: List of tables
3. Appendix III: Table of Load cases
4. Appendix IV: Section and material properties of the TLB S:
5. Appendix V: Section and material properties of the TLB B:
6. Appendix VI: Section and material properties of the TLB X3:

### **Electronic appendix:**

- ANSYS input files
- DNV-OS-J101
- DNV-RP-C205
- Flintec data sheet
- Full list of Load cases
- Linak Linear actuator data sheet
- Simulation results
  - TLB S
  - TLB B
  - TLB X3
- Video documentation

The digital appendix is found on the DVD in the back of the paper edition of the master thesis. The full sample of results from the experiment is not included in the appendix because of confidentiality concerns. The photo and video material in the appendix is private material, which is not confidential.

## Appendix I: Figure list

Figure 1: Modes of motion in water. Credit: Lancaster University Renewable Energy Group .....	IX
Figure 2: Illustration of wind speed and roughness (Knapp, 2012) .....	3
Figure 3: Wind speeds at sea and at shore in Europe (Petersen & Troen, 2012) .....	4
Figure 4: Example of mooring types. Illustration by renewableenergyworld.com .....	6
Figure 5: The TLB Concept (Myhr & Nygaard, Load Reductions and optimizations on a tension legged buoy offshore wind turbine platforms., 2012) .....	8
Figure 6: Illustration of the TLB research project .....	9
Figure 7: Wave moving past model B in the IFREMER water tank. ....	11
Figure 8: Ranges of wave theory validity. Be aware of the length unit (Det Norske Veritas, 2013) .....	12
Figure 9: Illustration of wave motion (Lohmann, 2013) .....	14
Figure 10: Illustration of horizontal drag and inertia wave forces .....	15
Figure 11: The combined influence of KC and Reynolds numbers on inertia coefficient and drag coefficient (Sarpkaya & Isaacson, 1981) .....	17
Figure 12: Drag coefficients for cylinder and sphere (Smits, 2013) .....	18
Figure 13: Illustration of experiment set up .....	19
Figure 14: Bird view of the experiment setup .....	20
Figure 15: Picture of the test site, the wave tank at IFREMER .....	22
Figure 16: IFREMER Deep seawater tank. (IFREMER, 2013) .....	22
Figure 17: Illustration of prototypes with height in mm .....	23
Figure 18: Photography of the prototypes (from left: Tower, TLB S, TLB B and TLB X3) .....	24
Figure 19: Sections of the simple prototype .....	25
Figure 20: Illustration of section in the TLB B .....	26
Figure 21: Sections of the TLB X3 .....	28
Figure 22: Setup of Tower, Load cell, Actuator, spring and mooring line .....	30
Figure 23: Tower section .....	30
Figure 24: Adjustable spring .....	31
Figure 25: Illustration of adjustable springs (Spæren, 2013) .....	31
Figure 26: Pulley plates with the modified pulleys .....	32
Figure 27: Illustration of 3D camera, tracking ball, video camera and wave gauge .....	32
Figure 28: Illustration of load cell, actuator and spring setup (Spæren, 2013) .....	33
Figure 29: Beam type load cell (Flintec sensor solutions, 2013) .....	33
Figure 30: Tracking balls on top of prototype .....	34
Figure 31: Linear actuator LA23 from LINAK .....	34
Figure 32: TLB B: Experiment 45, Force line 1: 0.3 m, 1.58 sec .....	35
Figure 33: TLB B: Experiment 45, UX movement: 0.3 m, 1.58 sec .....	35
Figure 34: Comparing UX Movement: 0.3 meter and 1.58 sec period .....	36
Figure 35: Forces in line 1: from all prototypes in 0.3 m waves and 1.58 sec period .....	39
Figure 36: Forces in line 4 from all prototypes in 0.3 m waves and 1.58 sec period .....	39
Figure 37: TLB Simple: 0.13 m waves .....	40
Figure 38: TLB Simple: 0.30 m waves .....	40

Figure 39: TLB simple: 0.40 m waves .....	40
Figure 40: TLB Simple: 50 m waves .....	40
Figure 41: TLB B: 0.13 m wave.....	41
Figure 42: TLB B: 0.30 m wave.....	41
Figure 43: TLB B: 0.5 m wave height .....	41
Figure 44: TLB X3: 0.13 meter wave.....	42
Figure 45: TLB X3: 0.3 meter wave.....	42
Figure 46: TLB X3: 0.5 m wave.....	42
Figure 47: UZ movement in wave cases 0.5m wave and 2.5 sec period .....	43
Figure 48: UX movement of prototypes in 0.5 meter and 2.5 sec period.....	43
Figure 49: Illustration of forces pulling the TLB B and X3 under water at wave top.....	44
Figure 50: Illustration of balance point (drawing not to scale) .....	44
Figure 51: Plot of x direction movement against wave frequency (Myhr, 2013) .....	46
Figure 52: Plot of z direction movement against wave frequency (Myhr, 2013) .....	47
Figure 53: Plot of force in line 4 against wave frequency (Myhr, 2013) .....	48
Figure 54: Plot of pitch movement against wave frequency (Myhr, 2013).....	49
Figure 55: 0.13 meter and 1.58 sec period for three prototypes .....	51
Figure 56: Wave measurement in load case 45 .....	51
Figure 57: Line model of the TLB S. (6 dots on model are point masses of mooring points. Water line at origin in xy-plane).....	53
Figure 58: Figure of the PIPE288 element (ANSYS, inc., 2012) .....	55
Figure 59: Illustration of the LINK180 element (ANSYS Inc. (b), 2013).....	56
Figure 60: Illustration of the modelling of X3 columns.....	60
Figure 61: Illustration of the three computational models .....	60
Figure 62: TLB S time convergence max .....	63
Figure 63: TLB B time convergence max.....	63
Figure 64: TLB X3 time convergence max.....	63
Figure 65: TLB S element convergence max.....	64
Figure 66: TLB B element convergence max.....	64
Figure 67: TLB X3 element convergence max.....	64
Figure 68: Drag parameter testing TLB S (tested with $C_m = 2.0$ ).....	66
Figure 69: Drag parameter testing TLB B (tested with $C_m = 2.0$ ) .....	66
Figure 70: Drag parameter testing TLB X3 (tested with $C_m = 2.0$ ) .....	66
Figure 71: Parameter testing of coefficient of inertia on TLB S (tested with $C_d = 1.3$ ).....	67
Figure 72: Parameter testing of coefficient of inertia on TLB B (tested with $C_d = 1.3$ ).....	67
Figure 73: Parameter testing of coefficient of inertia on TLB X3 (tested with $C_d = 1.3$ ).....	67
Figure 74: Illustration of decay loads.....	70
Figure 75: Decay pitch/ROTY .....	71
Figure 76: Simple decay heave .....	71
Figure 77: Test 53: TLB B Decay pitch .....	72
Figure 78: Damping of heave motion (UZ) .....	72
Figure 79: TLB X3: Decay pitch .....	73

Figure 80: TLB X3: Heave decay (UZ).....	73
Figure 81: Forces in lower lines load case 37 .....	76
Figure 82: Forces in upper lines load case 37.....	77
Figure 83: Rotational movement load case 37.....	77
Figure 84: Translational movement load case 37 .....	78
Figure 85: Wave resultant working on the model .....	79
Figure 86: Forces in lines load case 45.....	79
Figure 87: Forces in upper lines load case 45.....	79
Figure 88: Translation in load case 45.....	80
Figure 89: Rotation in load case 45.....	80
Figure 90: Forces in lower lines simulation 67 .....	81
Figure 91: Forces in upper lines simulation 67.....	81
Figure 92: Translation in simulation 67.....	81
Figure 93: Rotations in simulation 67 .....	82
Figure 94: Load case 45, UX movement in top node and UX movement corrected for pitch movement..	83
Figure 95: Comparison of forces in lower lines case 37 .....	84
Figure 96: Comparison of forces in upper lines case 37 .....	85
Figure 97: Comparison of translation in load case 37.....	85
Figure 98: Comparison of Rotation movement case 37 .....	86
Figure 99: Comparison of forces in lower lines case 45 .....	86
Figure 100: Comparison of forces in upper lines in load case 45.....	87
Figure 101: Comparison of translation in load case 45 .....	87
Figure 102: Comparison of Rotation movement in load case 45.....	88
Figure 103: Comparison of forces in lower lines.....	89
Figure 104: Comparison of forces in upper lines .....	89
Figure 105: Comparison of translation .....	90
Figure 106: Comparison of Rotation movement.....	91

## Appendix II: List of tables

Table 1: Labels on the simulated and experimental results.....	IX
Table 2: World electricity production and capacity .....	1
Table 3: Table of the theoretical potential energy from renewable energy sources (Knapp, 2012) .....	2
Table 4: Roughness of the ground (Knapp, 2012).....	4
Table 5: Cost of generating renewable energy toward 2035. (International Energy Agency, 2010) .....	5
Table 6: Extreme wave cases in experiment: highest and lowest wave period and wave height.....	13
Table 7: Wave and sea parameters.....	16
Table 8: Reynolds number and Keulegan Carpenter number .....	16
Table 9: Placing of towers.....	20
Table 10: Anchor point coordinates.....	21
Table 11: Stiffness of anchor lines.....	21
Table 12: The TLB S with geometry.....	25
Table 13: Geometry of TLB B .....	27
Table 14: Geometry of TLB X3 .....	29
Table 15: Eigen periods measured in the wave tank .....	36
Table 16: UX deflections from all the simulations with 0.30 m waves.....	37
Table 17: Pretension in the lines (Myhr, 2013) .....	61
Table 18: Table of tested coefficients in drag/inertia coefficient test .....	65
Table 19: Coefficients of drag and inertia.....	68
Table 20: Eigen periods calculated in ANSYS.....	68
Table 21: Finding and controlling yaw Eigen periods .....	69
Table 22: Difference in eigen periods between experimental decay tests and simulated decay test results .....	69
Table 23: Best fitting parameters for the TLB S decay test .....	71
Table 24: Best fitting parameters for the TLB B decay test .....	72
Table 25: Best fitting parameters for the TLB X3 decay test .....	73
Table 26: Damping parameters all models.....	74
Table 27: Input values for the hand calculation.....	75
Table 28: Table of experiments used for the analysis .....	76

### Appendix III: Table of Load cases

Test Number	Waves	Period [s]	Wave Height [m]	Gamma	Duration [s]
TLB S					
25	Calm water				
26	Regular Waves	0.95	0.13		60
27	Regular Waves	1.26	0.13		60
28	Regular Waves	1.26	0.30		60
29	Regular Waves	1.80	0.13		60
30	Regular Waves	1.80	0.30		60
31	Regular Waves	1.58	0.13		60
32	Regular Waves	1.58	0.30		60
33	Regular Waves	1.58	0.40		60
34	Regular Waves	1.80	0.50		60
35	Irregular waves	1.58	0.13	2.87	300
36	Irregular waves	3.04	0.28	1.05	300
37	Regular Waves	2.50	0.50		120
38	Irregular waves	2.53	0.28	2	300
39	Regular Waves	1.80	0.40		60
40	Decay test				
41	Irregular waves	3.04	0.28	1.05	300
TLB B					
43	Regular Waves	1.80	0.30		60
44	Regular Waves	1.58	0.13		60
45	Regular Waves	1.58	0.30		60
46	Irregular waves	3.04	0.28	1.05	300
47	Regular Waves	1.80	0.50		60
48	Irregular waves	1.58	0.13	2.87	300
49	Irregular waves	2.53	0.28	2	300
50	Regular Waves	0.95	0.13		60
51	Irregular waves	3.04	0.28	1.05	300
52	Regular Waves	1.26	0.13		60
53	Decay test				
54	Regular Waves	1.80	0.13		60
55	Regular Waves	1.26	0.30		60
56	Regular Waves	2.50	0.50		60
57	Regular Waves	1.80	0.50		60
TLB X3					
60	Decay test				
61	Regular Waves	0.95	0.13		60
62	Irregular waves	3.04	0.28	1.05	300
63	Irregular waves	1.58	0.13	2.87	300
64	Irregular waves	2.53	0.28	2	300
65	Irregular waves	3.04	0.28	1.05	300
66	Regular Waves	1.58	0.13		60
67	Regular Waves	1.58	0.30		60
68	Regular Waves	1.26	0.13		60
69	Regular Waves	1.26	0.30		60
70	Regular Waves	1.80	0.13		60
71	Regular Waves	1.80	0.30		60
72	Regular Waves	2.50	0.50		60
73	Regular Waves	1.80	0.50		60
74	Regular Waves	2.80	0.30		60
75	Regular Waves	2.80	0.13		60
76	Irregular waves	3.04	0.28	1.05	300
77	Regular Waves	2.50	0.50		180



#### Appendix IV: Section and material properties of the TLB S:

		material num.		
Young's modulus [N/m <sup>2</sup> ]				
Sections	all	1.20E+09		
Mooring lines	all	2.10E+11		
Anchoring bracket	all	2.10E+12		
Poisson ratio				
Sections	all	0.3		
Mooring lines	all	0.3		
Anchoring bracket	all	0.3		
Density of material [kg/m <sup>3</sup> ]				
Floater element	1	1463.4		
Floater element	2	922.5		
Floater element	3	1136.6		
Floater element	4	932.6		
Floater element	5	1480.4		
Mooring lines	all	1		
Anchor bracket	all	0		
Section properties	secnum	Outer diameter [m]	Inner diameter [m]	Area [m <sup>2</sup> ]
Floater element	1	0.25	0.1245	
Floater element	2	0.25	0.1245	
Floater element	3	0.25	0.005	
Floater element	4	0.25	0.1245	
Floater element	5	0.25	0.1245	
Mooring Bracket	999	0.25	0.1245	
Mooring line	1			5.20E-08
Mooring line	2			5.10E-08
Mooring line	3			5.15E-08
Mooring line	4			5.01E-08
Mooring line	5			4.97E-08
Mooring line	6			4.92E-08

## Appendix V: Section and material properties of the TLB B:

Young's modulus		[N/m <sup>2</sup> ]
Section number	1	7.00E+10
Section number	2	7.00E+10
Section number	3	1.20E+09
Section number	4	1.20E+09
Section number	5	7.00E+10
Section number	6	7.00E+10
Section number	7	7.00E+10
Section number	8	3.00E+09
Section number	9	3.00E+09
Section number	10	7.00E+10
Section number	11	7.00E+10
Section number	12	7.00E+10
Section number	13	7.00E+10
Section number	14	7.00E+10
Section number	15	7.00E+10
Mooring lines	all	2.10E+11
Mooring brackets	all	2.10E+12
Density of element		[kg/m <sup>3</sup> ]
Section number	1	2698
Section number	2	2353
Section number	3	1201
Section number	4	1201
Section number	5	2183
Section number	6	3084
Section number	7	1672
Section number	8	1547
Section number	9	1547
Section number	10	2022
Section number	11	3079
Section number	12	2996
Section number	13	2868
Section number	14	2007
Section number	15	1537
Weight of lower brackets [kg]	all	0.022
Weight of upper brackets [kg]	all	0.042
Mooring lines	all	1
Mooring brackets	all	0

Poisson ratio				
Section number	all	0.3		
Mooring lines	all	0.3		
Mooring brackets	all	0.3		
Section properties		Outer diameter [m]	Wall thickness [m]	Area [m <sup>2</sup> ]
section	1	0.163	0.081	
section	2	0.150	0.075	
section	3	0.150	0.004	
section	4	0.150	0.009	
section	5	0.160	0.017	
section	6	0.160	0.010	
section	7	0.160	0.005	
section	8	0.160	0.008	
Tapered section upper dia.	9	0.160	0.004	
Tapered section lower dia.	9	0.298	0.004	
section	10	0.298	0.006	
section	11	0.298	0.003	
section	12	0.298	0.006	
section	13	0.297	0.146	
mooring line	1			5.125E-08
mooring line	2			5.024E-08
mooring line	3			5.074E-08
mooring line	4			5.014E-08
mooring line	5			4.969E-08
mooring line	6			4.924E-08
Mooring brackets		0.297	0.146	

## Appendix VI: Section and material properties of the TLB X3:

Young's modulus		N/m <sup>2</sup>		
Section number	1	7.00E+10		
Section number	2	7.00E+10		
Section number	3	1.20E+09		
Section number	4	7.00E+10		
Section number	5	7.00E+10		
Section number	6	7.00E+10		
Section number	7	7.00E+10		
Section number	8	7.00E+10		
Section number	9	7.00E+10		
Section number	10	7.00E+10		
Section number	11	7.00E+10		
Density of material		kg/m <sup>3</sup>		
Section number	1	2697.8		
Section number	2	2353		
Section number	3	1201		
Section number	4	2344		
Section number	5	7715		
Section number	6	3833		
Section number	7	3312		
Section number	8	2864		
Section number	9	3001		
Section number	10	2164		
Section number	11	2705		
Mooring lines	all	2.10E+11		
Mooring brackets	all	2.10E+13		
Weight of mooring brackets [kg]		0.022		
Poisson ratio		all		
Sections	all	0.3		
Mooring lines	all	0.3		
Mooring brackets	all	1.3		
Section properties		Outer diameter [m]	Wall thickness [m]	Area [m <sup>2</sup> ]
Section number	1	0.1625	0.0812	
Section number	2	0.150	0.0749	
Section number	3	0.150	0.0040	
Section number	4	0.150	0.0128	
Section number	5	0.200	0.0378	
Section number	6	0.261	0.1302	
Section number	7	0.261	0.0045	
Section number	8	0.261	0.0025	
Section number	9	0.261	0.0045	
Section number	10	0.261	0.1302	
Section number	11	0.022	0.0030	

Section properties		Outer diameter [m]	Wall thickness [m]	Area [m <sup>2</sup> ]
Mooring line	1			4.43E-08
Mooring line	2			4.41E-08
Mooring line	3			4.31E-08
Mooring line	4			4.95E-08
Mooring line	5			4.98E-08
Mooring line	6			4.78E-08
Mooring bracket		0.297	0.1485	